

**EFFECT OF COARSE AGGREGATE POROSITY ON THE
COMPRESSIVE BEHAVIOR OF CONCRETE AFTER HIGH
TEMPERATURE EPISODES**

MD. SYIED MAHBUB MORSHED



**DEPARTMENT OF CIVIL ENGINEERING
BANGLADESH UNIVERSITY OF ENGINEERING AND TECHNOLOGY
DHAKA-1000, BANGLADESH**

MAY, 2014

**EFFECT OF COARSE AGGREGATE POROSITY ON THE
COMPRESSIVE BEHAVIOR OF CONCRETE AFTER HIGH
TEMPERATURE EPISODES**

A THESIS

**SUBMITTED TO THE DEPARTMENT OF CIVIL ENGINEERING
IN PARTIAL FULFILLMENT OF THE REQUIREMENTS FOR THE DEGREE
OF
MASTER OF ENGINEERING IN CIVIL ENGINEERING (STRUCTURAL)**

BY

MD. SYIED MAHBUB MORSHED



**DEPARTMENT OF CIVIL ENGINEERING
BANGLADESH UNIVERSITY OF ENGINEERING AND TECHNOLOGY
DHAKA-1000, BANGLADESH
MAY, 2014**

The thesis titled “Effect of coarse aggregate porosity on the compressive behavior of concrete after high temperature episodes”, Submitted by: Md. Syied Mahbub Morshed, Student ID no : 0409042308 P, Session: April’ 2009; has been accepted as satisfactory in partial fulfillment of the requirements for the degree of Master of Engineering in Civil Engineering (Structural) on May 26, 2014.

BOARD OF EXAMINERS

Dr. A. F. M. Saiful Amin
Professor
Department of Civil Engineering
BUET, Dhaka

Chairman
(Supervisor)

Dr. Syed Ishtiaq Ahmed
Professor
Department of Civil Engineering
BUET, Dhaka

Member

Dr. Mohammad Al Amin Siddique
Assistant Professor
Department of Civil Engineering
BUET, Dhaka

Member

TO
ABU ASRAR SAURAV

DECLARATION

It is hereby declared that, except where specific references are made, the work embodied in this thesis is the result of investigation carried out by the author under the supervision of Dr. A. F. M. Saiful Amin, Professor, Department of Civil Engineering, BUET.

Neither this thesis nor any part of it is concurrently submitted to any other institution in candidature for any degree.

Md. Syied Mahbub Morshed

ACKNOWLEDGEMENT

It is indeed a great pleasure and also a great privilege for me to express my deepest gratitude to Dr. A.F.M. Saiful Amin, Professor, Department of Civil Engineering, BUET for his constant guidance and continuous encouragements to carry out the research. His untiring efforts, great patience and keen interest to work contained in this report into the new areas of research have made this work real and exciting. His invaluable suggestions and arrangement of wonderful research facilities will always be remembered.

Many thanks go to Mr. Nafis Fuad, Ms. Pauline Laila Bela and Ms. Rokeya Sharmin, students of undergraduate, Department of Civil Engineering, BUET, for their continuous assistance throughout the research work. I remember Mr. Abu Asrar Saurav, student of Department of Civil Engineering, BUET, he assisted me during experiment works along with other three but left us forever before finishing this work.

The author would like to express his gratefulness to Mr. Abdul Mozid Shikder, Additional Chief Engineer (Retd.), Public Works Department (PWD) for his inspiration and support.

I would like to acknowledge his thanks to the staffs and technicians of Concrete Laboratory and Structural Mechanics Laboratory, Department Civil Engineering, BUET for their cooperation. Special thanks go to Mr. Jafor Iqbal, Senior Craft Instructor, Foundry Shop, BUET for the technical help in constructing the electric furnace. The cooperation indeed made our work away from classical ones.

Finally, the author would like to thank all of his family members, friends, colleagues and well wishers for their encouragement and help.

Concrete loses strength when exposed to high temperature. The thermo-chemo-rheological processes that take place within the concrete matrix at high temperature not only produce gaseous matters and vapors but may also bring concrete to a new chemical composition. Pressure built-up within concrete matrix due to formation of gases often leads to cracking and eventual spalling of concrete. However, built-up pressure responsible for concrete spalling should be directly related to the extent of permeable pores within the concrete matrix. Thus, damage due to temperature episodes should be different in concretes having different porosities. In general, concretes of higher strengths are known to be less porous. Furthermore, brick aggregate concretes are generally more porous than stone aggregate concretes. The porosities of recycled concrete fall in between. However, there is no information based on a systematic study on strength losses for these fundamental cases. The present work is motivated to characterize the effect of coarse aggregate porosity and concrete porosity on the strength loss after different thermal episodes.

Concrete having 10 MPa, 20 MPa and 35 MPa made of four types of coarse aggregates having different absorption capacities (0.8%-14.4%) were tested for compressive strengths after heat treatments at a purpose built electrical furnace. Four different heating paths having fast to gradually slower heating rates were used. Heating paths were so chosen that to reach at 600°C temperature at one step, at two steps and at three steps. Variation in heating paths was found to have significant effect on loss of compressive strength after episodes of heat treatment. Absorption capacities of concrete (5.58% - 31.19%) were measured. Losses of masses at different stages of heat treatment were also measured.

It is seen that compressive strength loss is generally proportional to the temperature and heating rate for a given aggregate porosity. Strength loss was found to be proportional to parent concrete strength. A conspicuous decrease of strength loss with increase in heat input keeping maximum temperature of heating path at a constant value has been well resolved. Statistical significance gathered from test data out of 384 specimens were generally noted to be higher for slower heating rates and larger porosities. Concrete with coarse aggregate porosity between 3% to 8% and concrete porosity between 10% to 20% were found to be most susceptible to strength loss due to high temperature events.

CONTENTS

| | Page |
|--|-----------|
| DECLARATION | v |
| ACKNOWLEDGEMENT | vi |
| ABSTRACT | vii |
| CONTENTS | viii |
| LIST OF TABLES | xi |
| LIST OF FIGURES | xii |
| | |
| Chapter 1 | |
| INTRODUCTION | 1 |
| 1.1 General | 1 |
| 1.2 Background and present state of the problem | 2 |
| 1.2.1 General | 2 |
| 1.2.2 International status | 5 |
| 1.2.3 Bangladesh status | 6 |
| 1.3 Objectives with specific aims | 7 |
| 1.4 Possible outcome | 8 |
| 1.5 General methodology and experimental plan | 8 |
| | |
| Chapter 2 | |
| LITERATURE REVIEW | 12 |
| 2.1 General | |
| 2.2 Physical properties of hardened concrete | 12 |
| 2.2.1 Compressive strength | 12 |
| 2.2.2 Thermal expansion | 13 |
| 2.2.3 Thermal conductivity | 14 |
| 2.2.4 Specific heat | 14 |
| 2.2.5 Fire resistance | 15 |
| 2.2.6 Aging of concrete | 17 |
| 2.3 Responses of concrete to high temperatures | 18 |
| 2.3.1 Physical and chemical responses of concrete to fire | 17 |
| 2.3.2 Effects of elevated temperature on Ordinary Portland Cement concrete materials | 21 |
| 2.4 Damage mechanisms of concrete under high temperatures | 23 |
| 2.4.1 Phase transformations in cement paste | 24 |
| 2.4.2 Phase transformations taking place in aggregate | 25 |
| 2.4.3 Thermal incompatibility between cement paste and aggregate | 25 |

| | Page |
|--|-----------|
| 2.4.4 Spalling | 25 |
| 2.5 Loss of strength of concrete in fire | 28 |
| 2.6 Cracking | 29 |
| Chapter 3 MATERIALS AND EQUIPMENTS | 31 |
| 3.1 General | 31 |
| 3.2 Properties of concrete | 31 |
| 3.2.1 Ordinary Portland cement | 31 |
| 3.2.2 Aggregates | 31 |
| 3.2.3 Water | 36 |
| 3.3 Equipments used for casting of concrete | 37 |
| 3.3.1 Mould | 37 |
| 3.3.2 Vibrator | 37 |
| 3.3.3 Compressive strength testing machine | 37 |
| 3.3.4 Sieves | 38 |
| 3.3.5 Sieve shaker | 39 |
| 3.4 Mix design | 39 |
| 3.5 Heating in gas furnace | 39 |
| 3.5.1 Problems and reasons for abandoning gas furnace | 40 |
| 3.5.2 Infrared thermometer | 41 |
| 3.6 Electric furnace | 41 |
| 3.6.1 Materials | 43 |
| 3.6.2 Design | 44 |
| 3.6.3 Construction of furnace | 44 |
| Chapter 4 LABORATORY PROCEDURE AND DATA ACQUISITION | 46 |
| 4.1 Casting of concrete cylinders | 46 |
| 4.1.1 Preparation of materials | 46 |
| 4.2 Heat treatment in electric furnace | 48 |
| 4.3 Strength testing of concrete cylinders | 49 |
| 4.4 Correction of strength | 49 |
| 4.5 Estimation of porosity | 51 |
| 4.6 Estimation of heat input | 52 |
| Chapter 5 RESULTS AND DISCUSSION | 53 |
| 5.1 General | 53 |
| 5.2 Effect of temperature on compressive strength | 53 |
| 5.2.1 Compressive strength loss (%) at different temperatures and heating paths | 54 |
| 5.2.2 Compressive strength loss (%) of different types of concrete with respect to different heat inputs | 61 |

| | Page |
|--|-----------|
| 5.2.3 Compressive strength loss (%) at 600°C with respect to coarse aggregate porosity at different heating paths | 65 |
| 5.2.4 Compressive strength loss (%) at 600°C with respect to concrete porosity at different heating paths | 68 |
| 5.2.5 Residual compressive strength at different temperatures and heating paths | 72 |
| 5.2.6 Mass loss (%) at 600°C with respect to coarse aggregate porosity and concrete porosity for different types of concrete | 79 |
| 5.2.7 Mass loss (%) at different temperatures for different types of concrete at different heating paths | 81 |
| Chapter 6 CONCLUSIONS | 88 |
| 6.1 General | 88 |
| 6.2 Effect of strength | 88 |
| 6.3 Effect of heating rate | 88 |
| 6.4 Effect of aggregate | 89 |
| 6.5 Scope for future studies | 90 |
| REFERENCES | 91 |
| APPENDICES | |
| Appendix A | 97 |
| A.1 Sample of collected compressive strength data | 97 |
| A.2 Sample of collected mass loss data | 98 |
| A.3 Concrete porosity and coarse aggregate porosity | 99 |
| A.4 Mass loss data | 99 |
| A.5 Residual compressive strength data | 102 |
| A.6 Compressive strength loss data | 104 |
| A.7 Summary of mix design | 106 |
| A.8 Sample calculation of porosity | 106 |
| A.9 Summary of age of concrete | 107 |
| A.10 Sample calculation of heat input | 107 |
| A.11 Summary of estimation of heat input | 108 |
| Appendix B | 109 |
| B.1 Fire incidents and losses in Bangladesh | 109 |
| B.1.1 Standard Garments Ltd., Konabari, Gazipur | 109 |
| B.1.2 Tazreen Fashion Factory in Ashulia | 110 |

| | Page |
|--|------|
| B.1.3 Fire in Chemical Factory, Dhaka | 110 |
| B.1.4 Ha-Meem Group in Ashulia | 111 |
| B.1.5 Fire in Shoe Factory, Dhaka | 112 |
| B.2 Fire incidents around the world | 112 |
| B.2.1 Hotel Roosevelt Fire, USA | 112 |
| B.2.2 Fire at the Ozone Disco Club in Quezon City, Philippine | 114 |
| B.2.3 Kader Toy Factory Fire, Thailand | 114 |
| B.2.4 2010 Shanghai Fire , China | 115 |
| B.2.5 Santiago Prison Fire, Chile | 116 |
| Appendix C Photographs of materials and activities | 117 |

LIST OF TABLES

| | Page | |
|------------|--|-----|
| Table 1.1 | Experiment plan | 10 |
| Table 2.1 | Coefficients of thermal expansion of coarse aggregate and concrete | 13 |
| Table 3.1 | Properties of coarse aggregates | 32 |
| Table 3.2 | Mix proportions of coarse aggregates | 33 |
| Table 3.3 | Properties of fine aggregate | 35 |
| Table 3.4 | Sieve numbers and openings | 38 |
| Table 4.1 | Porosity in coarse aggregates | 51 |
| Table 4.2 | Porosity in concrete | 52 |
| Table A.1 | Sample of collected compressive strength data | 97 |
| Table A.2 | Sample of collected mass loss data | 98 |
| Table A.3 | Concrete porosity and aggregate porosity | 99 |
| Table A.4 | Mass loss data | 99 |
| Table A.5 | Residual compressive strength data | 102 |
| Table A.6 | Compressive strength loss data | 104 |
| Table A.7 | Summary of mix design | 106 |
| Table A.9 | Summary of age of concrete | 107 |
| Table A.11 | Summary of estimation of heat input | 108 |

LIST OF FIGURES

| | Page | |
|-------------|--|----|
| Figure 1.1 | Fire triangle | 1 |
| Figure 1.2 | Schematic representation of concrete matrix | 4 |
| Figure 1.3 | Schematic representation of the heating paths | 11 |
| Figure 2.1 | The effect of temperature on compressive strength of high-strength concrete according to Eurocode 2 | 16 |
| Figure 2.2 | The concrete composite | 18 |
| Figure 2.3 | Different types of water in concrete | 19 |
| Figure 2.4 | a) Color of concrete before fire b) Color of concrete after fire | 21 |
| Figure 2.5 | View of a spall on a fire-damaged concrete slab soffit | 26 |
| Figure 2.6 | Interior column spalling | 27 |
| Figure 2.7 | Cracking in the proximity of column | 30 |
| Figure 2.8 | Longitudinal cracking in column | 30 |
| Figure 3.1 | Types of coarse aggregate used in the research | 33 |
| Figure 3.2 | Sand as fine aggregate | 35 |
| Figure 3.3 | Grain size distribution for fine aggregate (Sand) | 36 |
| Figure 3.4 | Gas furnace | 40 |
| Figure 3.5 | Infrared thermometer | 41 |
| Figure 3.6 | Electric furnace and temperature control unit | 42 |
| Figure 3.7 | Electric furnace back and front view | 42 |
| Figure 3.8 | Materials used for constructing electric furnace | 43 |
| Figure 3.9 | Design of electric furnace | 44 |
| Figure 3.10 | Construction of electric furnace | 45 |
| Figure 4.1 | Concrete being heated in furnace | 48 |
| Figure 4.2 | Concrete after burning in furnace and testing | 49 |
| Figure 4.3 | Effect of age on compressive strength | 50 |
| Figure 5.1 | Compressive strength loss (%) at different temperatures and heating paths for all types of concrete. | 54 |
| Figure 5.2 | Compressive strength loss (%) at different temperatures and heating paths for S10 concrete | 55 |
| Figure 5.3 | Compressive strength loss (%) at different temperatures and heating paths for S20 concrete | 55 |
| Figure 5.4 | Compressive strength loss (%) at different temperatures and heating paths for S35 concrete | 56 |

| | Page | |
|-------------|---|----|
| Figure 5.5 | Compressive strength loss (%) at different temperatures and heating paths for B10 concrete | 56 |
| Figure 5.6 | Compressive strength loss (%) at different temperatures and heating paths for B20 concrete | 57 |
| Figure 5.7 | Compressive strength loss (%) at different temperatures and heating paths for B35 concrete. | 57 |
| Figure 5.8 | Compressive strength loss (%) at different temperatures and heating paths for RS10 concrete. | 58 |
| Figure 5.9 | Compressive strength loss (%) at different temperatures and heating paths for RS20 concrete. | 58 |
| Figure 5.10 | Compressive strength loss (%) at different temperatures and heating paths for RS35 concrete | 59 |
| Figure 5.11 | Compressive strength loss (%) at different temperatures and heating paths for RB10 concrete | 59 |
| Figure 5.12 | Compressive strength loss (%) at different temperatures and heating paths for RB20 concrete | 60 |
| Figure 5.13 | Compressive strength loss (%) at different temperatures and heating paths for RB35 concrete | 60 |
| Figure 5.14 | Compressive strength loss (%) at 600° C with respect to different heat inputs for all types of concrete. | 61 |
| Figure 5.15 | Compressive strength loss (%) at 600° C of 10 MPa concrete (all aggregate). | 62 |
| Figure 5.16 | Compressive strength loss (%) at 600° C of 20 MPa concrete (all aggregate). | 62 |
| Figure 5.17 | Compressive strength loss (%) at 600° C of 35 MPa concrete (all aggregate). | 63 |
| Figure 5.18 | Compressive strength loss (%) at 600° C of concrete of stone aggregate (all strength) | 63 |
| Figure 5.19 | Compressive strength loss (%) of concrete of brick aggregate (all strength) | 64 |
| Figure 5.20 | Compressive strength loss (%) of concrete of recycle brick aggregate (all strength) | 64 |
| Figure 5.21 | Compressive strength loss (%) of concrete of recycle stone aggregate (all strength) | 65 |
| Figure 5.22 | Compressive strength loss (%) at 600° C with respect to coarse aggregate porosity at different heating paths for all types of concrete. | 66 |
| Figure 5.23 | Compressive strength loss (%) at 600° C with respect to coarse aggregate porosity for 10 MPa concrete at different heating paths. | 66 |

| | Page | |
|-------------|---|----|
| Figure 5.24 | Compressive strength loss (%) at 600° C with respect to coarse aggregate porosity for 20 MPa concrete at different heating paths. | 67 |
| Figure 5.25 | Compressive strength loss (%) at 600° C with respect to coarse aggregate porosity for 35 MPa concrete at different heating paths. | 67 |
| Figure 5.26 | Compressive strength loss (%) at 600° C with respect to concrete porosity for all types of concrete. | 68 |
| Figure 5.27 | Compressive strength loss (%) at 600° C with respect to concrete porosity for 10 MPa concrete at different heating paths. | 69 |
| Figure 5.28 | Compressive strength loss (%) at 600° C with respect to concrete porosity for 20 MPa concrete at different heating paths. | 69 |
| Figure 5.29 | Compressive strength loss (%) at 600° C with respect to concrete porosity for 35 MPa concrete at different heating paths. | 70 |
| Figure 5.30 | Compressive strength loss (%) at 600° C for stone aggregate concrete at different heating paths. | 70 |
| Figure 5.31 | Compressive strength loss (%) at 600° C for brick aggregate concrete at different heating paths. | 71 |
| Figure 5.32 | Compressive strength loss (%) at 600° C for recycled brick aggregate concrete at different heating paths. | 71 |
| Figure 5.33 | Compressive strength loss (%) at 600° C for recycled stone aggregate concrete at different heating paths. | 72 |
| Figure 5.34 | Residual compressive strength at different heating path for S10 concrete | 73 |
| Figure 5.35 | Residual Compressive Strength at different Heating Path for S20 concrete | 73 |
| Figure 5.36 | Residual Compressive Strength at different Heating Path for S35 concrete | 74 |
| Figure 5.37 | Residual Compressive Strength at different Heating Path for RS10 concrete | 74 |
| Figure 5.38 | Residual Compressive Strength at different Heating Path for RS20 concrete | 75 |
| Figure 5.39 | Residual Compressive Strength at different Heating Path for RS35 concrete | 75 |
| Figure 5.40 | Residual Compressive Strength at different Heating Path for B10 concrete | 76 |
| Figure 5.41 | Residual Compressive Strength at different Heating Path for B20 concrete | 76 |

| | Page |
|---|------|
| Figure 5.42 Residual Compressive Strength at different Heating Path for B35 concrete | 77 |
| Figure 5.43 Residual Compressive Strength at different Heating Path for RB10 concrete | 77 |
| Figure 5.44 Residual Compressive Strength at different Heating Path for RB20 concrete | 78 |
| Figure 5.45 Residual Compressive Strength at different Heating Path for RB35 concrete | 78 |
| Figure 5.46 Mass loss (%) at 600° C with respect to coarse aggregate porosity for all types of concrete. | 79 |
| Figure 5.47 Mass loss (%) at 600° C with respect to concrete porosity for all types of concrete. | 80 |
| Figure 5.48 Mass loss (%) at 600° C with respect to coarse aggregate porosity at different heating paths for all types of concrete. | 80 |
| Figure 5.49 Mass loss (%) at 600° C with respect to concrete porosity at different heating paths for all types of concrete. | 81 |
| Figure 5.50 Mass loss (%) at different temperatures and different heating paths for S10 concrete. | 82 |
| Figure 5.51 Mass loss (%) at different temperatures and different heating paths for S20 concrete. | 82 |
| Figure 5.52 Mass loss (%) at different temperatures and different heating paths for S35 concrete. | 83 |
| Figure 5.53 Mass loss (%) at different temperatures and different heating paths for RS10 concrete. | 83 |
| Figure 5.54 Mass loss (%) at different temperatures and different heating paths for RS20 concrete. | 84 |
| Figure 5.55 Mass loss (%) at different temperatures and different heating paths for RS35 concrete. | 84 |
| Figure 5.56 Mass loss (%) at different temperatures and different heating paths for B10 concrete. | 85 |
| Figure 5.57 Mass loss (%) at different temperatures and different heating paths for B20 concrete. | 85 |
| Figure 5.58 Mass loss (%) at different temperatures and different heating paths for B35 concrete. | 86 |
| Figure 5.59 Mass loss (%) at different temperatures and different heating paths for RB10 concrete. | 86 |
| Figure 5.60 Mass loss (%) at different temperatures and different heating paths for RB20 concrete. | 87 |
| Figure 5.61 Mass loss (%) at different temperatures and different heating paths for RB35 concrete. | 87 |

| | Page | |
|-------------|--|-----|
| Figure B.1 | Fire incident in Standard Garments Ltd | 109 |
| Figure B.2 | Fire incident in Tazreen fashion factory, Ashulia | 110 |
| Figure B.3 | Fire incident in a chemical factory, Old Dhaka | 111 |
| Figure B.4 | Fire hazard in Ha-Meem group, Ashulia | 112 |
| Figure B.5 | Hotel Roosevelt fire incident, Florida | 113 |
| Figure B.6 | Fire incident in the Ozone disco club in Quezon city, Philippines | 114 |
| Figure B.7 | Shanghai fire, China | 115 |
| Figure B.8 | Santiago prison fire, Chile | 116 |
| Figure C.1 | Stone aggregate | 117 |
| Figure C.2 | Brick aggregate | 117 |
| Figure C.3 | Recycled brick aggregate | 118 |
| Figure C.4 | Recycled stone aggregate | 118 |
| Figure C.5 | Sylhet sand | 119 |
| Figure C.6 | Cement | 119 |
| Figure C.7 | Water | 120 |
| Figure C.8 | Fresh cast concrete | 120 |
| Figure C.9 | Compaction of concrete sample | 121 |
| Figure C.10 | Hammering | 121 |
| Figure C.11 | Numbering of sample | 122 |
| Figure C.12 | Sample of concrete cylinder | 122 |
| Figure C.13 | Curing of sample | 123 |
| Figure C.14 | Burning of sample | 123 |
| Figure C.15 | Crushing strength test | 124 |
| Figure C.16 | Failure pattern after testing | 124 |

1.1 GENERAL

Concrete is one of the most important construction material used in the construction of high rise buildings and special structures for long time. Concrete is specified in building and civil engineering projects for several considerations including life cycle cost and architectural appearance. Historically, the fire performance of concrete as a building material has not been emphasized due to its non-combustible nature and ability to function as a thermal barrier, preventing heat and fire to spread. However, heating temperature, duration and stages of exposure to high temperatures in practical fire occurrences differ a lot from the ideal ones. In a real fire incident, initially fire can grow very fast at a rapid heating rate, sometimes even very slow. At times, heat may build up within the structure at different stages. The attained temperature during fire mostly depends on the rate of combustion, fuel and access to oxygen (Figure 1.1). Both of these conditions can impose additional stresses on concrete.



Figure 1.1 Fire triangle

At high temperature, the properties of concrete changes from the designed ones. After a fire, changes in the structural properties of concrete do not reverse themselves. Irreversible transformations changes in the physical and chemical properties of the

cement itself. It has been found that, the strength properties of a concrete structure can be considerably deteriorated after a fire, even if there is no visible sign of damage.

After high temperature episodes cracks are seen to develop in concrete that lead to eventual loss of structural integrity and shortening of service life. Hence, it is important to understand the change in the concrete properties after various temperature exposures. When concrete is used in buildings as the construction material, structural members must be designed to satisfy appropriate fire resistance requirements in addition to load carrying requirements to ensure that, when other measures of controlling the fire fail, structural integrity is the last line of defense.

1.2 BACKGROUND AND PRESENT STATE OF THE PROBLEM

1.2.1 General

The versatility of concrete in construction owes much to its flexibility in using local aggregates for attaining the design strength. However, the local aggregates of different geological origins diverge in respective physical properties. Furthermore, brick aggregates are known to be of lower unit weight and high absorption capacity than stone aggregates. In contrast, the gel spaces of high strength concrete usually have larger densities. Thus, high strength concrete with a particular aggregate type tend to have lower porosities than low strength ones. Concrete subjected to high temperature loses weight due to release vapor and other gaseous matters as a result of temperature actuated physicochemical events occurring within the solid matrix. The composition of gaseous matters so released depends on the chemo-rheological composition of concrete and respective phase transition events. This formation of gases cause a built-up stress within the concrete itself which results in cracks in concrete or spalling which eventually reduces strength. In these events, the concrete with larger porosities releases the gaseous matters more easily than other ones and therefore offer better performances of concrete under fire. The extent of damage in strength is higher for the concrete with lesser porosities as those have lesser ability to readily release the vapors and gases.

Concrete may experience unexpected fire events that may induce thermal episodes during its life time to change its strength properties. Three distinct aspects, namely density/porosity/absorption capacity, bound moisture content and chemical composition of major components, namely aggregates and cement affect the performance of concrete at an elevated temperature. Furthermore, the scale of temperature, heating rate and duration govern the event. Nevertheless, the thermal resistance properties of concrete depend much on the properties of coarse aggregates that generally occupy 70% to 80% of the concrete volume. In Bangladesh, brick aggregate concrete is common due to low cost, local availability and being used historically for long time (Akhteruzzaman et al. 1983). Use of stone aggregate is also more common in producing concrete of higher strength requirements. Demolition of old concrete buildings and other structures produce, however, a huge quantity of waste concrete of each type. Due to lack of sources of natural aggregate, recycled concrete or crushed waste concrete is now considered to be an alternate source of aggregates. Brick aggregate, recycled stone aggregate and recycled brick aggregate have higher porosity and absorption capacity than stone aggregate. The absorption capacities of these aggregates vary in between 1% to 15%. Stone aggregate, brick aggregate, recycled stone aggregate, and recycled brick aggregate have different physical properties, in terms of strength, absorption capacity, porosity, modulus of elasticity, Poisson's ratio and unit weight. Eventually, these aggregates invariably have the important effect on the behavior of concrete after high temperature episodes. Porous aggregate contain larger amount of moisture and it may be trapped or bound in concrete. During fire, bound water become vaporized and creates excessive pore pressure inside concrete and has the potential to spall the concrete (Figure 1.2). These effects can vary with the changes of the grade of strength of warranted concrete.

There are a number of physical and chemical changes which occur in concrete subjected to heat. Among these there are changes both reversible and non-reversible upon cooling. The irreversible one can significantly weaken the concrete structure.

Numerous studies on the behavior of different types of concrete have been performed under different fire exposure conditions, experimentally from small to big scale full systems testing or by mathematical modeling. Unfortunately, the exact mechanisms

controlling the behavior of concrete in fire exposure have still not been understood fully and this is due to the complexity of parameters that play a role in the events. Each of these parameters has a different response to thermal exposures in itself, and thus the behavior of the composite system is even more complex to define or model. Still today, experimental results are the only reliable way of assessing the fire resistance of concrete. The effect of these uncertainties in the thermal response can be understood by extensive testing, mostly based on standard heating curves and presented as a “fire resistance” time, typically a function of thickness or cover, for different types of concrete (Fletcher et al., 2007; Pimienta et al. 2010).

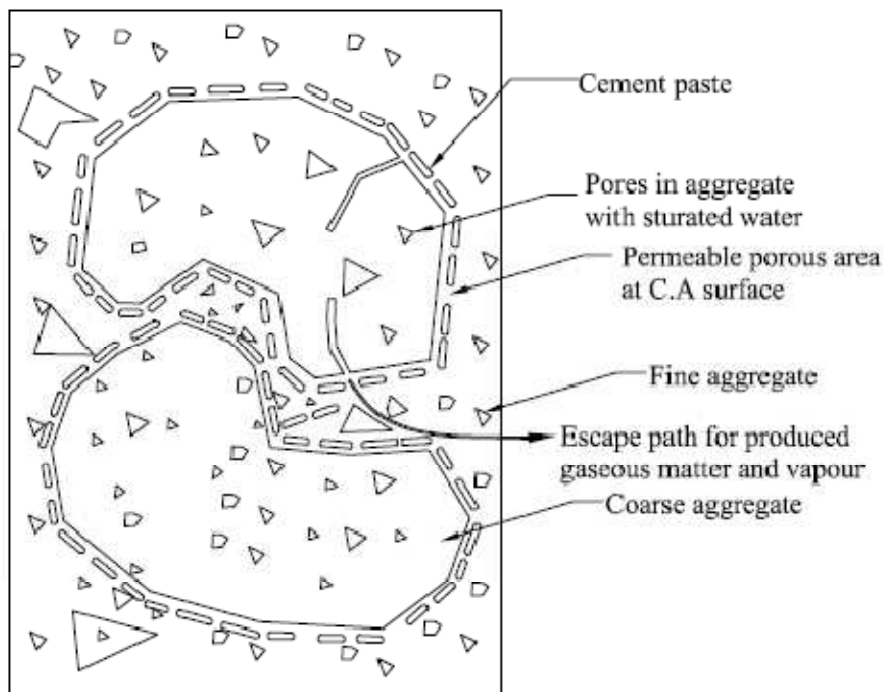


Figure 1.2 Schematic representation of concrete matrix

In the past, substantial laboratory tests were conducted to evaluate the behavior of high strength stone aggregate concrete under elevated temperature. These pioneering works suggest decreases in residual compressive strength, split tensile strength and shear strength after high temperature episodes. On the other hand, a few results show distinct increase in compressive strength of concrete with laterite soil as partially or wholly substituting fine aggregates after exposure to high temperature (Ikponmwosa, et al., 2010). However, such information on concrete of lower strengths and higher

porosities, for example brick aggregate concrete are not much known. Furthermore, the concretes with the recycled aggregates were not studied in the past for high temperature effect. This limits our ability in assessment of residual strength of concrete structures after a fire incident but indicates the necessity of conducting fundamental research in this area to evaluate and predict the performance of the concrete after elevated temperature episodes. Therefore, it is also important to compare the thermal behavior of concrete with different strength and different porosities to understand the effect of high temperature on the physical properties of concrete with different types of coarse aggregates.

The concrete with stone aggregate was extensively studied in the past for high temperature effect. However, the behavior of concretes with the other three aggregate types has not been under such extensive study in the past. This limits the evaluation of residual strength in concrete buildings made of local aggregate after a fire incident. So there exists the necessity of conducting fundamental research in this area to evaluate and predict the performance of the concrete after elevated temperature episodes.

1.2.2 International status

In the past two decades, a significant amount of research has been conducted into the performance of composite steel frame structures in fire. For reinforced concrete structures, the research of fire resistance of the structures was started in early 1970 and mainly focused on the behavior of isolated members. In terms of reinforced concrete construction, design is still based on simplistic methods which have been developed from standard fire tests that do not necessarily represent real building behavior. In current design codes, such as *Eurocode* more advanced computer modeling methods are allowed.

A study of 16 industrialized nations (13 in Europe plus the USA, Canada and Japan) found that, in a typical year, the number of people killed by fires was 1 to 2 per 100,000 inhabitants and the total cost of fire damage amounted to 0.2% to 0.3% of Gross National Product. In USA specifically, statistics collected by the National Fire

Protection Association for the year 2000 showed that more than 4,000 deaths, over 100,000 injuries and more than \$10bn of property damage were caused by fire. UK statistics suggest that of the half a million fires per annum attended by firefighters, about one third occur in occupied buildings and these result in around 600 fatalities (almost all of which happen in dwellings). The loss of business resulting from fires in commercial and office buildings runs into millions of pounds each year. One of the most significant changes in the field of fire-protection engineering in the last 20 years has been the introduction of the performance based design. Historically, concrete structures and systems in regards to fire have been designed based on a set of prescriptive codes and standards where the performance values are provided for in tables or through a series of simplistic mathematical equations. Design criteria have been based on the results of testing to “standard” fire exposures, typically expressed in terms of required reinforcement cover. Performance-based design utilizes engineering design to achieve a specified fire-protection goal for a whole building system (*Appendix B*).

1.2.3 Bangladesh status

Bangladesh is the most densely populated country (With population above 150 million) in the world. But till now there is no facility with adequate provisions for fire situations in Bangladesh. So, if fire occurs it will create serious damage to the infrastructure of our country. In 2012, there occurs serious fire incident to the *Tazreen fashion factory* in Ashulia for the lacking of the fire escape and fighting facility. At least 124 people were killed in the fire and at least 200 were injured. The fire caused by an electrical short circuit, started on the ground floor of the nine-story building. Because of the large amount of fabrics and yarn in the factory, the fire quickly spread to the other floors, which complicates the fire fighting operations. It is worst ever fire incident in Bangladesh’s history (*Appendix B*).

To predict the fire performance of the concrete made of local materials, this research will be useful.

In view of above, there is urgent need to take following measures:

- i. Proper utilization of fire frightening facility & improve the existing facility.
- ii. National level support on research studies on fire performance.
- iii. Arrange proper fire structure facility to minimize its effect.
- iv. Formulation of guidelines, specifications and provisions.
- v. Provisions of list of experts available in this field who can supply knowledge and information in this topic.
- vi. Preparation of techno-financial regime, financial support for introducing fire existing system in construction.
- vii. Gathering much knowledge on residual strength of concrete.

1.3 OBJECTIVES WITH SPECIFIC AIMS

This research aims to study the changes in the compressive strength properties of concrete after thermal episodes. the following objectives are intended to be met:

- i) To produce high strength concrete (35 MPa), moderate strength concrete (20 MPa) and low strength concrete (10 MPa) using stone aggregates, brick aggregates, recycled stone aggregates and recycled brick aggregates.
- ii) To obtain fundamental data on loss of compressive strength due to high temperature exposures for four types of concrete having different strengths.
- iii) To study the effect of sustained high temperature on compressive strength and weight loss with respect to porosity of coarse aggregate and concrete.
- iv) To determine loss of weight due to high temperature exposures for four types of concrete.

1.4 POSSIBLE OUTCOME

The outcome of the study will be to ascertain the changes in properties of different types of concrete after different temperature episodes. Relation of loss of strength with porosity, total heat input and rate of heating will be understood. Such information will be much relevant in the evaluation of concrete structures after a thermal event. General suggestion could be made for the use of concrete as a building material aimed at better performance in fire occurrence.

1.5 GENERAL METHODOLOGY AND EXPERIMENTAL PLAN

Basic thermal properties of concrete for different aggregates are reviewed. Concrete of three strength grades having 10 MPa (1450 psi), 20 MPa (2900 psi) and 35 MPa (5075 psi) compressive strength, following BS 5328 mix design method and confirming concrete cylinder from trial mixes, were produced using four types of coarse aggregates such as crushed stone aggregate (S), crushed brick aggregate (B), recycled stone aggregate (RS) and recycled brick aggregate (RB) having same gradation conforming BS 882-1992. Mix ratio, water cement ratio, and other component of concrete were determined by mix design for each strength grade of concrete before the experiment with BRE (Building Research Establishment) manual. Crushed stone and brick aggregate was collected from nearest available place of Dhaka city and recycled stone and recycled brick aggregates was used from ready stock of Concrete Laboratory, Department of Civil Engineering, BUET. Ordinary Portland cement/CEM-I conforming BS 12-1996, Sylhet sand of F.M. 2.5 and no admixture were used to produce the plain concrete. Physical properties of aggregates especially, specific gravity, absorption capacity and unit weight were determined. Proper specimen identification mark was used. 384 nos. cylindrical specimens (100mm dia. and 200 mm height) of all four types of plain concrete were cast and cured for 28 days by ponding of water. Then the specimens were brought out from water and took weight in saturated and surface-dry (SSD) condition. After that the specimens were allowed to air dry under shed in room temperature until those were burnt in a custom made high temperature electric furnace. The electric furnace having

the facility to control heating rate using a digital device was used delivering a uniformly distributed thermal load to the specimens. Heating in gas furnace was not considered as uniformly heating could not be ensured. In this electric furnace, temperature can be controlled up to 1000^o C with a tolerance of $\pm 5^{\circ}$ C. The temperature can be observed from the digital screen.

The specimens were divided into ninety six groups, four in each group, as planned for heat treatment under different temperature following four heating paths in an electric furnace shown in Table 1.1. PATH 1, temperature monotonically increased to 200^o C, 400^o C, and 600^o C in each case and specimens were heated under that for 5 hours separately (Figure 1.3). PATH 2, was stepped increased; first temperature was increased to 200^o C and allowed it to remain constant for 5 hours then increased to 600^o C and allowed it again to remain constant for 5 hours. PATH 3, was stepped increased; first temperature was increased to 400^o C and maintained constant for 5 hours then increased to 600^o C and maintained constant for 5 hours again. PATH 4, was stepped increased; first temperature was increased to 200^o C, allowed it to remain constant for 5 hours then increased to 400^o C again allowed it to remain constant for 5 hours, finally increased to 600^o C and allowed it again to remain constant for 5 hours. Weights of all specimens were taken before and after heat treatment. Testing of cylindrical specimens for measuring compressive strength and dilation behavior were done before and after heat treatment. Synthesis of all data obtained from the experiments was done and finally some results, recommendations and conclusions were made about the behavior of different types of concrete under elevated temperatures.

Table 1.1 Experiment plan

| Strength of concrete | Type of coarse aggregate | Number of specimen to be tested after temperature episodes | | | | | | | | | | | | Total number of specimens | |
|---------------------------|--------------------------|--|--------------------|--------------------|--------------------|--------------------|--------------------|--------------------|--------------------|--------------------|--------------------|--------------------|--------------------|---------------------------|--------------------|
| | | Room Temp. | Heating | | | Heating | | | Heating | | | Heating | | | |
| | | | PATH 1 | | | PATH 2 | | | PATH 3 | | | PATH 4 | | | |
| | | | 200 ^o C | 400 ^o C | 600 ^o C | 200 ^o C | 400 ^o C | 600 ^o C | 200 ^o C | 400 ^o C | 600 ^o C | 200 ^o C | 400 ^o C | | 600 ^o C |
| 10 MPa (1450 psi) | S | 4 | 4 | 4 | 4 | - | - | 4 | - | - | 4 | - | 4 | 4 | 32 |
| | B | 4 | 4 | 4 | 4 | - | - | 4 | - | - | 4 | - | 4 | 4 | 32 |
| | RS | 4 | 4 | 4 | 4 | - | - | 4 | - | - | 4 | - | 4 | 4 | 32 |
| | RB | 4 | 4 | 4 | 4 | - | - | 4 | - | - | 4 | - | 4 | 4 | 32 |
| 20 MPa (2900 psi) | S | 4 | 4 | 4 | 4 | - | - | 4 | - | - | 4 | - | 4 | 4 | 32 |
| | B | 4 | 4 | 4 | 4 | - | - | 4 | - | - | 4 | - | 4 | 4 | 32 |
| | RS | 4 | 4 | 4 | 4 | - | - | 4 | - | - | 4 | - | 4 | 4 | 32 |
| | RB | 4 | 4 | 4 | 4 | - | - | 4 | - | - | 4 | - | 4 | 4 | 32 |
| 35 MPa (5075 psi) | S | 4 | 4 | 4 | 4 | - | - | 4 | - | - | 4 | - | 4 | 4 | 32 |
| | B | 4 | 4 | 4 | 4 | - | - | 4 | - | - | 4 | - | 4 | 4 | 32 |
| | RS | 4 | 4 | 4 | 4 | - | - | 4 | - | - | 4 | - | 4 | 4 | 32 |
| | RB | 4 | 4 | 4 | 4 | - | - | 4 | - | - | 4 | - | 4 | 4 | 32 |
| Total number of specimens | | 48 | 48 | 48 | 48 | - | - | 48 | - | - | 48 | - | 48 | 48 | 384 |

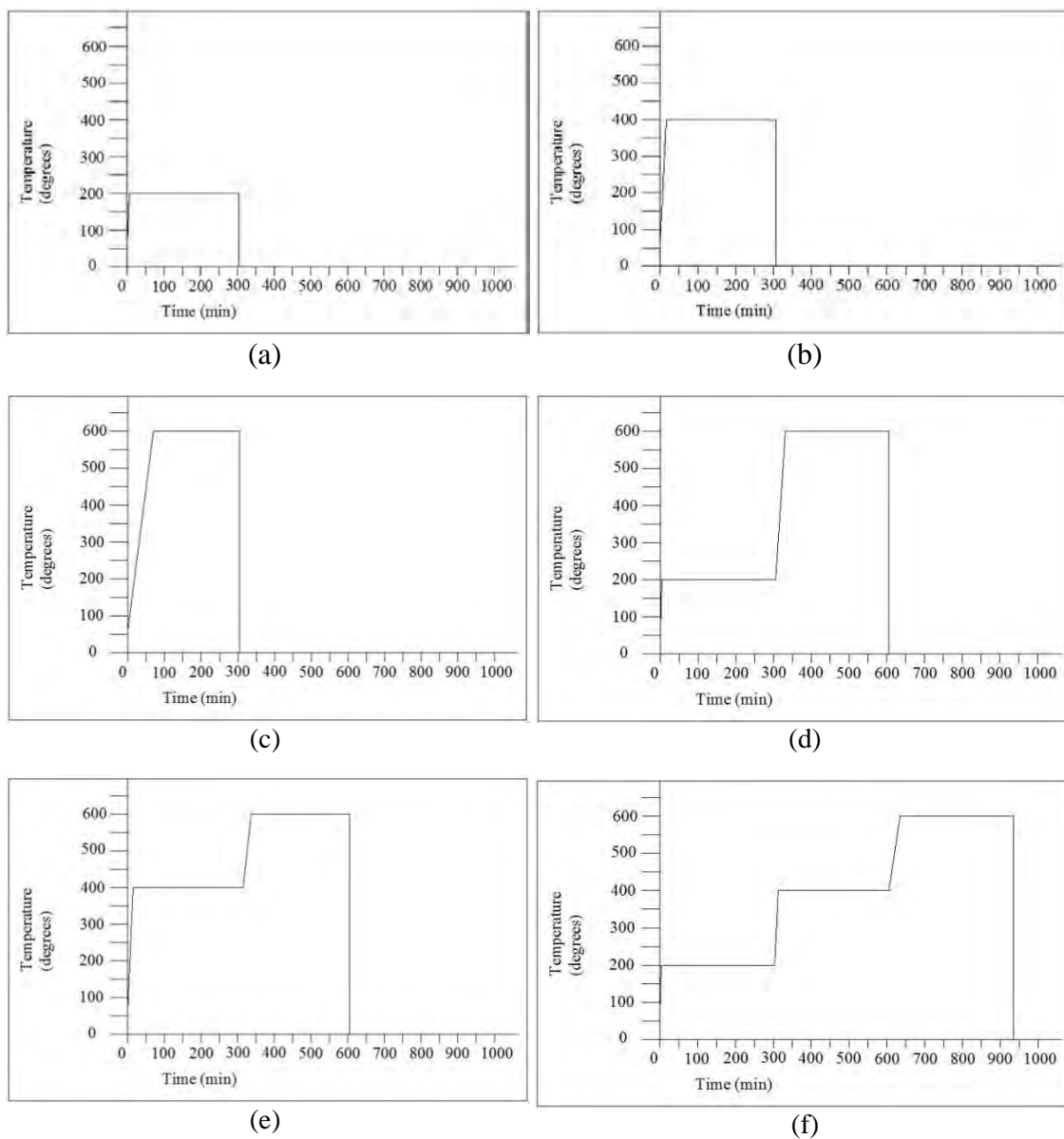


Figure 1.3 Schematic representations of heating paths; (a), (b), (c) represent PATH 1, (d) represents PATH 2, (e) represents PATH 3 and (f) represents PATH 4.

2.1 GENERAL

Concrete is a widely used construction material in all the modern concrete structures because of ease of getting wide range of compressive strength from low to high and good durability. Most important mechanical property of concrete is compressive strength which is the capacity to withstand axially directed compressive forces. It is measured from the failure load divided by the cross sectional area resisting the load. Thermal expansion and thermal conductivity are important properties of concrete and have significant effect on behavior of concrete structure during fire incident. Concrete is non-combustible and does not support the spread of flames and has a slow rate of heat transfer which makes it an effective fire shield. The effects of fire on concrete are loss of strength and spalling of the concrete surface. Extensive research has been performed on the fire resistance of concrete under high temperature where stiffness and strength are degraded due to temperature-dependent material properties.

2.2 PHYSICAL PROPERTIES OF HARDENED CONCRETE

2.2.1 Compressive strength

Concrete mixtures can be designed to provide a wide range of mechanical and durability properties to meet the design requirements of structures. Compressive strength is the capacity of a material or structure to withstand axially directed compressive forces. It provides data of force versus deformation for the conditions of the test method. When the limit of compressive strength is reached, brittle materials are crushed. The compressive strength is measured by breaking cylindrical concrete specimens in a compression testing machine. It is calculated from the failure load divided by the cross sectional area resisting the load and reported in units of pound per square inch (psi) in US and Mega Pascal (MPa) in SI units. Concrete can be made

to have high compressive strength, that is, many concrete structures have compressive strengths in excess of 50 MPa, whereas a material such as soft sandstone may have a compressive strength as low as 5 or 10 MPa. In contrast, a small plastic container might have a compressive strength of less than 250 N. Concrete compressive strength requirements can vary from 17 MPa (2500 psi) for residential concrete to 28 MPa (4000 psi) and higher in commercial structures. Higher strengths up to and exceeding 70 MPa (10000 psi) are specified for certain applications.

2.2.2 Thermal expansion

The coefficient of thermal expansion, α_c of concrete is a measure of the free strain produced in concrete subject to a unit change in temperature and is usually expressed in micro strain per degree centigrade ($\mu\epsilon/^\circ\text{C}$). Values are typically in the range 8–13 $\mu\epsilon/^\circ\text{C}$. As aggregate comprises about 70% to 80% of the concrete volume, this has the dominant effect on the coefficient of thermal expansion as shown in Table 2.1(Neville

Table 2.1 Coefficients of thermal expansion of coarse aggregate and concrete.

| Coarse aggregate/rock group | Thermal Expansion coefficient (micro strain/ $^\circ\text{C}$) | | |
|--|---|--------------------|--------------|
| | Rock | Saturated concrete | Design value |
| Chert or flint | 7.4-13.0 | 11.4-12.2 | 12 |
| Quartzite | 7-13.2 | 11.7-14.6 | 14 |
| Sandstone | 4.3-12.1 | 9.2-13.3 | 12.5 |
| Marble | 2.2-16.0 | 4.4-7.4 | 7 |
| Siliceous limestone | 3.6-9.7 | 8.1-11.0 | 10.5 |
| Granite | 1.8-11.9 | 8.1-10.3 | 10 |
| Dolerite | 4.5-8.5 | Average 9.2 | 9.5 |
| Basalt | 4.0-9.7 | 7.9-10.4 | 10 |
| Limestone | 1.8-11.7 | 4.3-10.3 | 9 |
| Glacial gravel | -- | 9.0-13.7 | 13 |
| Sintered fly ash(coarse and fine) | -- | 5.6 | 7 |
| Sintered fly ash(coarse and natural aggregate fines) | -- | 8.5-9.5 | 9 |

A. M, 1995). Reducing paste volume will lead to a small reduction in the coefficient of thermal expansion but this change is significantly less than that achieved by changing aggregate type.

2.2.3 Thermal conductivity

The thermal conductivity of concrete, λ_c , determines the rate at which heat will be transported through it and hence the rate of heat loss. While it is not required for general design it may be necessary when estimating temperature rise and temperature differentials in some specific situations as follows:

- i. Predicting early-age temperature rise and differentials due to heat of hydration.
- ii. Estimating temperature differentials under transient conditions, for example, in oil storage vessels that are regularly filled and emptied.

There are three principal factors influencing the thermal conductivity of concrete:

1. The aggregate type.
2. The aggregate volume: Aggregate has a higher thermal conductivity than both cement and water.
3. The moisture content: As concrete hydrates and dries, the space previously occupied by water empties and the conductivity reduces.

2.2.4 Specific heat

The specific heat of concrete, c_p is required in the determination of thermal diffusivity, D (through the expression, $D = \lambda_c / c_p \rho$) used in thermal analysis. The range of values for concrete may vary from 0.75 to 1.17 kJ/kg-K. This is a very significant variation, indicating that the temperature rise associated with a particular amount of heat generated may vary by as much as $\pm 20\%$ from a mean value of about 0.96 kJ/

kg-K. It is particularly important, therefore, that a representative value is used in early age models for temperature prediction based on heat generation from the cement. Specific heat is generally measured using calorimetry, although it is evident that it may be predicted with a reasonable degree of accuracy using the method of mixtures and values for the individual constituents.

Two factors in particular influence to the specific heat of concrete:

1. Aggregate type: Aggregate constitutes the largest proportion of the mass. The specific heat for rocks ranges from 0.8 to 1.0 kJ/kg-K and for a typical structure this may result in a 15% difference for concrete.
2. Water content: Water has a specific heat that is four to five times that of the other mix constituents. Dealing with the water content is more complicated as the specific heat differs for free water (4.18 kJ/kg-K) and bound water (2.22 kJ/kg-K) in concrete.

2.2.5 Fire resistance

Concrete is non-combustible and does not support the spread of flames. It produces no smoke, toxic gases or emissions when exposed to fire and does not contribute to the fire load. Not surprisingly, the European Commission has given concrete the highest possible fire designation, namely A1. Concrete has a slow rate of heat transfer which makes it an effective fire shield for adjacent compartments, and under typical fire conditions concrete retains most of its strength. The effects of fire on concrete are loss of strength of the matrix and spalling of the concrete surface. Loss of strength of concrete starts as a result of moisture loss and micro cracking but the effect is modest up to about 300°C, being of the order of 15%. At temperatures above 300°C the strength loss is much more severe and at 500°C the loss may be approaching 50% (Abdel Alim et al. 2009). Due to the slow heat transfer through concrete, high temperatures are normally limited to the surface zone and the section retains most of its strength. Spalling can occur with most types of concrete but the severity depends

upon the aggregate type, the strength class and the moisture content. Sometimes explosive spalling can be caused by the increase in vapor pressure as water turns into steam. Spalling is more likely in higher-strength concrete as its ability to relieve the vapor pressure reduces. Even when spalling occurs, the integrity of the remaining reinforced concrete is usually adequate.

The effect of temperature on the compressive strength of these classes is shown in Figure 2.1. No distinction is made for aggregate type. High-strength concrete is assumed to be more adversely affected by temperature.

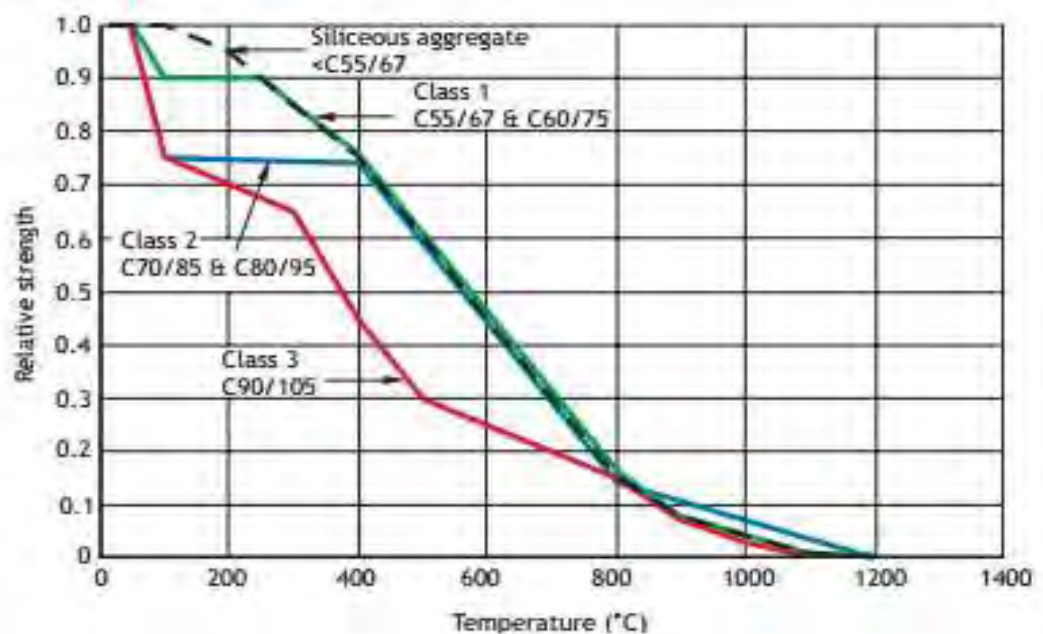


Figure 2.1 The effect of temperature on compressive strength of high-strength concrete according to *Eurocode 2*

In most normal situations, concrete can be considered to be sufficiently fire resistant, so that further enhancement is not necessary. For a few extreme situations some enhancement of the fire protection or resistance may be required. Some possible approaches are as follows:

1. Use of limestone aggregates rather than siliceous aggregates such as flint.

2. Use of light weight aggregate concretes. When dry, performance in fire is very good, but laboratory tests indicate possible poor performance, if these are saturated when the fire begins.
3. Calcium aluminate cement has a higher resistance to strength loss than other cement types. While this cement is widely used for non-structural applications, for example, refractory linings, there is still debate over its suitability for structural applications and local provisions need to be followed.
4. Recognition that high-strength, low-permeability concrete is more prone to spalling. In some situations, structural considerations override that of fire performance, and there may be little practical scope for reducing concrete strength. In such circumstances BS EN 1992-1-2 recommends the option of using not less than 2kg/m^3 of monofilament polypropylene fibres. The mechanism is believed to be the fibres melting and being absorbed in the cement matrix, providing voids for release of high pressure in the pores caused by steam build-up. However, further research is required to confirm the exact mechanism.

2.2.6 Aging of concrete

The strength of concrete is traditionally characterized by the 28-day value. Normal strength concrete gains compressive strength very fast to some extent. It achieves 80% of its ultimate strength after or about 28 days. Usually, 28-day compressive strength of concrete is used as design strength. After 28 days, compressive strength increases to some extent with slower rate which is not taken into account in the design.

2.3 RESPONSES OF CONCRETE TO HIGH TEMPERATURES

2.3.1 Physical and chemical responses of concrete to fire

Under high temperatures, concrete (Figure 2.2) is exposed to several degradation processes, because of multi-chemo-physical mechanisms occurring in the porous concrete media which leads to thermal softening as well as thermal expansion, drying shrinkage and internal pore pressure build-up. When exposed to high temperature, heat is conducted and convected through material, resulting in changes in the chemical composition, physical structure and fluid (water, gas and vapor) contents in the porous material which in turn affect the overall mechanical (strength, stiffness, fracture, etc) and other

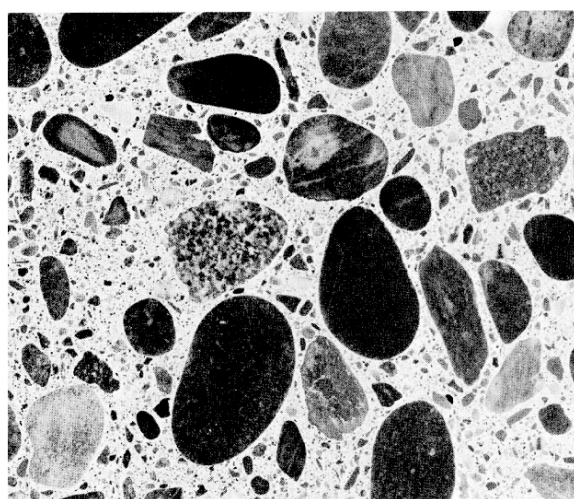


Figure 2.2 The concrete composite (After Mehta and Monteiro, 1993)

physical properties (thermal conductivity, permeability, porosity, etc). Extensive research has been performed on the fire resistance of concrete under high temperature where stiffness and strength are degraded due to temperature-dependent material properties (Bažant et al., 1996; Phan et al., 2001; Willam et al., 2009). Internal restraints may lead to the cracking of the concrete even during the ideal situation of free thermal expansion due to the mismatch of temperature-dependent material properties of heterogeneous concrete constituents under transient temperature but

constant humidity condition. The behavior of concrete is more complicated when considering water mass transport especially under high temperature. Concrete is considered a multiphase medium comprised of solid, liquid (Capillary free water), gaseous mixture (water vapor and dry air) and adsorbed water (Figure 2.3).

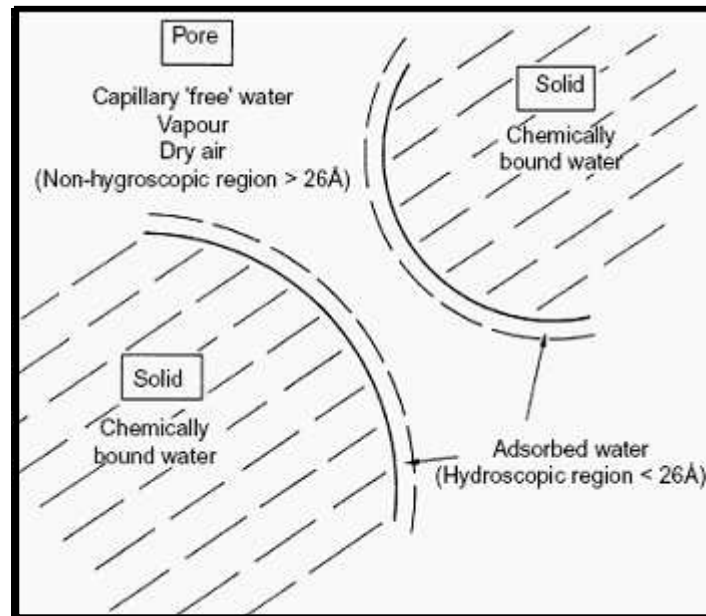


Figure 2.3 Different types of water in concrete

The solid phase consists of cement paste and aggregate, both of which are porous materials. The cement paste is more porous and contains very small gel pores (diameter about 2 nm) and capillary pores (about 1 μm). The products of hydration in the cement paste contain chemically bound water. The gel pores hold water absorbed on large surface. The capillary pores may be fully filled or partially filled with water. The gel and capillary water is called free water. The gaseous phase exists in the partially filled capillary pores. When a concrete structure is exposed to high external temperature heat is transferred by both conduction and convection and the free water begins to evaporate. At higher temperature the chemically bound water is released by dehydration and then evaporates. The transport of vapor and water is governed by the pressure gradient, moisture, and temperature gradients (Lee, 2008). The escape of water chemically bounded in the Calcium Silicate Hydrates (CSH) leads progressively to the failure of concrete for temperatures over 450°C.

Type of aggregates influence strongly the behavior of concrete submitted to high temperature. Aggregate thermal expansion is partly opposed to the drying of cement paste. This phenomenon makes it possible to think that limestone aggregates whose thermal coefficient of expansion is lower than that of siliceous aggregates is more favorable to the behavior at high temperature of concrete.

When subjected to heat, concrete responds not just in instantaneous physical changes, such as expansion, but by undergoing various chemical changes. This response is especially complex due to the non-uniformity of the material. Concrete contains both cement and aggregate elements, and these may react to heating in a variety of ways. There are a number of physical and chemical changes which occur in the concrete subjected to heat. Some of these are reversible upon cooling, but others are nonreversible and may significantly weaken the concrete structure after a fire. Most porous concretes contain a certain amount of liquid water in them. This will obviously vaporize if the temperature significantly exceeds the moisture plateau range of 100-140°C or so, normally causing a build-up of pressure within the concrete. If the temperature reaches about 400°C, the calcium hydroxide in the cement will begin to dehydrate, generating further water vapor and also bringing about a significant reduction in the physical strength of the material. Other changes may occur in the aggregate at higher temperatures, for example quartz-based aggregates increase in volume, due to a mineral transformation, at about 575°C and limestone aggregates will decompose at about 800°C. In isolation, the thermal response of the aggregate itself is more straightforward but the overall response of the concrete due to changes in the aggregate may be much greater. For example, differential expansion between the aggregate and the cement matrix may cause cracking and spalling (Kulkarni, et al., 2011; Kim et al. 2009).

These physical and chemical changes in concrete will have the effect of reducing the compressive strength of the material. Generally, concrete will maintain its compressive strength until a critical temperature is reached, above which point it will rapidly drop off. This generally occurs at around 600°C (Toumi, 2009). This is only a little higher than critical temperatures for steel, but because of the much lower conductivity of concrete the heat tends not to penetrate very far into the depth of the

material, meaning that the structure as a whole normally retains much of its strength (timber is similar in being able to retain strength in its depth once surface layers have been attacked by fire).

Color change of heat exposed concrete (Figure 2.4) as a major parameter in conjunction with material property changes, such as weight loss and compressive strength degradation, for the purpose of identifying the relationship between concrete color change and material property changes at high exposure temperatures. Experiment results show that the color change into red in concrete samples exposed to higher temperatures has a consistent relationship with weight loss rate and residual compressive strength. This result indicates that measuring the hue value in a concrete material can enable assessment of its material property changes. Damage to concrete exposed to fire can be determined by petro graphic studies. Interestingly, it is often best revealed by changes in color of the cement paste and the aggregates. "Effects of Fire on Characteristics of Concrete" in ASTM C856, provides information about color changes as an index to identifying concrete exposure temperatures, attendant cracking, and general effects on strength.

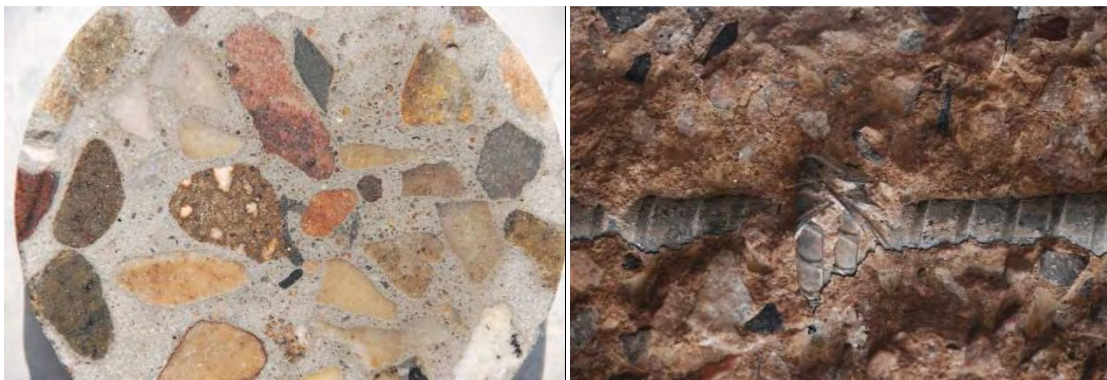


Figure 2.4 (a) Color of concrete before fire

(b) Color of concrete after fire

2.3.2 Effects of elevated temperature on ordinary Portland cement concrete materials

It has been established that compressive strength of concrete decreases with increasing temperature. However, determination of temperature at which the

reduction of strength should start is not an easy task. This is mainly because test data do not show the simple monotonic decreasing trend for concrete strength in ACI 216, instead, many test data showed that the strength of concrete decreases first, and regains or even exceeds the original strength in the temperature range of 100 to 200°C, and then decreases with further temperature increase. This phenomenon may be described as a first down, then up, and further down trend (or simply the down-up-down trend) in compressive strength of concrete under high temperatures. There are some explanations on the physical mechanisms responsible for the down-up-down trend, although there is no widely accepted theory validated by systematic experimental studies. The current design codes did not consider such a variation in strength of concrete under high temperature.

Portland cement is manufactured by mixing finely divided calcareous materials (i.e., lime containing) and argillaceous materials (i.e., clay). Four compounds that make up more than 90% of the dry weight of the cement are tricalcium silicate, dicalcium silicate, tricalcium aluminate, and tetracalcium aluminoferrite. When water is added to cement, an exothermic reaction occurs, and new compounds are formed (i.e., hydrated cement paste): tobermorite gel calcium hydroxide, calcium aluminoferrite hydrate, tetracalcium aluminate hydrate, and calcium monosulfoaluminat. Mature cement paste is normally composed of 70-80% layered calcium-silicate-hydrate, and other chemical compounds. The C-S-H gel structure is made up of three types of groups that contribute to bond across surfaces or in the interlayer of partly crystallized tobermorite material: calcium ions, siloxanes, and water molecules. Bonding of the water within the layers (gel water) with other groups via hydrogen bond determines the strength, stiffness, and creep properties of the cement paste. Tobermorite gel is the primary contributor to the cement paste structural properties. Concrete is a heterogeneous multiphase material with relatively inert aggregates that is held together by the hydrated cement paste. When, concretes are exposed to high elevated temperature exposure, the cement paste experiences physical and chemical changes that contribute to development of shrinkage, transient creep, and changes in strength. Key material features of hydrated Portland cement paste affecting the properties of concrete at elevated temperature are its moisture state (i.e., sealed or unsealed), chemical structure, average pore size and amorphous/crystalline structure of solid,

temperatures, changes in mechanical properties and durability. Nonlinearities in material properties, variation of mechanical and physical properties with temperature, tensile cracking and creep effects affect the buildup of thermal forces, the load-carrying capacity and the deformation capability (i.e., ductility) of the structural members. The property variations result largely because of changes in the moisture condition of the concrete constituents and the progressive deterioration of the cement paste-aggregate bond, which is especially critical where thermal expansion values for the cement paste and aggregate differ significantly. The bond region is affected by the surface roughness of the aggregate and its chemical and physical interactions. Chemical interaction relates to the chemical reactions between the aggregate and cement paste that can be either beneficial or detrimental. Physical interaction relates to dimensional compatibility between aggregate materials and cement paste. Behavior of concrete at high temperature depends on exposure conditions (i.e., temperature-moisture-load-time regime). Curing influences the degree of hydration, while the temperature and load history prior to exposure to elevated temperature could have a significant effect on the behavior of the Portland cement paste and therefore the concrete. Concrete at elevated temperature is sensitive to the temperature level, heating rate, thermal cycling, and temperature duration (as long as chemical and physical transformations occur).

2.4 DAMAGE MECHANISMS OF CONCRETE UNDER HIGH TEMPERATURES

There are four types of major damage mechanisms responsible for deterioration of properties of concrete under high temperatures (William et al. 2009):

1. Phase transformations taking place in cement paste (destruction of gel structure).
2. Phase transformations taking place in aggregate.
3. Thermal incompatibility between the cement paste and aggregate.
4. Spalling of concrete.

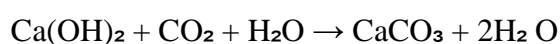
The first three damage mechanisms result in reduced strength and stiffness of concrete, while the last one leads to reduced cross section of structural members and loss of structural integrity. This research deals extensively with the first one.

2.4.1 Phase transformations in cement paste

Major products of hydration reactions of Portland cement are Calcium Silicate Hydrates (C-S-H), Calcium Hydroxide (CH), and Ettringite (C₃A·3H₂O). All of the hydration products decompose under high temperatures. The chemical reactions for the decomposition processes can be described as following



The formation of CaCO₂ is due to accelerated carbonation reaction of CH



Then, CaCO₃ decomposes at high temperatures.

Water evaporates under high temperatures. Free water evaporates in relatively low temperature and the bond water evaporates even higher temperature. If the capillary pores are too fine, the steam pressure that builds up may generate tensile stresses in the concrete at this point such that the concrete's limit of resistance is exceeded.

Associated with the formation of new phases in the chemical reactions are change in volume as well as in stiffness of cement paste. There are cracks and voids formed in cement paste along with the decomposition of CH, which results in major damage of concrete. Similarly, the stiffness's of the new products are different from the stiffness of the original phases, which leads to a change in stiffness of concrete when temperature rises.

2.4.2 Phase transformations taking place in aggregate

For normal weight concrete, there are two common aggregate groups: siliceous aggregates such as quartzite, gravel, granite and flint; calcareous aggregates such as limestone, dolomite and anorthosite. It is generally known that siliceous aggregates, especially quartzite, experience phase transformation at approximately 570° C from α -quartz to β -quartz.

2.4.3 Thermal incompatibility between cement paste and aggregate

Concrete is a composite material with aggregates as inclusions and cement paste as matrix. While concrete is exposed to heat its strength loss occurs not only because of the loss of bond between binding materials particles but also because of interaction between different materials. This phenomenon takes place mainly because the two phases have different thermal and mechanical properties and thus respond differently upon a temperature rise. The aggregates in concrete expand with increasing temperature. Cement paste may expand if the thermal expansion is dominant and may shrink if the moisture loss is dominant. The combined effect of the deformation mechanisms of the two phases depends on many factors such as heating rate, holding period, and composition of the concrete. The thermal incompatibility between the two phases causes very large mismatch in the deformation between aggregates and cement paste, which results in cracks in the interface transition zone around aggregates. Subsequent heating, drying, and loading may cause coalescence of the cracks to form discrete large cracks leading to spalling of concrete and/or failure of concrete structures.

2.4.4 Spalling

One of the most poorly understood processes in the reaction of concrete to high temperatures or fire is that of 'explosive spalling' (Figure 2.5). This is the process whereby chunks of concrete break off and are ejected from the surface of the concrete

slab, often at fairly high velocities. The phenomenon is generally assumed to occur at high temperatures, yet it has also been observed in the early stages of a fire and at temperatures as low as 200° C. If severe, spalling can have a deleterious effect on the strength of reinforced concrete structures, due to enhanced heating of the steel reinforcement. Spalling may significantly reduce or even eliminate the layer of concrete cover on the reinforcement bars, thereby exposing the reinforcement to high temperatures, leading to a reduction of strength of the steel and hence a deterioration of the mechanical properties of the structure as a whole (Figure 2.6). The mechanism leading to spalling is generally thought to involve large build-up of pressure within the porous material which the structure of the concrete is not able to sufficiently dissipate, so fractures occur and chunks of the material are forced suddenly outward. While still in its early stages, modeling of spalling is beginning to show promise.



Figure 2.5 View of a spall on a fire-damaged concrete slab soffit.

The main prerequisites for spalling are relatively well established, these being moisture content of at least 2% and most importantly steep temperature gradients within the material. A value of 5 K/mm is a rough minimum and at 7-8 K/mm spalling is very likely. Temperature gradients are dependent not only on gas-phase temperatures but also heating rates, so that it is not possible to define a threshold temperature per se. However, these values may be affected by the type of concrete, including the strength of the material and the presence of fibers, as described below.

There has been a large amount of recent research on the potential for inclusion of various types of fibers into concrete to mitigate the effects of spalling. Some studies have included polypropylene fibers into the concrete matrix. The theory is that when the concrete is subjected to heat, the polypropylene will melt, creating pathways within the concrete for the exhaust of water vapor and any other gaseous products, which will thereby reduce the build-up of pressure within the concrete. There has been some debate as to whether mono-filament or multi-filament fibers are better able to mitigate spalling. It has also been suggested that the melted polypropylene fibers can form a barrier to the transport of moisture further into the concrete, preventing pressure build-up at greater depth and forcing the moisture to escape instead. The same report suggests that the polypropylene fibers may provide a mechanism for cracking deeper within the concrete, which may mitigate spalling at the surface, but may have adverse structural consequences. Clearly, more work needs to be done in this area. Other studies have added steel fibres to concrete systems; the theory behind this is that the steel will increase the ductility of the concrete and make it more able to withstand the high internal pressures. Results are, so far, inconclusive.



Figure 2.6 Interior column spalling

Recently there has been increasing use of ‘high strength concrete’. This material typically has considerably higher compressive strength than normal strength concrete, however it is also considerably less porous and moisture absorbent. While this

generally reduces the water content of the cement, it is also harder for water vapor to escape during heating. Spalling has been suggested to be relatively more common in high strength concrete, due to the lower porosity of high strength concrete and hence the increased likelihood of high pressure developing within the concrete structure. However, some recent research has shown that this is not necessarily the case, with testing showing higher spalling resistance in high strength concrete than in normal strength (Hachemi et al. 2014).

An aspect of concrete behavior in fire that has not been revealed by testing based on standard fire curves is the post-fire cooling stage. The importance of a cooling-off phase in the assessment of a sample's resistance to heat was demonstrated during a test of some concrete structural elements at Hagerbach test gallery, Switzerland. During the test a concrete sample resisted temperatures of up to 1600° C for two hours without collapsing, but half an hour into the cooling-off phase the sample collapsed explosively.

2.5 LOSS OF STRENGTH OF CONCRETE IN FIRE

The compressive strength of concrete at high temperature is largely affected by the following factors: 1) Individual constituent of concrete, 2) Sealing and moisture conditions, 3) Loading level during heating period, 4) Testing under 'hot' or 'cold residual' conditions, 5) Rate of heating or cooling, 6) Duration under an elevated temperature (holding period), 7) Time maintained in moist conditions after cooling before the strength test is carried out, and 8) Number of thermal cycles (Khoury, 2002). Before discussing thermal responses of concrete under high temperatures, it is important to distinguish several different loading scenarios for strength testing. Three testing methods are commonly used to examine the strength and stiffness of concrete under a high temperature. These testing methods are referred to as stressed test, unstressed test and unstressed residual strength test (Phan, 1996).

This research is based on unstressed residual strength test. Unstressed residual strength test is a test in which the specimen is cooled to room temperature after one or

several cycles of heating without preloading. The mechanical load is then applied (after the heat treatment) at room temperature under stress or strain control until the specimen fails. The results of this test are most suitable for assessing the post fire (or residual) properties of concrete.

The cooling of concrete actually generates very significant damage in concrete, as shown recently by Lee (2008). Test data showed that high strength concrete has higher rate of reduction in residual compressive strength (Morita, et al. 1992). This may be attributed to the fact that. Concrete has many pores in it which contain water, vapor and many gases. While being exposed to heat the water and gases expands and try to come out. The sudden raise of heat leads to sudden expansion of gases which leads to local failures along the pores which finally creates cracks and causes total failure. But if the rise of heat is not sudden rather gradual then the gases inside the pores expand gradually and can come out gradually which results in less or no failure.

2.6 CRACKING

The processes leading to cracking are believed to be essentially the same as those leading to spalling. Thermal expansion and dehydration of the concrete due to heating may lead to the formation of fissures in the concrete rather than, or in addition to, explosive spalling. These fissures may provide pathways for direct heating of the reinforcement bars, possibly bringing about more thermal stress and further cracking (Figure 2.7). Under certain circumstances the cracks may provide pathways for hot combustion products to spread through the barrier to the adjoining compartment with particular emphasis on the depths to which cracking penetrates the concrete. It was found that this relates to the temperature of the fire, and that generally the cracks extended quite deep within the concrete member. Major damage was confined to the surface near to the fire origin, but the nature of cracking and discoloration of the concrete suggested that the material around the reinforcement had reached about 700° C (Figure 2.8). Cracks which extended more than 3cm into the depth of the structure were attributed to a short heating or cooling cycle due to the fire being extinguished.



Figure 2.7 Cracking in the proximity of column



Figure 2.8 Longitudinal cracking in column

3.1 GENERAL

Concrete with four aggregate types were used in this study. The aggregates are brick (B), stone (S), recycled brick (RB) and recycled stone (RS) aggregates. The concrete mix ratio was designed in accordance to the British Standard (BS 5328-1997) with the BRE (Building Research Establishment) concrete mix design-British method (1988) manual. Concrete having three different strengths were designed using four types of coarse aggregates. Compressive strength of 10 MPa, 20 MPa and 35 MPa was attained with each of the four coarse aggregate types for heat treatments in a purpose built electric furnace. This chapter presents the properties of used materials and outlines the construction of the electric furnace.

3.2 PROPERTIES OF MATERIALS

3.2.1 Ordinary Portland cement

All cement used for the casting of concrete columns is Ordinary Portland Cement conforming to the requirements of the BS 12-1996. Different batch of concrete cylinders were cast with same brand of cement (Seven Rings Gold). All cement for casting purposes are delivered in bags from the same production batch and stored inside the laboratory. The stored cements are carefully protected against moisture.

3.2.2 Aggregates

Coarse and fine aggregates used for concrete were clean, strong and free from clay lumps or other impurities. Fine aggregate size is less than 4.75 mm and coarse

aggregates size is greater than 4.75 mm and less than 19mm. Both the aggregates (coarse and fine) were conforming BS 882-1992.

Coarse aggregates

In this research, four types of coarse aggregates; e.g. crushed stone (S), crushed brick (B), recycled stone (RS) and recycled brick (RB) having same gradation were used (Figure 3.1). The stone aggregates and bricks were collected from Bholagonj quarry, Sylhet, Bangladesh. The stone and brick concrete cylinders after compressive strength test from BUET Concrete Laboratory are taken as recycled concrete. After crushing aggregates are graded in BS standard sieves to attain a specific gradation. The basic engineering properties of coarse aggregates are given in Table 3.1. Los Angeles Abrasion values (LAA) are generally higher in brick and recycled aggregates than the stone aggregates due to higher porosity and lower unit weight of brick and recycled aggregates. Mix proportions of coarse aggregate of sizes used in this research are given in Table 3.2.

Table 3.1 Properties of coarse aggregates

| Type of coarse aggregate (ID) | LAA Value (%) | Porosity through absorption capacity (%) | Bulk specific gravity (OD) | Bulk specific gravity (SSD) | Unit wt. kg/m ³ (lb/ft ³) |
|-------------------------------|---------------|--|----------------------------|-----------------------------|--|
| Stone (S) | 29.5 | 0.8 | 2.6 | 2.6 | 1568 (98) |
| Recycled stone (RS) | 38.1 | 5.8 | 2.2 | 2.4 | 1223 (76) |
| Recycled brick (RB) | 40.8 | 12.4 | 1.9 | 2.1 | 1000 (62) |
| Brick (B) | 38.0 | 14.4 | 1.7 | 2.0 | 936 (60) |

Table 3.2 Mix proportion of coarse aggregate

| Particle size | | % of total coarse aggregate (by weight) |
|-----------------|-------------|--|
| Passing through | Retained on | |
| 19 mm | 12.5 mm | 10 |
| 12.5 mm | 9.5 mm | 32 |
| 9.5mm | 4.75 mm | 58 |



Figure 3.1 Types of coarse aggregate used in the research (a), (b), (c) are brick aggregates, (d), (e), (f) are stone aggregates, (g), (h), (i) are recycled brick aggregates and (j), (k), (l) are recycled stone aggregates. Here (a), (d), (g), (j) are 6.5mm passing and 4.75mm retained, (b), (e), (h), (k) are 12.5mm passing and 6.5mm retained and (c), (f), (i), (l) are 19mm passing and 12.5mm retained.

Aggregate generally contain pore, both permeable and impermeable, for which specific gravity has to be carefully determined. With the specific gravity of each constituent known, its weight can be converted into solid volume and hence a

theoretical yield of concrete per unit volume can be calculated. This test was conducted for determining the bulk and apparent specific gravity and absorption of fine aggregate.

Bulk specific gravity is defined as the ratio of weight of aggregate (oven-dry or saturated surface dry) to weight of water occupying a volume equal to that of solid including permeable pores. This is used for

1. Calculation of volume occupied by the aggregate in various admixtures containing aggregate on an absolute basis.
2. The computation of void in aggregate.
3. The determination of moisture content in aggregate.

Apparent specific gravity is the ratio of weight of the aggregate dried in an oven at 100°C to 110°C for 24 hours to the weight of water occupying a volume equal to that of solid excluding permeable pores. This pertains to the relative density of the solid material making up the constituent particles not including the pore space within the particles that is accessible to water.

Absorption volume is used to calculate the change in the weight of an aggregate due to water absorption in the pore spaces within the constituent particles, compared to the dry condition. For an aggregate that has been in contact with water and that has free moisture on particle surfaces, the percentage of free moisture can be determined by deducting the absorption from the total moisture content. This test procedure conforms to ASTM standard C128-88.

The test procedure covers the determination of unit weight in compacted or loose condition of fine and coarse aggregates. However, the procedure may also be used for determining mass/volume relationship for conversions and calculating the percentages of voids in aggregates. Voids within particles, either permeable or impermeable, are not included in voids as determined by this test method. The test was conducted according to ASTM standard C29.

Fine aggregates

Sand is normally dredged from river bed and stream in the dry season when the river bed is dry or when there is not much flow in the river. According to the size and source there are two types of sands (Figure 3.2) are available in Bangladesh such as Sylhet sand (F.M. 2.5) and local sand (F.M. 1.2). Sylhet sands are available from the eastern part of the Bangladesh and are obtained from the bed of flowing river. Sylhet sands are reddish in color and the fineness modulus (FM) is 2.5-2.9. Sylhet sand is composed of angular grains which are coarser than any other sand. The basic engineering properties of fine aggregates are given in Table 3.3. Sylhet sand was used in this research as fine aggregate (Figure 3.3).

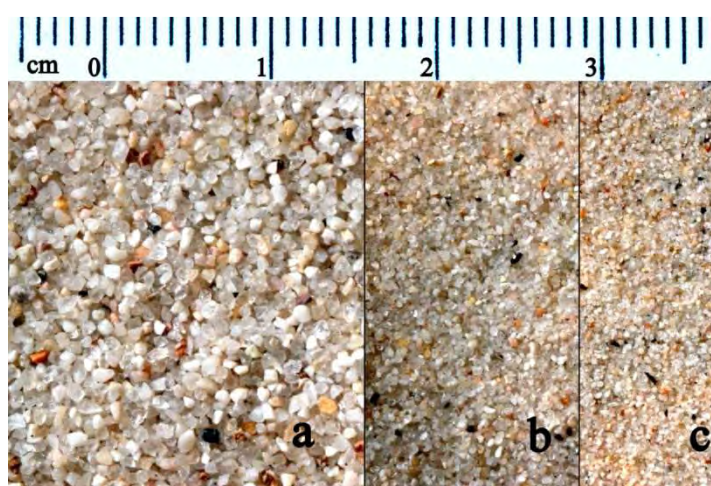


Figure 3.2 Sand as fine aggregate

Table 3.3 Properties of fine aggregate.

| Type of fine aggregate | Bulk specific gravity (OD) | Bulk specific gravity (SSD) | Bulk unit wt. (SSD) kg/m ³ (lb/ft ³) | Fineness modulus |
|------------------------|----------------------------|-----------------------------|---|------------------|
| Sylhet sand | 2.54 | 2.58 | 1520 (95) | 2.62 |

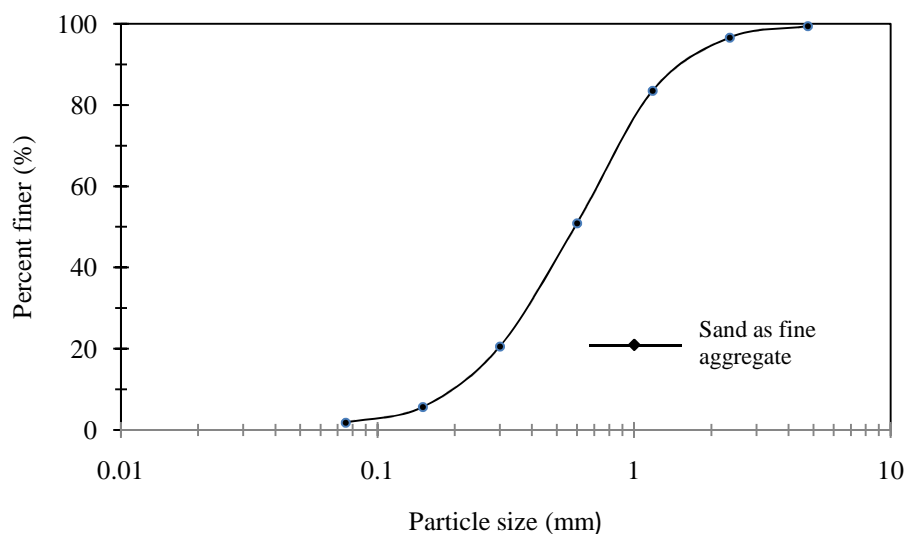


Figure 3.3 Grain size distribution for fine aggregate (Sand)

3.2.3 Water

Water is an important ingredient of concrete as it actively participates in the chemical reaction with cement. On an average 23% of water by weight of cement known as bound water is required for chemical reaction with Portland cement compound. A certain quantity of water is also embedded within the gel-pores. This water is known as gel water. Bound water and gel water are complimentary to each other. 15 percent of water by weight of cement is required to fill up the gel-pores. Therefore a total 38 percent of water by weight of cement is required for the complete chemical reactions and also to occupy the space within gel-pores (Neville A. M., 1995).

The slump was maintained in the range of 75 mm to 125 mm. The total free water content was taken to be 210 kg (10 MPa and 20 MPa) and 225 kg (35 MPa) for 1.0 m³ fresh concrete. Water cement ratio was found to be 0.81, 0.64 and 0.51 for 10 MPa, 20 MPa and 35 MPa respectively from mix design.

Chemically $W/C \approx 0.38$ is needed for complete hydration. If the water cement ratio is high, the chemically not-needed-water will cause pores termed as “capillary pores”.

- i. $W/C < 0.60$ → capillary pores are not interconnected.
- ii. $W/C > 0.60$ → capillary pores will be more and more interconnected.

3.3 EQUIPMENTS USED FOR CASTING OF CONCRETE

To cast the concrete specimens some equipment were used. These equipments are discussed in below:

3.3.1 Mould

Moulds are used for casting cylinders in definite shape. Two main factors are associated regarding the mold with the testing process.

- i. Type of mould
- ii. Capping and surface plainness

100 mm in diameter and 200 mm in height cylindrical mould was used for casting of concrete.

3.3.2 Vibrator

A concrete vibrator uses an off-centered weight, which is spun as much as 10,000 times a minute, causing large air pockets in the concrete to disperse as the concrete is shaken. A concrete vibrator is used to ensure that a concrete pour is even and free of air bubbles so that the concrete will remain strong and have a smooth finish.

3.3.3 Compressive strength testing machine

Compression strength is a measure of mechanical compressive strength and materials properties such as yield strength, modulus, ultimate strength, poissons ratio and per

cent strain to failure. Specimens are fixed in multiple ways including the use of compression platens, spherical seat platens, cages, and bend or flexural fixtures. Test parameters to configure a test system include load, speed of machine, test method, sample geometry, and maximum sample deflection. Test sample thicknesses and types affect equipment requirements. Compression test machines perform tension or compressive tests on materials and products.

Compressive testing helps to select materials to confirm the adequacy and thereby ensures quality of adopted casting procedure. In addition, compressive properties can predict material behavior under forms of loading other than tension. Material strength is of primary concern. Strength may be measured as stress necessary to cause plastic deformation or maximum stress the material can withstand.

The compressive strength is measured by breaking cylindrical concrete specimens in a compression-testing machine. Concrete cylinders was centered in compressive testing machine and loaded to complete failure. This test procedure conforms to ASTM standard C39.

3.3.4 Sieves

A small sieve such as that used for sifting aggregate has very small holes which allow only very fine particles to pass through. Following sieves were used (Table 3.4).

Table 3.4: Sieve numbers and openings

| Sieve opening (mm) | Sieve no. |
|--------------------|-----------|
| 37.5 | 1.5" |
| 19.00 | 3/4" |
| 9.5 | 3/8" |
| 4.75 | #4 |
| 2.36 | #8 |
| 1.18 | #16 |
| 0.6 | #30 |

3.3.5 Sieve shaker

Mechanical vibratory sieve shaker also commonly referred to as gyratory separators or screening machines are a traditional part of processing dry bulk powders. They classify materials by separating them by particle size through a screen mesh. Using a combination of horizontal and vertical movements by means of a vibratory motor, they spread the material over a screen in controlled flow patterns and stratify the product. There are three main functions a vibratory sieve or separator can achieve:

- i. Check/safety screening: used for quality assurance by checking for foreign contaminants and oversized material and removing them from the product.
- ii. Grading/sizing screening: used to grade or classify material into different particle sizes.
- iii. Recovery screening: used to recover valuable materials in the waste stream for re-use.

3.4 MIX DESIGN

Mix design was performed in accordance to BS 5328-1997 with the BRE (Building Research Establishment) concrete mix design-British method (1988) to determine the mix proportion of the materials used in casting of concrete.

3.5 HEATING IN GAS FURNACE

Gas furnace (Figure 3.4) was first used in this work as burning equipment. Its temperature ranged from 300⁰ C to 1300⁰ C. Maximum 4 cylinders can be fitted inside the furnace. The heat treatment was started in an gas furnace. However, some serious problem arised, so it was needed to abundone the gas furnace and construct an electric furnace.



Figure 3.4 Gas furnace.

3.5.1 Problems and reasons for abandoning the gas furnace

There were some problem arised in gas furnace. As a result the gas furnace was abandoned. Following are the problems.

Control of temperature

In gas furnace the heat treatment was provided through gas and the temperature raised very quickly. Though, the desired temperature attained very quickly but it was not steady. It fluctuated in a very large range, $\pm 50^{\circ}$ C.

Space

In gas furnace the space needed for heat treatment was not sufficient. It was able to heat maximum five specimens at a time. So, heat treatment procedure became time consuming for large numbers of specimen.

Control of heating rate

In gas furnace the heating could not be controlled. To attain a desired temperature the heating rate varied from day to day.

3.5.2 Infrared thermometer

Infrared thermometer (Figure 3.5) is an instrument by which the temperature of an object can be measured from a distance without any contact with the object. The temperature of the furnace was measured with the help of infrared thermometer.



Figure 3.5 Infrared thermometer

3.6 ELECTRIC FURNACE

An electric furnace (Figures 3.6 and 3.7) was constructed to generate the effects of temperature episodes in a controlled laboratory environment. In this electric furnace temperature can be controlled up to 1000° C with a tolerance of $\pm 5^{\circ}$ C. The temperature can be observed from the digital screen.



(a)



(b)

Figure 3.6 (a) Electric furnace, (b) Thermocouple, data logger and temperature control unit.



(a)



(b)



(c)

Figure 3.7 Electric furnace; (a) Back view; (b) and (c) Inside views

3.6.1 Materials

The constructed electric furnace is box shaped. Following materials are used to construct the furnace (Figure 3.8):

1. Fire brick
2. Fire clay
3. Steel angles
4. Aluminum
5. Electric coil for heating
6. MS plates
7. Digital thermometer and control unit
8. Switch
9. Glass wool



(a)



(b)



(c)



(d)

Figure 3.8 Materials used for constructing electric furnace. (a) fire clay, (b) fire brick, (c) glass wool. (d) Electric coils

3.6.2 Design

The electric furnace is designed to raise temperature up to 1000° C. It is designed in such a way that heat generates from three sides of the furnace, from the bottom and from the two side wall. Heat is generated in the furnace by fourteen electric coils, six in bottom and four in each side wall. The outer dimension of the furnace is 115 cm long, 90 cm width and 76 cm height (Figure 3.9). The furnace can heat 24 cylinders at a time.

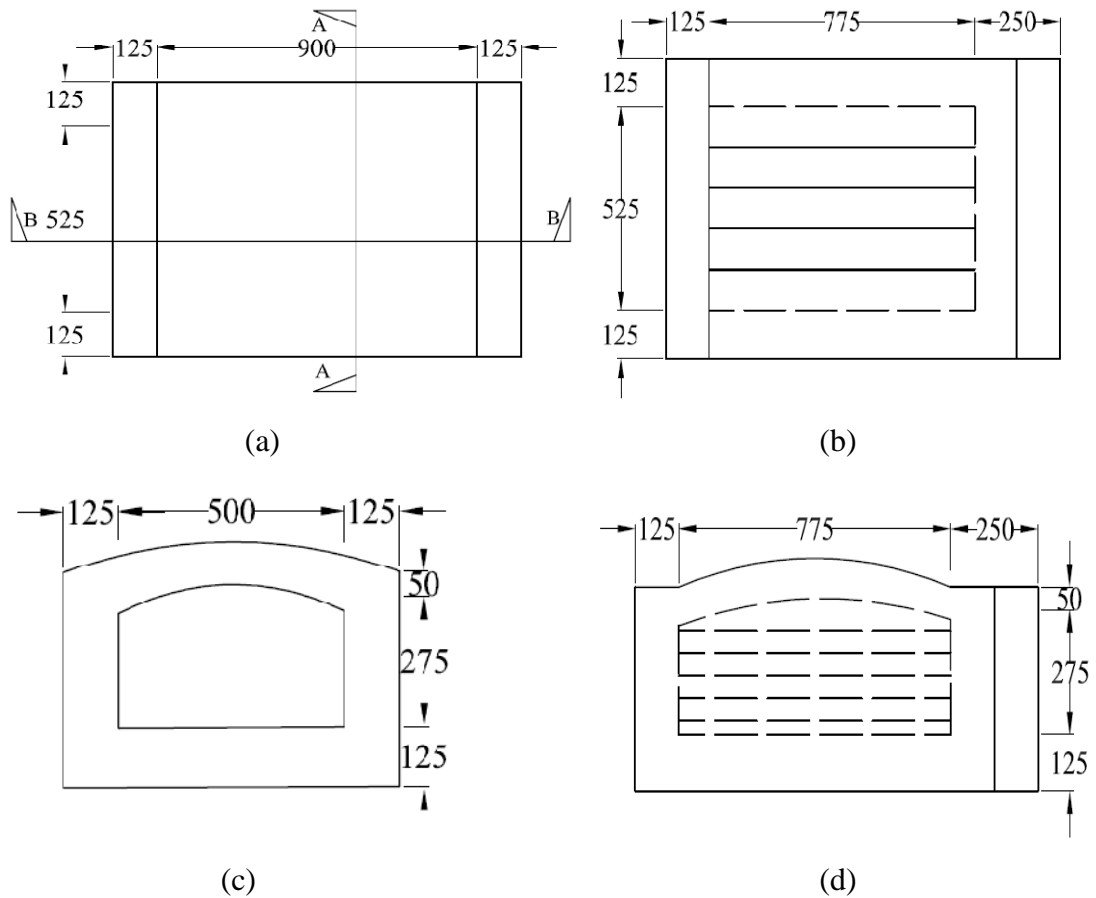
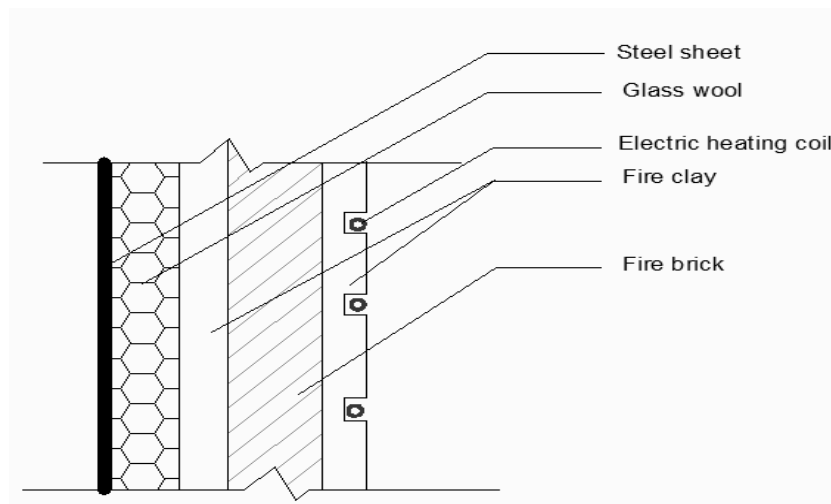


Figure 3.9 Design of electric furnace. (a) Plan view; (b) Cross sectional view; (c) Section A-A (back view); (d) Section B-B (side view).

3.6.3 Construction of electric furnace

The electric furnace has insulated wall in all sides with a slightly curved dome shaped insulated top. The walls are made of three layers mainly, a layer of fire brick in the

middle with a fire clay covering in both sides. These three layers form a total thickness of 125 mm. The slightly domed top is made of fire clay and has a thickness of 50 mm. The overall outer surface is then covered with glass wool and MS plates are placed over it as final covering to prevent heat loss (Figure 3.10). So, heat loss by the electric furnace becomes lowest and the heat inside the oven sustains uniformly and for a longer period. The electric heater coils which provide heat are embedded in the inner surface. Electric coils are powered by the electric control unit at 440 volts. 63 ampere current is required for operating the furnace. While operating the electric furnace keeps its temperature constant by the help of the thermocouple, data logger and electric control unit.



(a)



(b)

Figure 3.10 Construction of Electric Furnace; (a) Cross-section of wall; (b) Angle bars, Fire bricks and fire clays used for construction.

Chapter 4

***LABORATORY PROCEDURE AND
DATA ACQUISITION***

4.1 CASTING OF CONCRETE CYLINDERS

Concrete specimens having 100 mm in diameter and 200 mm in height were cast in steel moulds using four types of coarse aggregates. The aggregates are crushed brick, crushed stone and their recycled derivatives e.g. recycled brick, recycled stone. Concrete specimens were cast following standard laboratory procedures.

4.1.1 Preparation of materials

Preparation of materials is essential for casting specimens in desired quality. Without proper preparation of material, behavior of casting concrete may differ from the target specimen. Preparation of material is discussed in below:

Cleaning and pre-soaking

Coarse aggregates and fine aggregates may contain foreign materials including clay lumps. These foreign materials can be barrier to achieve quality concrete specimens. Cleaning of coarse and fine aggregate was done by screening and washing properly. Soaking of coarse aggregate has been done for 24 hours and allowed it in air to remove all visible water films from the surface of aggregates to reach saturated and surface-dry (SSD) condition.

Mixing

The mixing was done in three steps. These steps are adding water in dry mix, working it to the perfect consistency and clean up promptly. These three steps are very

important for proper mixing. Mixing is the important part of casting. Dense concrete mixture can be made by proper mixing.

Addition of water

A measured amount of water was poured into the mix from a bucket rather than squirting it in with a hose. Mixing was continued for a few minutes after all the water was absorbed because the concrete will often get soupy as it is mixed. It was ensured that all the dry particles were completely wet.

Slump

Slump measures the consistency of concrete and indicates workability. The slump test is carried out using a mould known as slump cone following ASTM standard C 143 and maintained 75 mm.

Compaction

Compaction is the process which expels entrapped air from freshly placed concrete and packs the aggregate particles together so as to increase the density of concrete. It increases significantly the ultimate strength of concrete, decreases the permeability. Casting was done by placing the concrete in layers in the mould and consolidate using vibrator. Vibrator was used for vibrating the concrete mix inside the mould. Moulds were filled in 2 equal layers and vibrated each layer until the concrete became smooth and there was no further egress of entrapped air bubbles. Care was taken that the vibrator is withdrawn in such a manner that no air pockets are left in the specimen. The surface was finished smoothly and the cylinders were covered with a plastic bag.

De-molding and curing

After 24 hours of casting the moulds were separated from the concrete cylinders. They were marked properly and then ready for curing. It has long been recognized that adequate curing is essential to obtain the desired structural and durability

properties of concrete. Curing was done by ponding the specimens in water ensuring uninterrupted curing for 28 days.

4.2 HEAT TREATMENT IN ELECTRIC FURNACE

Heat treatment has been done at three different temperatures with different durations using the constructed electric furnace (Sec. 3.6). In electric furnace the temperature was controlled by thermocouple, data logger and electric control unit. Maximum 24 cylinders can be placed in the electric furnace at a time (Figures 4.1 and 4.2). Monotonic short duration heating (PATH 1, Fig. 1.3, Sec. 1.5) and multi-steps long duration heat treatment (PATH 2, 3 and 4) were done by the purpose made digitally controlled electric furnace.

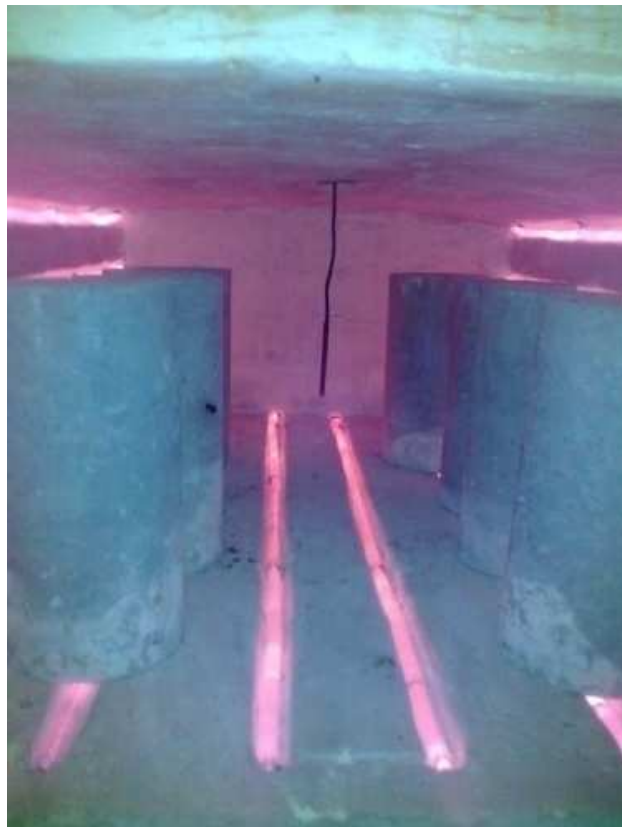


Figure 4.1 Concrete being heated in electric furnace



Figure 4.2 Concrete specimens after burning and testing

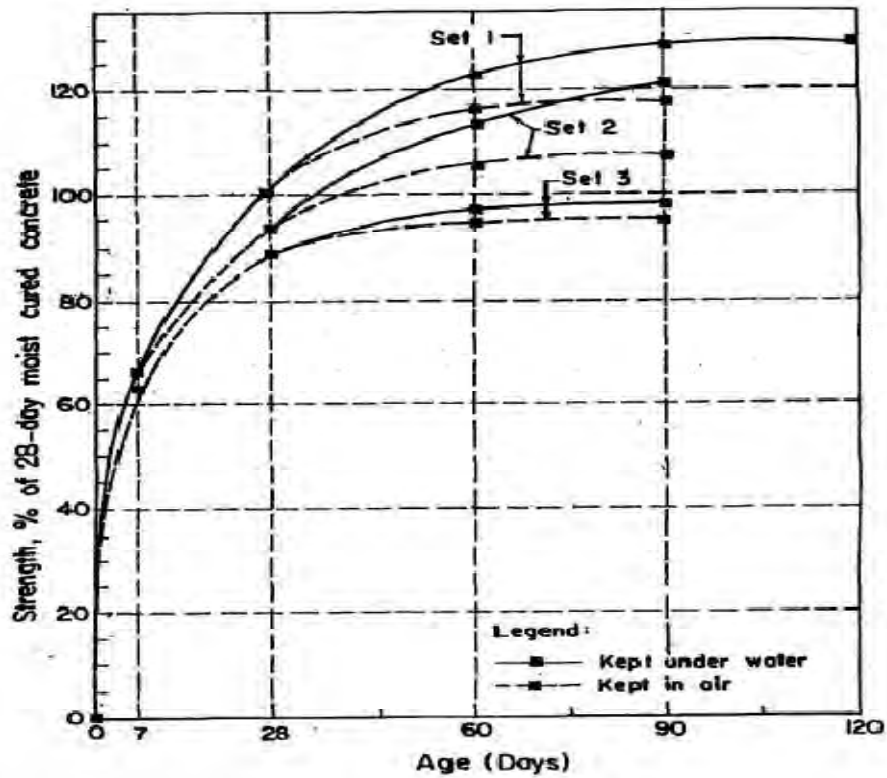
4.3 STRENGTH TESTING OF CONCRETE CYLINDERS

The compressive strength is the most common performance measure used by an engineer in designing or assessing a concrete structure. The compressive strength is usually measured by crushing cylindrical specimens in compressive testing machine. The compressive strength is calculated from dividing the failure load by the cross-sectional area resisting the load in accordance to ASTM C39.

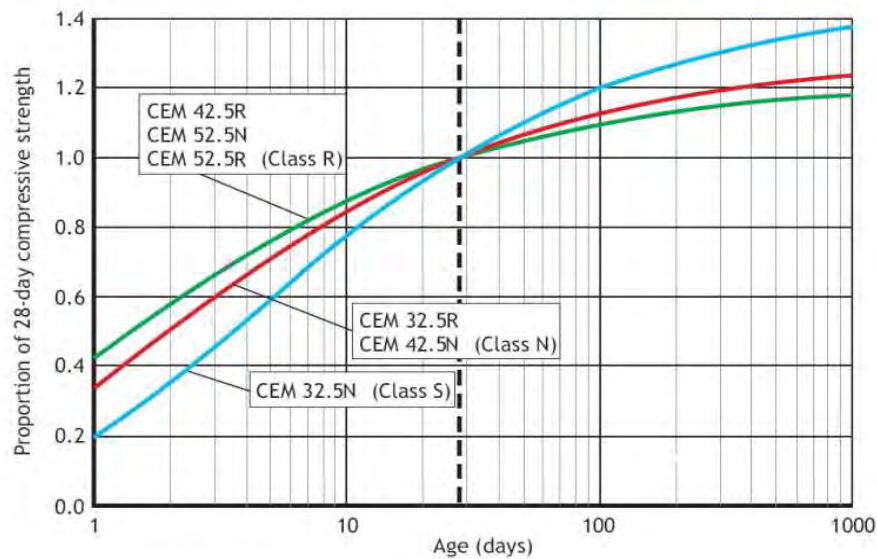
After burning, the cylinders were crushed in the compressive strength testing machine. Then the strength of the burnt cylinders was compared to un-burnt cylinders.

4.4 CORRECTION OF STRENGTH

The control concrete specimens were kept in air for 3 months after 28 days curing. So the strength that found from crushing of concrete was not the correct strength. To compare the strength of control concrete specimens strength with the heat treatment concrete specimens strength, control concrete specimens strength were corrected. Strength of brick aggregate concretes and stone aggregate concrete specimens were corrected using the graphs of Figure 4.3(a) and 4.3(b) respectively (Ahmad and Amin, 1998, Eurocode 2).



(a)



(b)

Figure 4.3 Effect of age on compressive strength. (a) represents compressive strength of brick aggregate concrete at different ages under different curing conditions as obtained from cylinder test (Ahmad and Amin, 1998) (b) represents effect of age on compressive strength of stone aggregate concrete, recycled stone aggregate concrete and recycled brick aggregate concrete (Eurocode 2).

4.5 ESTIMATION OF POROSITY IN COARSE AGGREGATES AND CONCRETES

Determination of porosity using porosimeter is a complex and expensive process. Due to unavailability of such experimental means, the porosity of the coarse aggregates and concretes were estimated through water absorption which is an indication of apparent porosity in aggregate. The assumptions that in a coarse aggregate and concrete there are interconnected voids to be filled with water are utilized here. Therefore, water absorption can be the indication of apparent porosity of coarse aggregates as well as concrete. This was done taking weight of a particular sample of concrete in saturated and surface-dry (SSD) and oven-dry (OD) condition and percentage of weight loss is calculated with respect to dry weight of the sample concrete using equation 4.1. Same concept and procedure has been followed in determining apparent porosity of coarse aggregates. Physical properties of coarse aggregates (Table 4.1) have been determined by other group for their study and coarse aggregate from the same known source has been used in this study (Islam, 2011). Therefore, the physical properties also used directly here. Porosity of concrete used in this research has been determined following above procedure and presented in Table 4.2.

Equation used for porosity (through absorption) calculation,

Apparent porosity, η

$$= \frac{\text{Wt. of sample in SSD condition} - \text{Dry wt. of sample at } 600^{\circ} \text{ C}}{\text{Dry weight of sample at } 600^{\circ} \text{ C}} \times 100\% \quad \dots\dots (4.1)$$

Table 4.1 Porosity in coarse aggregates

| Aggregate type (ID) | Porosity in coarse aggregates measured through absorption capacity (%) |
|---------------------|--|
| Stone (S) | 0.8 |
| Recycled stone (RS) | 5.8 |
| Recycled brick (RB) | 12.4 |
| Brick (B) | 14.4 |

Table 4.2 Porosity in concrete

| Aggregate type (ID) | Concrete specimen ID | Compressive strength (MPa) | Apparent porosity in concrete (%) |
|---------------------|----------------------|----------------------------|-----------------------------------|
| Stone (S) | S10 | 10 | 8.86 |
| | S20 | 20 | 5.58 |
| | S35 | 35 | 13.03 |
| Recycled stone (RS) | RS10 | 10 | 20.00 |
| | RS20 | 20 | 19.10 |
| | RS35 | 35 | 13.42 |
| Recycled brick (RB) | RB10 | 10 | 24.51 |
| | RB20 | 20 | 30.76 |
| | RB35 | 35 | 23.50 |
| Brick (B) | B10 | 10 | 28.94 |
| | B20 | 20 | 31.19 |
| | B35 | 35 | 26.21 |

4.6 ESTIMATION OF HEAT INPUT

As concrete is a composite heterogeneous material, thermal properties of concrete depend on its constituent materials but is different from them. So the determination of heat absorbed during the heat treatment is a difficult one. This parameter is thus estimated (*Equation 4.2*) on the basis of the calculated electrical energy used to produce heat by the furnace and the fraction of heat that was estimated to remain in the system after the losses encountered (*Appendix A*).

Equation used for heat input calculation,

$$\text{Heat} = \text{Electrical power} \times \text{Time}$$

Heat input

$$= \frac{\text{Power in watt} \times \text{Time of power supply in second}}{\text{Nos. of sample} \times \text{weight of each sample}} \text{ (J/kg)} \dots\dots\dots(4.2)$$

5.1 GENERAL

The change of mechanical properties of concrete subjected to high temperature is influenced by coarse aggregate porosity, concrete porosity and concrete strength. These factors determine the extent of spalling that may occur in concretes when subjected to a heat episode. The bound moisture content and the volume of gaseous matters are the driving force for the spalling phenomena to occur. In producing gaseous matters at high temperatures, the concretes pass through a chemo-rheological metamorphosis having an enough potential to further bear upon the mechanical strength properties of the subject concrete. The objective of finding these research results was to see the influence of high temperature episodes (time and duration) on compressive strength for four types of concrete having different strengths, to assess the loss of mass due to high temperature exposures, also to see the effect of sustained temperature with varying magnitudes and duration on compressive strength losses with respect to porosity.

5.2 EFFECT OF TEMPERATURE ON COMPRESSIVE STRENGTH

From the tests it has been observed that compressive strength generally decreases with the increase of temperature. This phenomenon is same for all types of concrete aggregate for all concrete strength grades. Strength decrease patterns vary at different heat episodes for all grades of concrete of all the four of coarse aggregate types.

5.2.1 Compressive strength loss (%) at different temperatures and heating paths

It has been observed from Figures 5.1 to 5.13 that compressive strength loss is proportional to temperature to which the specimens were subjected to. At a fast

heating path (PATH 1, Fig. 1.3, Sec. 1.5) compressive strength loss is high. Compressive strength loss gradually decreases when heating rate gradually becomes slower (PATH 2 – 4, Fig. 1.3, Sec. 1.5). In a particular aggregate type compressive strength loss was found to be higher for concrete with high initial strengths (Figures 5.4, 5.7, 5.10 and 5.13). Furthermore, compressive strength loss of brick aggregate concrete is higher than stone aggregate concrete (Figures 5.5 to 5.7). Compressive strength loss is maximum in low strength concrete made of recycled stone (Figures 5.8 to 5.10) and minimum in concrete made of stone (Figure 5.2 to 5.4). These findings are in conformity with the findings of past studies (Abdel Alim et al.; 2009; Bastami, M., et al., 2011; Lee, K. K. 2008; Schneider U. 1976).

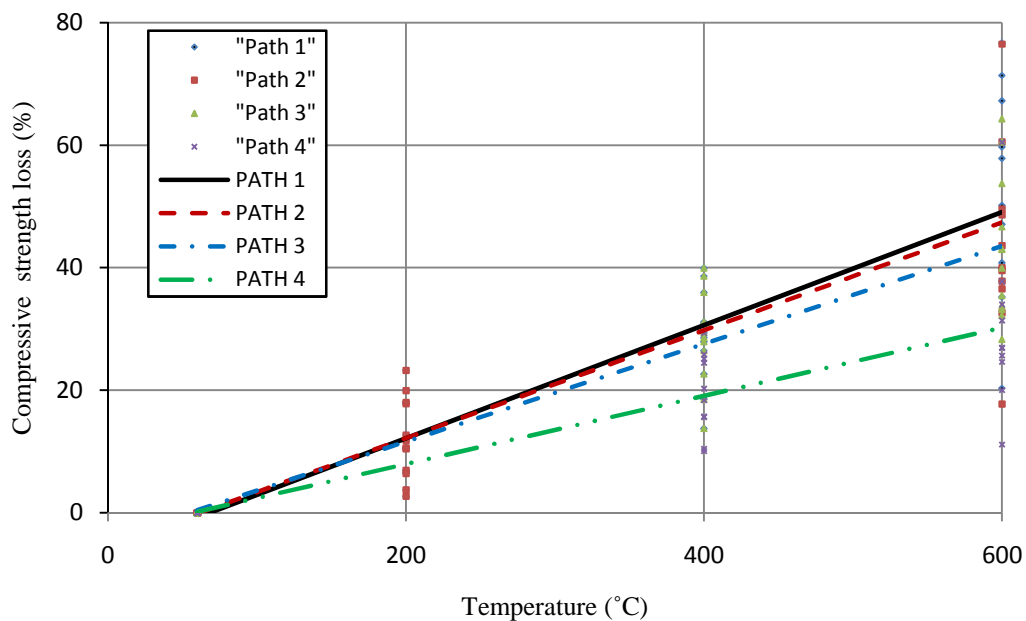


Figure 5.1 Compressive strength loss (%) at different temperatures and heating paths for all types of concrete.

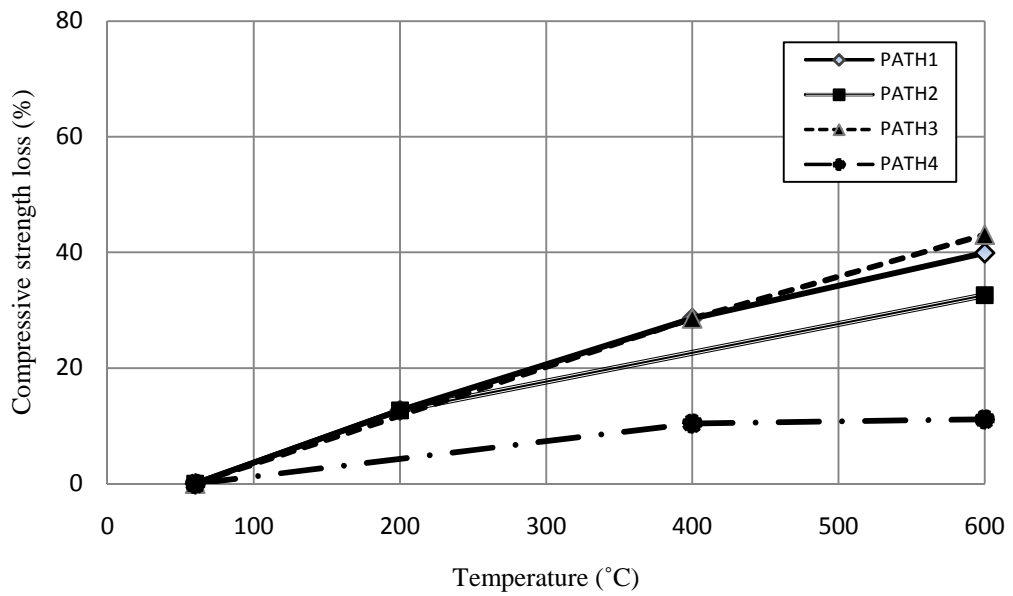


Figure 5.2 Compressive strength loss (%) at different temperatures and heating paths for S10 concrete.

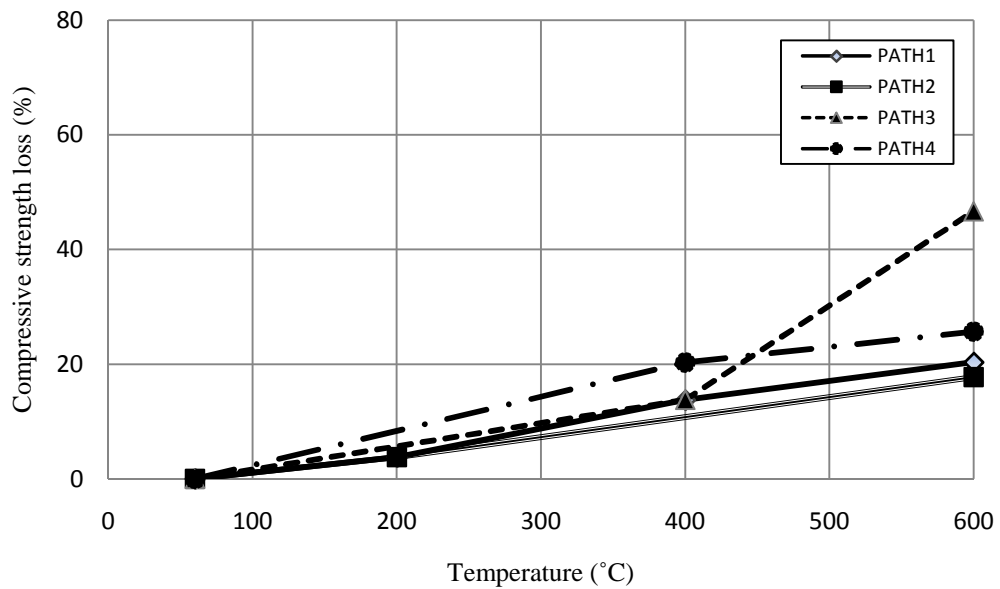


Figure 5.3 Compressive strength loss (%) at different temperatures and heating paths for S20 concrete.

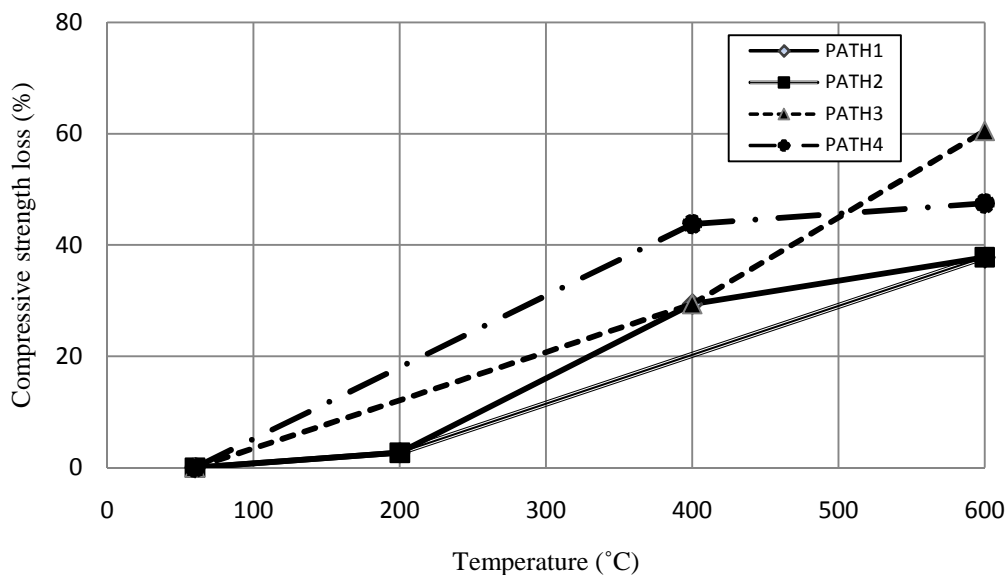


Figure 5.4 Compressive strength loss (%) at different temperatures and heating paths for S35 concrete.

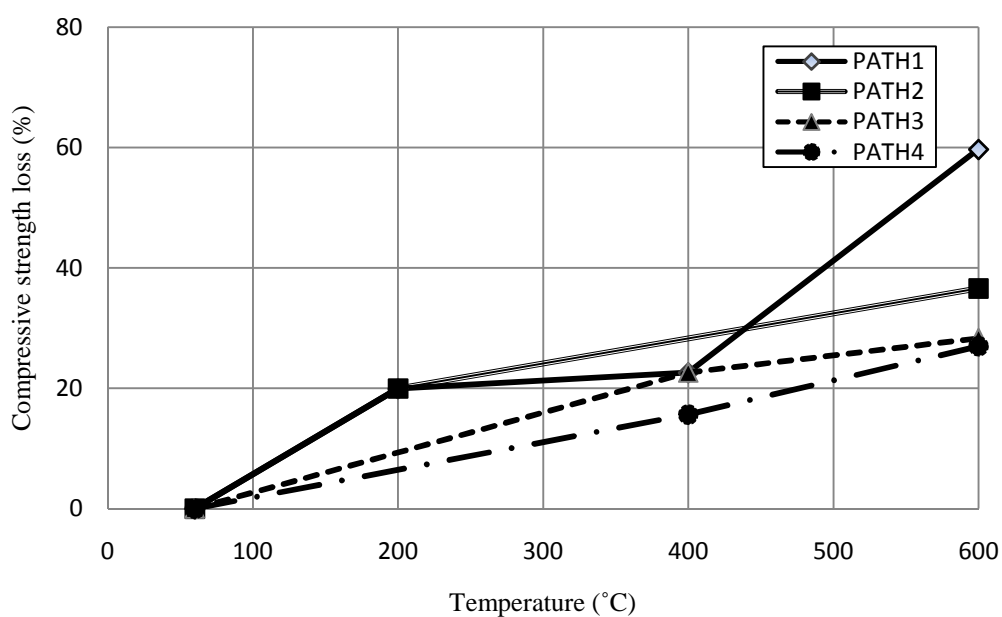


Figure 5.5 Compressive strength loss (%) at different temperatures and heating paths for B10 concrete.

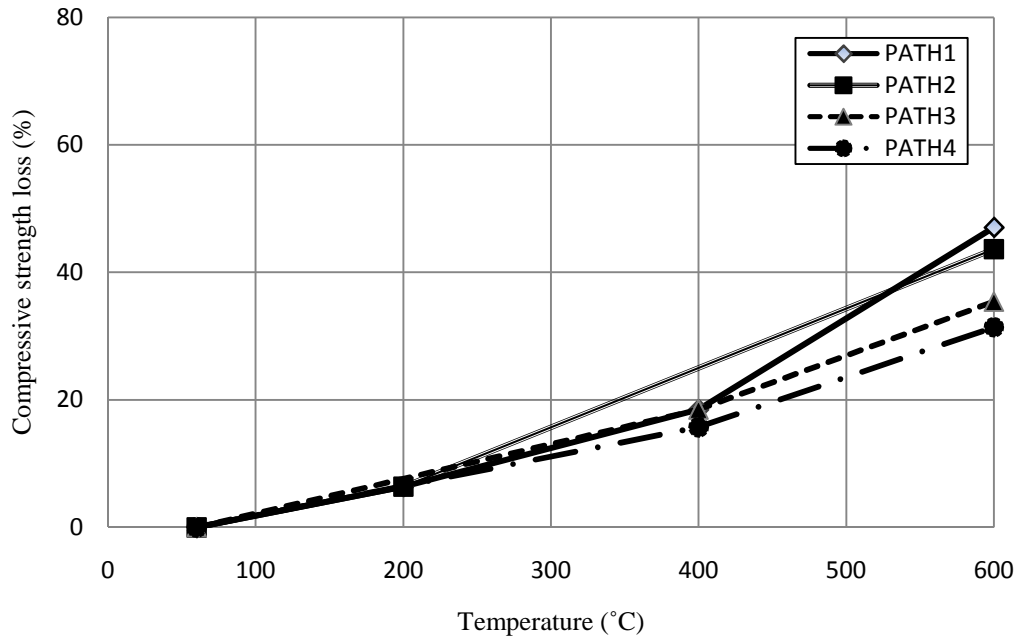


Figure 5.6 Compressive strength loss (%) at different temperatures and heating paths for B20 concrete.

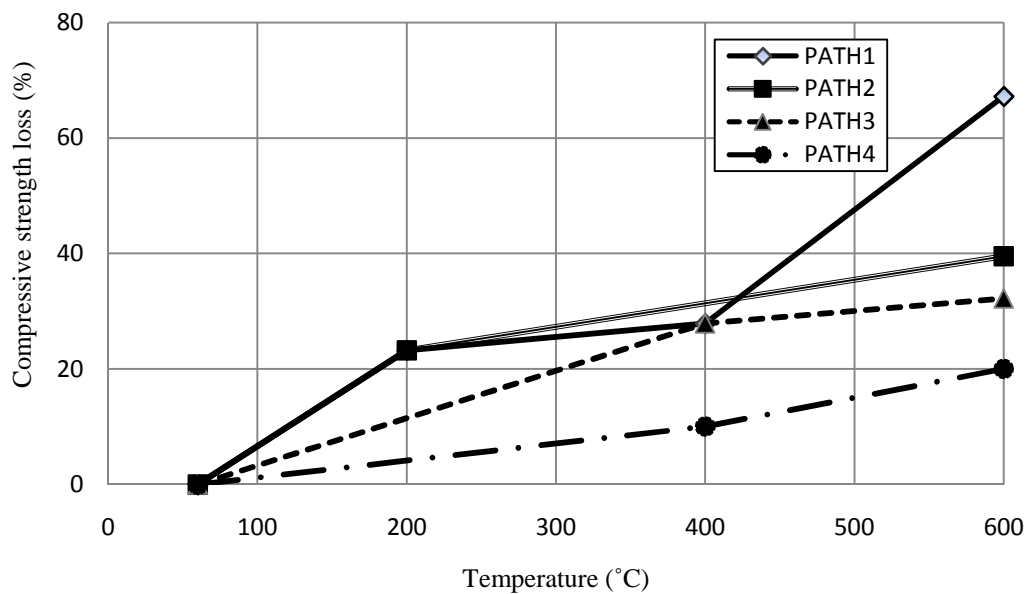


Figure 5.7 Compressive strength loss (%) at different temperatures and heating paths for B35 concrete.

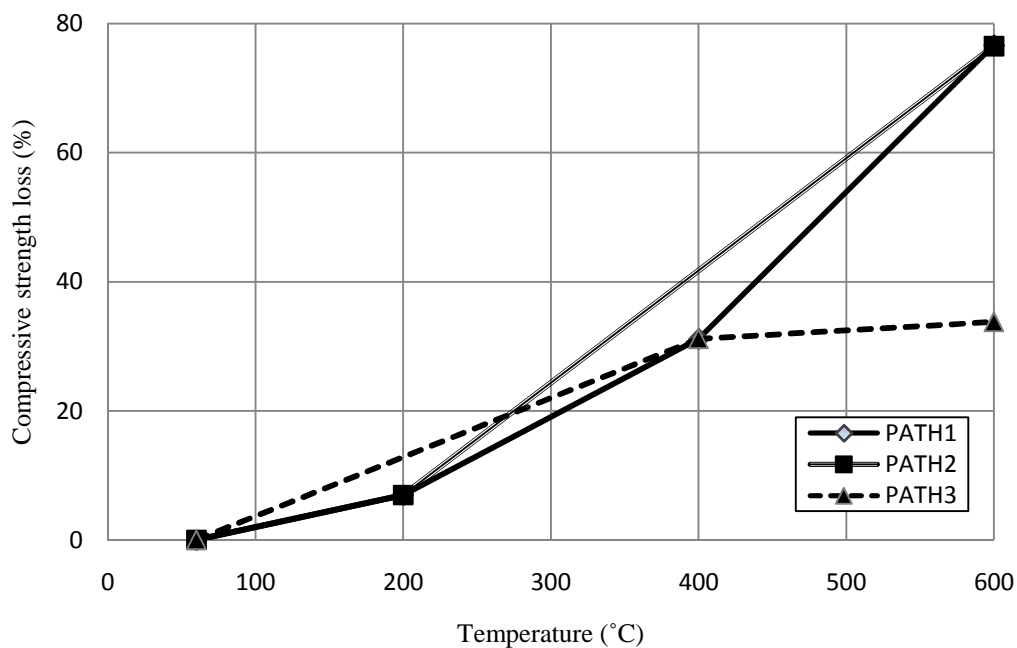


Figure 5.8 Compressive strength loss (%) at different temperatures and heating paths for RS10 concrete.

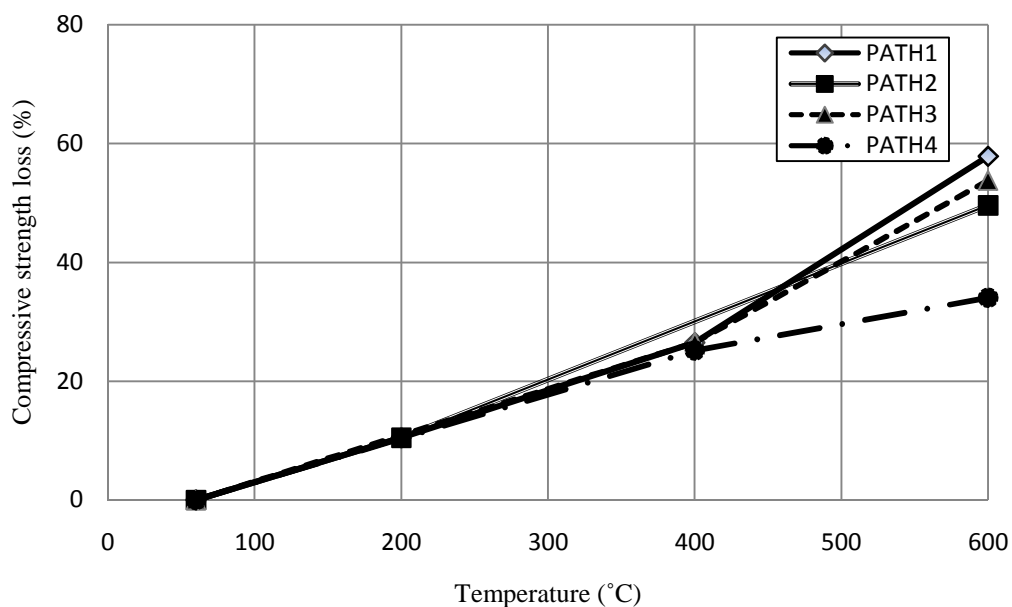


Figure 5.9 Compressive strength loss (%) at different temperatures and heating paths for RS20 concrete.

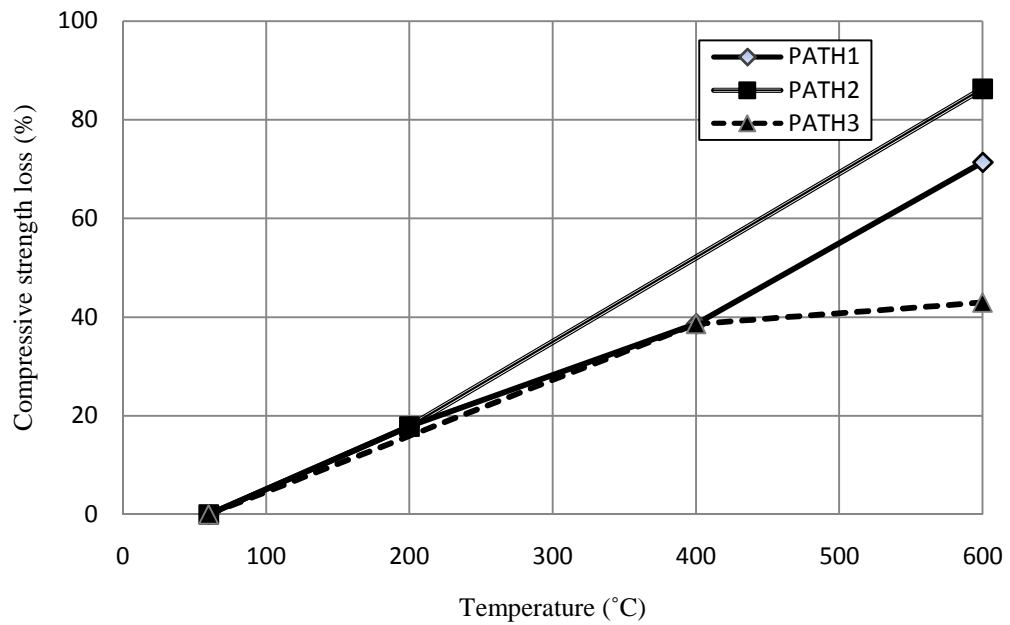


Figure 5.10 Compressive strength loss (%) at different temperatures and heating paths for RS35 concrete.

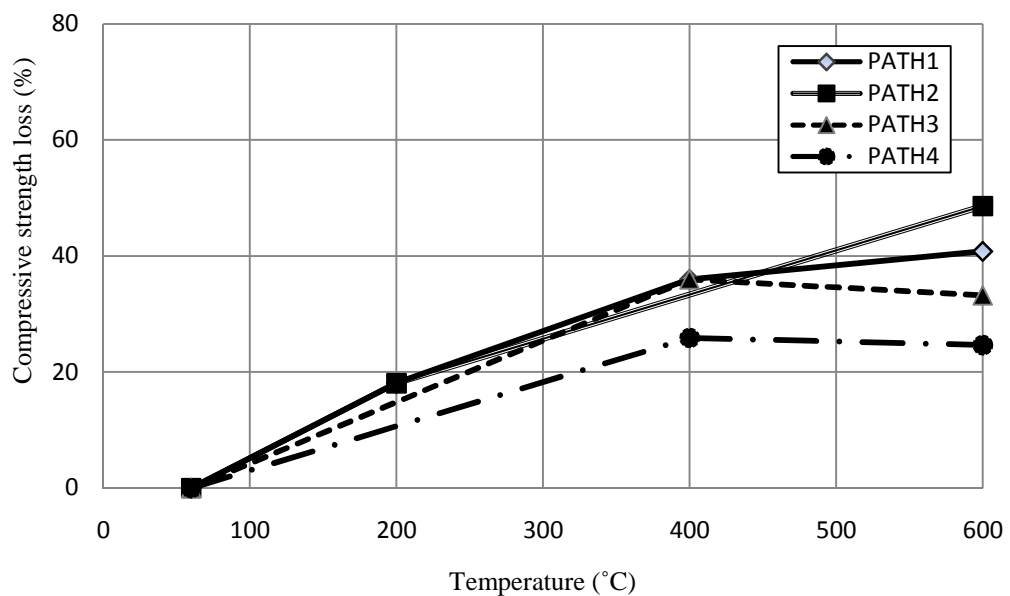


Figure 5.11 Compressive strength loss (%) at different temperatures and heating paths for RB10 concrete.

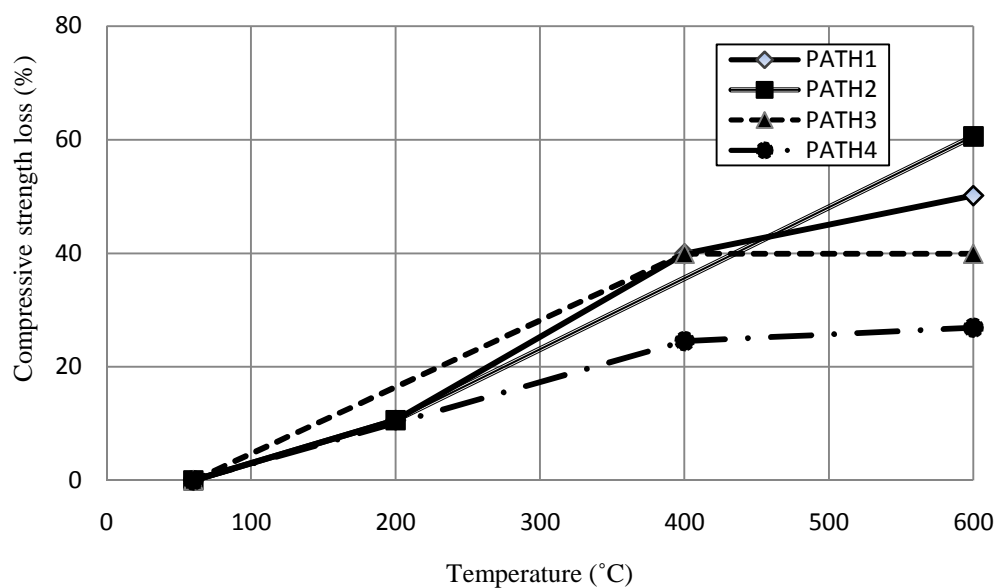


Figure 5.12 Compressive strength loss (%) at different temperatures and heating paths for RB20 concrete.

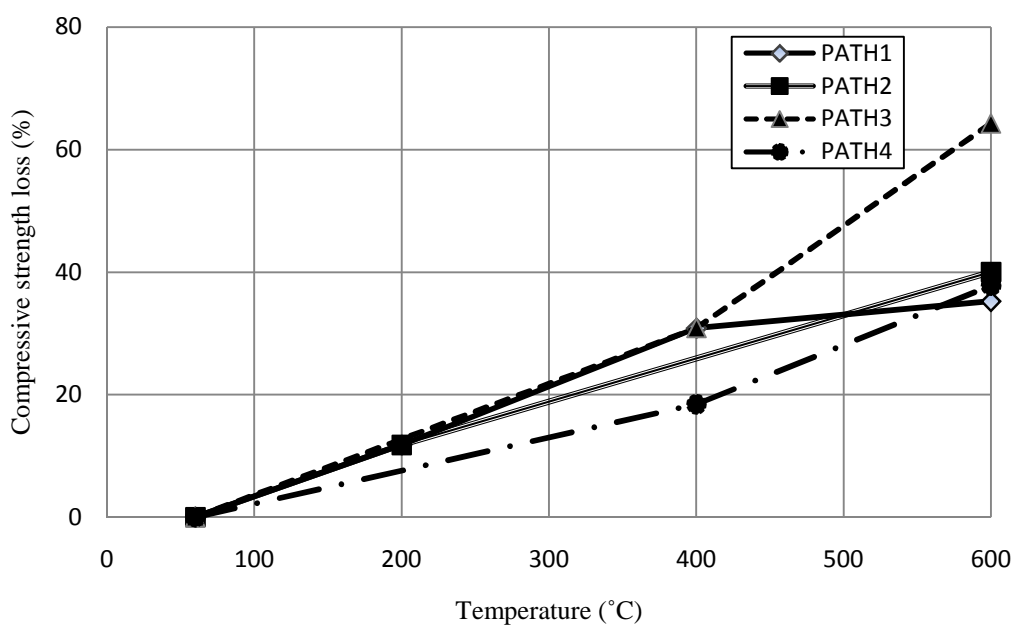


Figure 5.13 Compressive strength loss (%) at different temperatures and heating paths for RB35 concrete.

5.2.2 Compressive strength loss (%) of different types of concrete with respect to different heat inputs

In Figure 5.14, compressive strength losses for concrete of different porosities with respect to heat input are presented. Compressive strength loss is seen to be proportional to the rate of heating. Furthermore, to attain a specific ultimate temperature in all heating PATHs when heat input is gradually increased in PATH 1 to PATH 4, the strength loss was found to decrease at an inverse relation. It is also observed from Figures 5.15 to 5.21 that the same trend of decreasing rate of compressive strength loss with increase of heat input irrespective of coarse aggregate and grade (strength) of concrete. In a fast heating path (PATH 1, Fig. 1.3, Sec. 1.5), with less heat input used, compressive strength loss is found to be higher but gradually decreased with increase of heat input in PATH 2-4 (Fig. 1.3, Sec. 1.5). These heating PATHs generally have relatively slower heating rate. These findings are understandable from physical viewpoint but not visible in any past study reviewed in this dissertation.

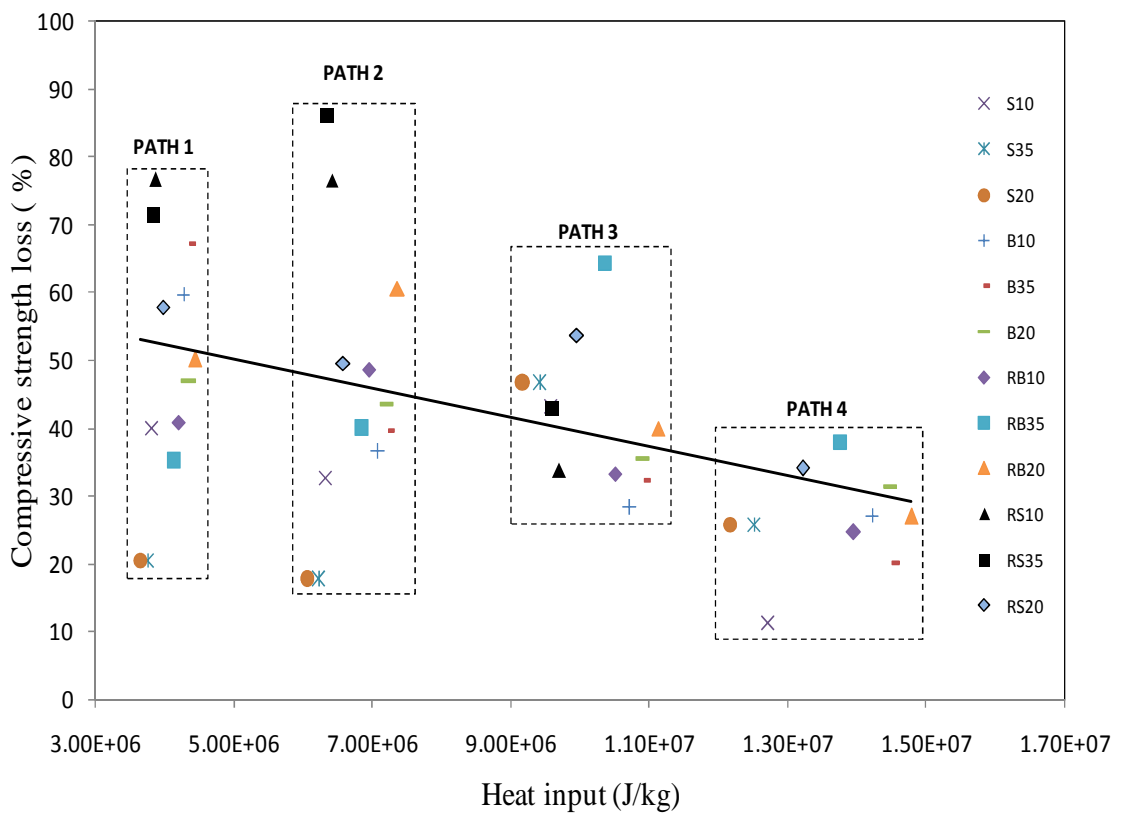


Figure 5.14 Compressive strength loss (%) at 600° C with respect to different heat inputs for all types of concrete.

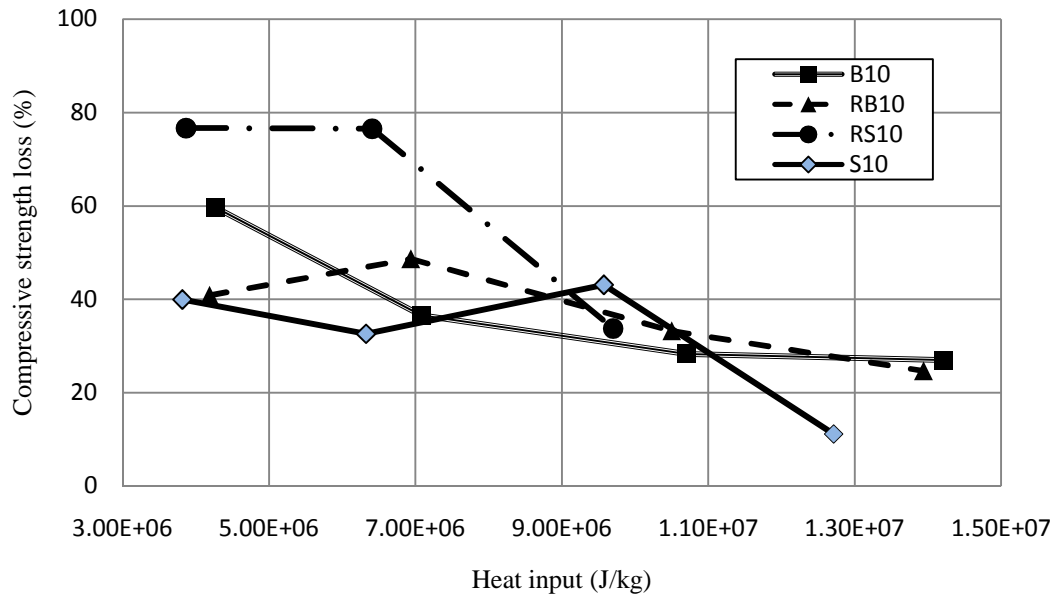


Figure 5.15 Compressive strength loss (%) at 600° C of 10 MPa concrete (all aggregate).

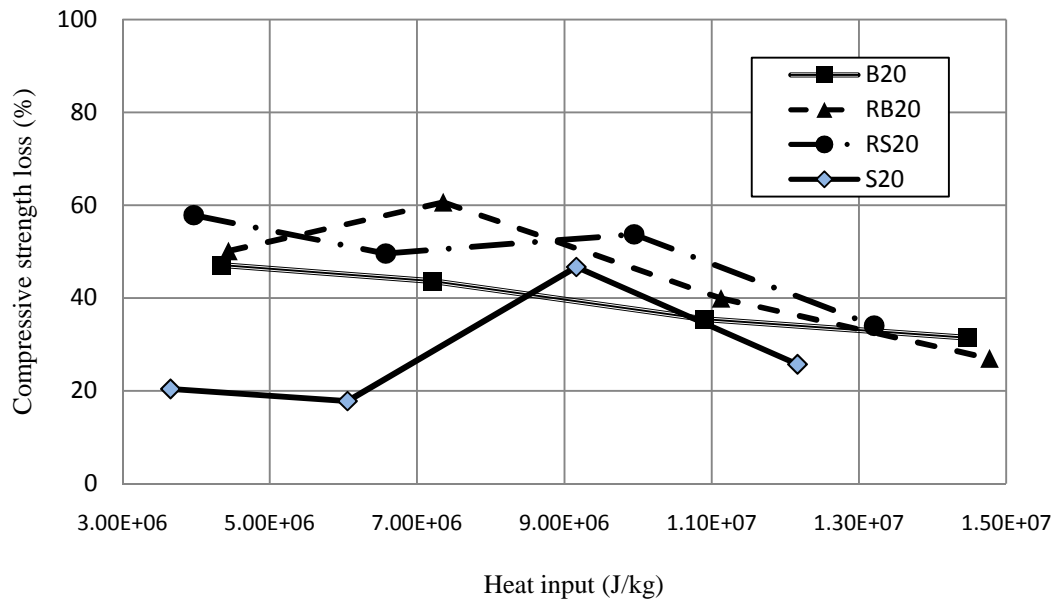


Figure 5.16 Compressive strength loss (%) at 600° C of 20 MPa concrete (all aggregate).

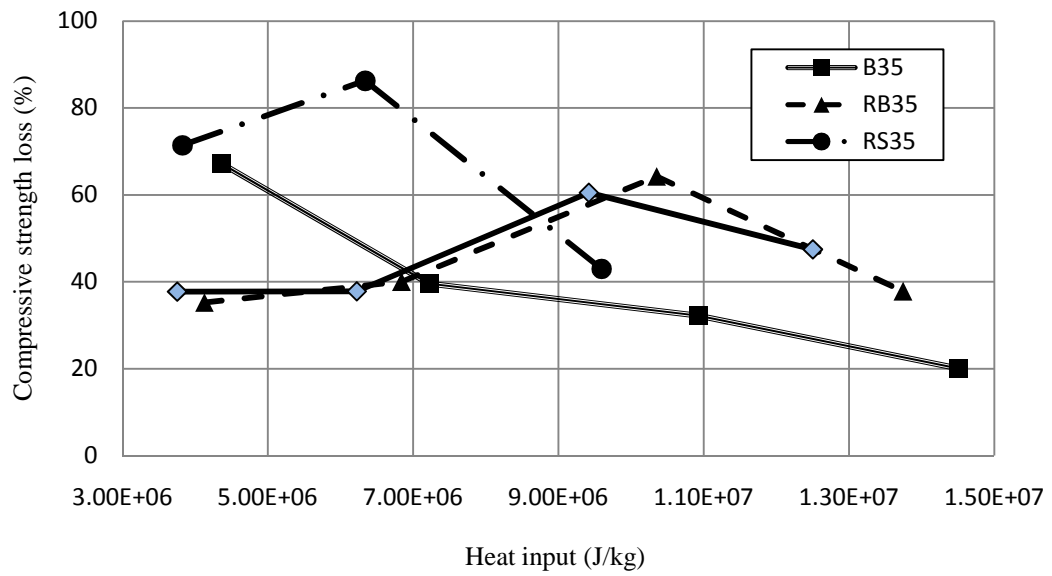


Figure 5.17 Compressive strength loss (%) at 600° C of 35MPa concrete (all aggregate).

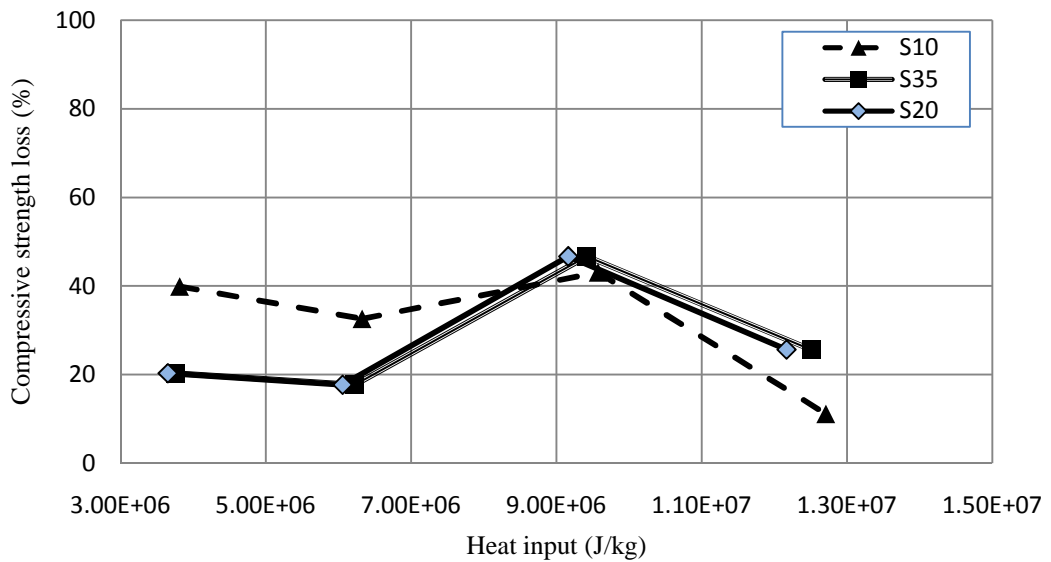


Figure 5.18 Compressive strength loss (%) at 600° C of concrete of stone aggregate (all strength)

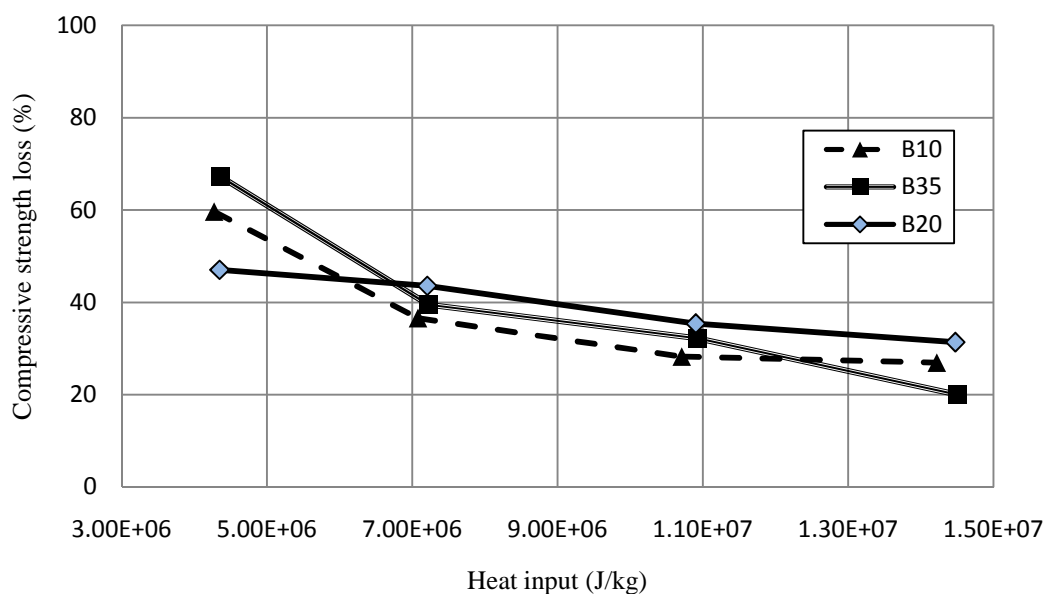


Figure 5.19 Compressive strength loss (%) at 600° C of concrete of brick aggregate (all strength)

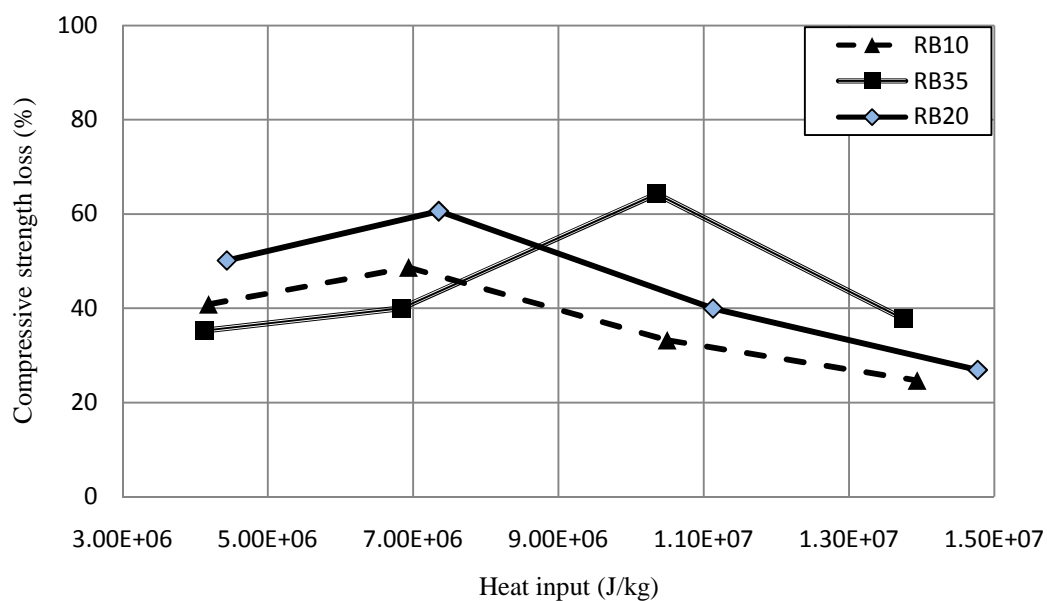


Figure 5.20 Compressive strength loss (%) at 600° C of concrete of recycled brick aggregate (all strength)

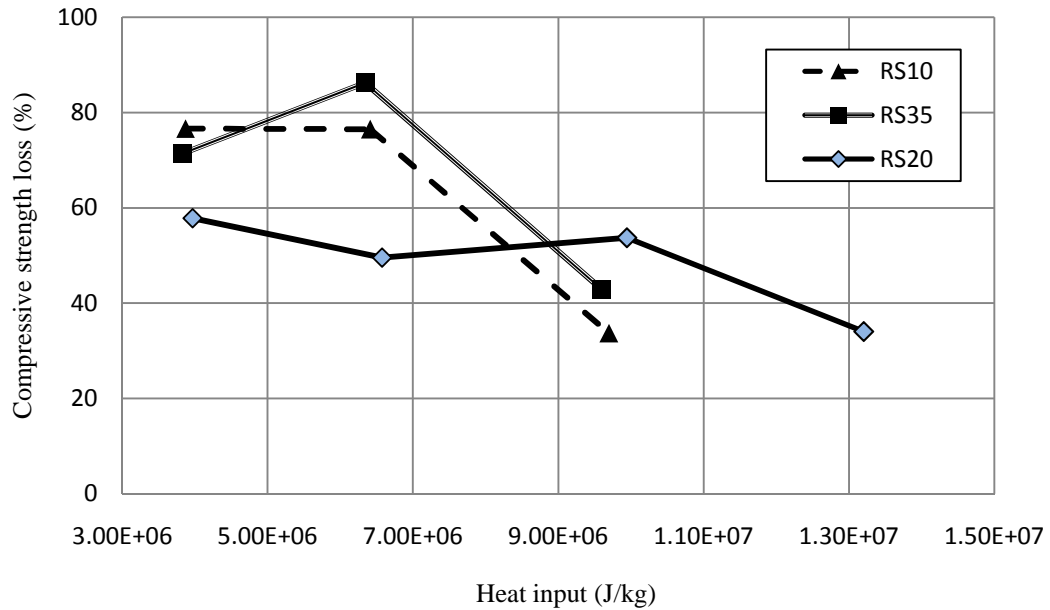


Figure 5.21 Compressive strength loss (%) at 600° C of concrete of recycled stone aggregate (all strength)

5.2.3 Compressive strength loss (%) at 600° C with respect to coarse aggregate porosity at different heating paths

In Figure 5.22 average of compressive strength losses of concrete of all types of aggregates with respect to coarse aggregate porosity is presented. Statistical significance of averaging is shown by marking high and low points. It is apparent that there is a range of coarse aggregate porosity (3% to 8%) in between which compressive strength loss is high. Beyond this band of coarse aggregate porosity, compressive strength loss is relatively low for concrete of coarse aggregate having both low and high value of porosity. It is also observed from Figures 5.23 to 5.25 that compressive strength loss is high at fast heating rate (PATH 1, Fig. 1.3, Sec, 1.5) and gradually decreases when heating rate gradually becomes slower (PATH 2 - 4). Furthermore, Compressive strength loss is more for concrete having high strength than low strength concrete of all types of aggregates.

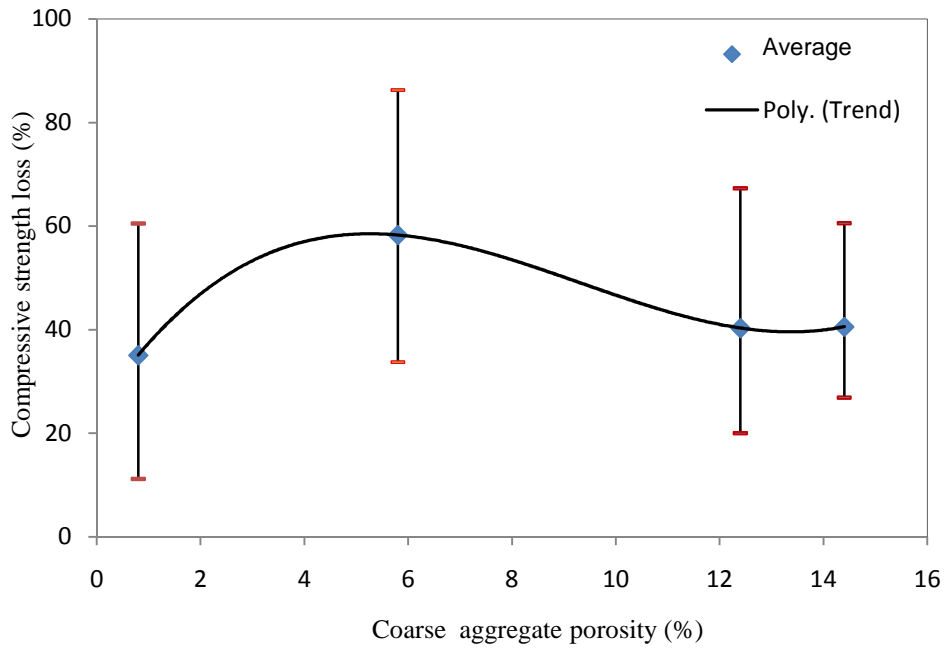


Figure 5.22 Compressive strength loss (%) at 600° C with respect to coarse aggregate porosity at different heating paths for all types of concrete.

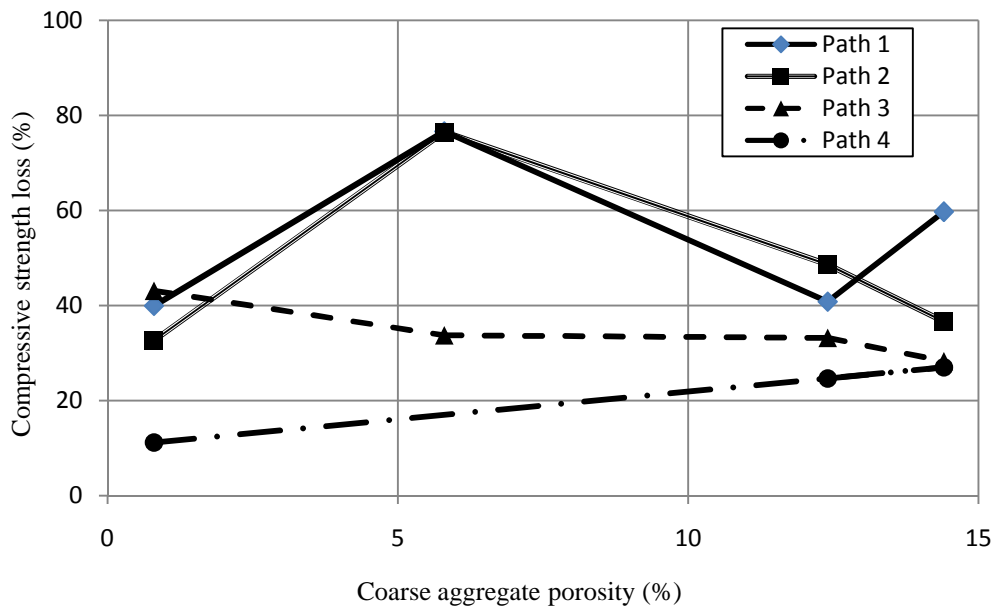


Figure 5.23 Compressive strength loss (%) at 600° C with respect to coarse aggregate porosity for 10 MPa concrete at different heating paths.

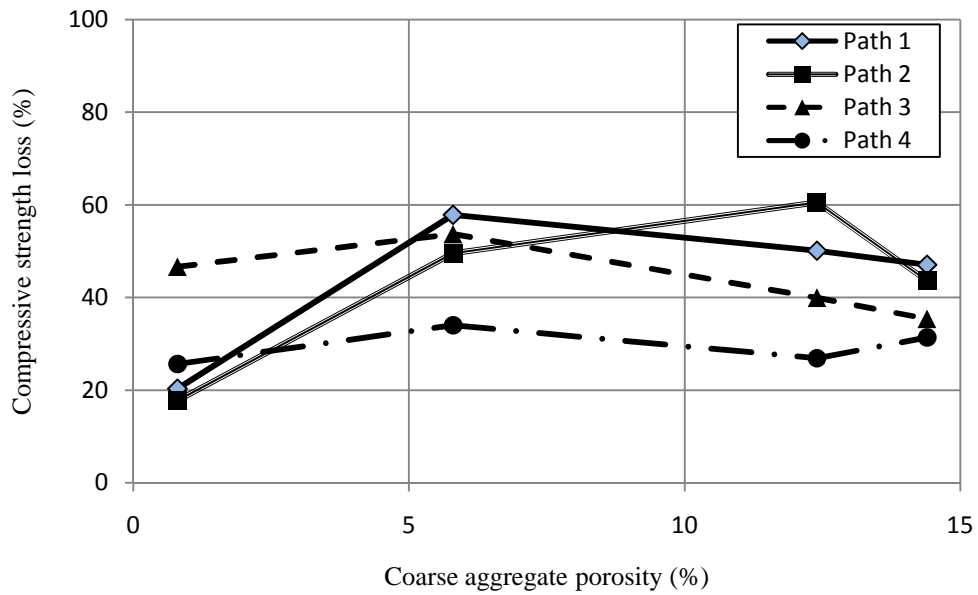


Figure 5.24 Compressive strength loss (%) at 600° C with respect to coarse aggregate porosity for 20 MPa concrete at different heating paths.

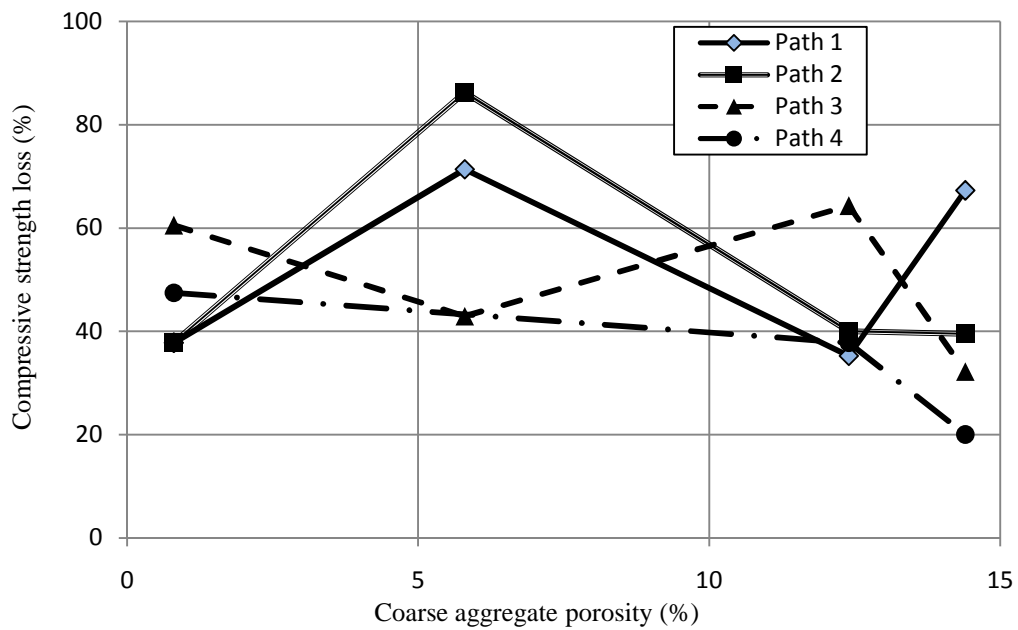


Figure 5.25 Compressive strength loss (%) at 600° C with respect to coarse aggregate porosity for 35 MPa concrete at different heating paths.

5.2.4 Compressive strength loss (%) at 600° C with respect to concrete porosity at different heating paths

In Figure 5.26 average of compressive strength losses of concrete after high temperature episode of all types of aggregates with respect to concrete porosity is presented. Data scatterings are also presented in the figure. It has been observed that there is a range of concrete porosity (10% to 20%) in between which compressive strength loss is high. Beyond this band of concrete porosity compressive strength loss is lower for concrete having both low and high value of porosity. It is also observed from Figures 5.27 to 5.33 that loss of compressive strength in slow heating path (PATH 1, Fig. 1.3, Sec, 1.5) is lower than that of fast heating path (PATH 4) for all types of concrete. Furthermore, compressive strength loss is high for recycled stone aggregate concrete (Figure 5.33) and low for stone aggregate concrete (Figure 5.30).

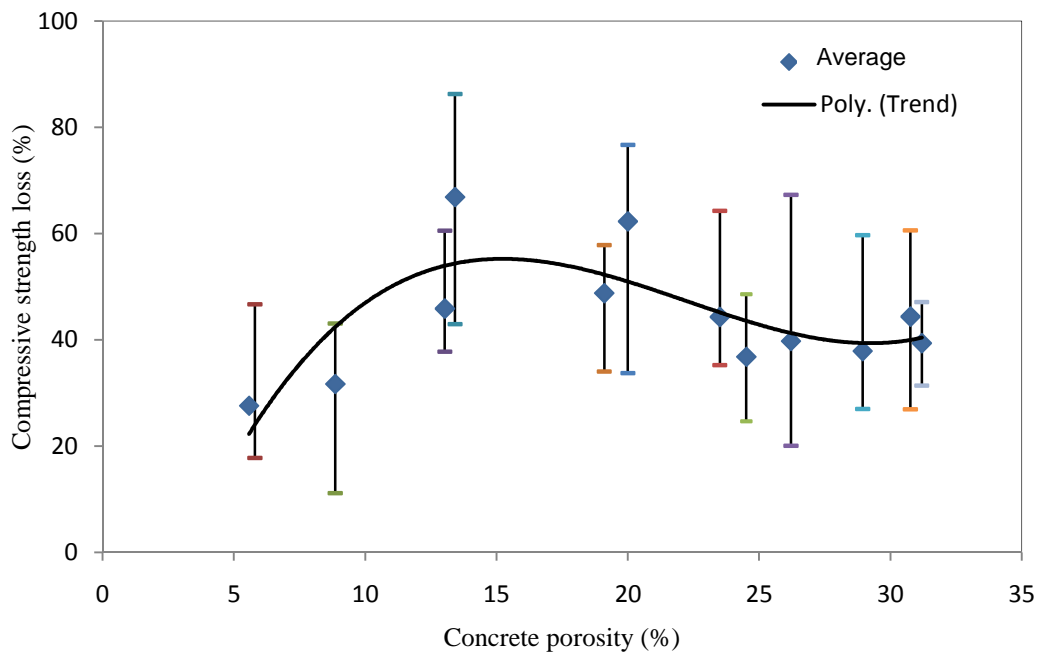


Figure 5.26 Compressive strength loss (%) at 600° C with respect to concrete porosity for all types of concrete.

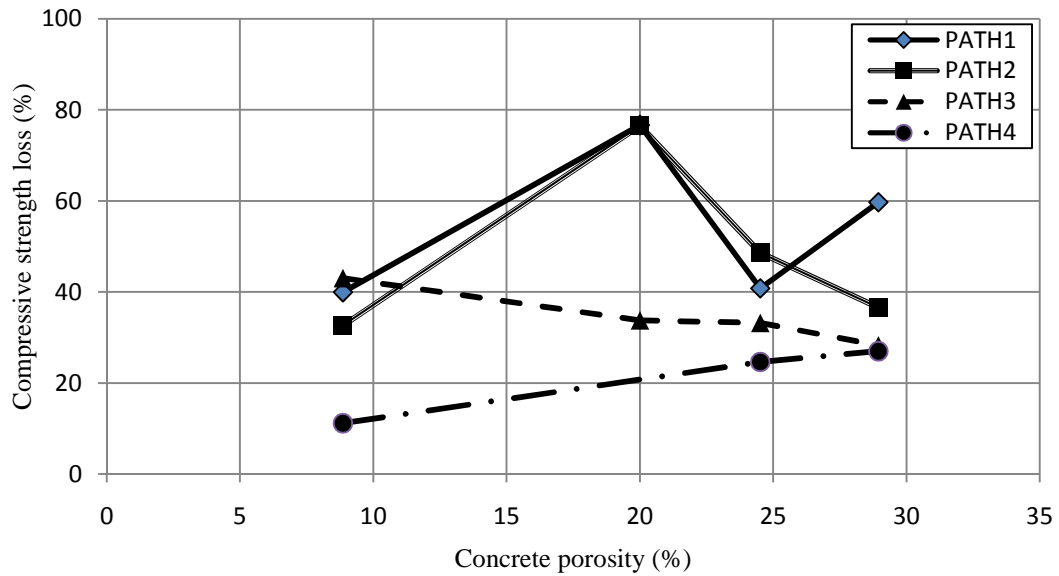


Figure 5.27 Compressive strength loss (%) at 600° C with respect to concrete porosity for 10 MPa concrete at different heating paths.

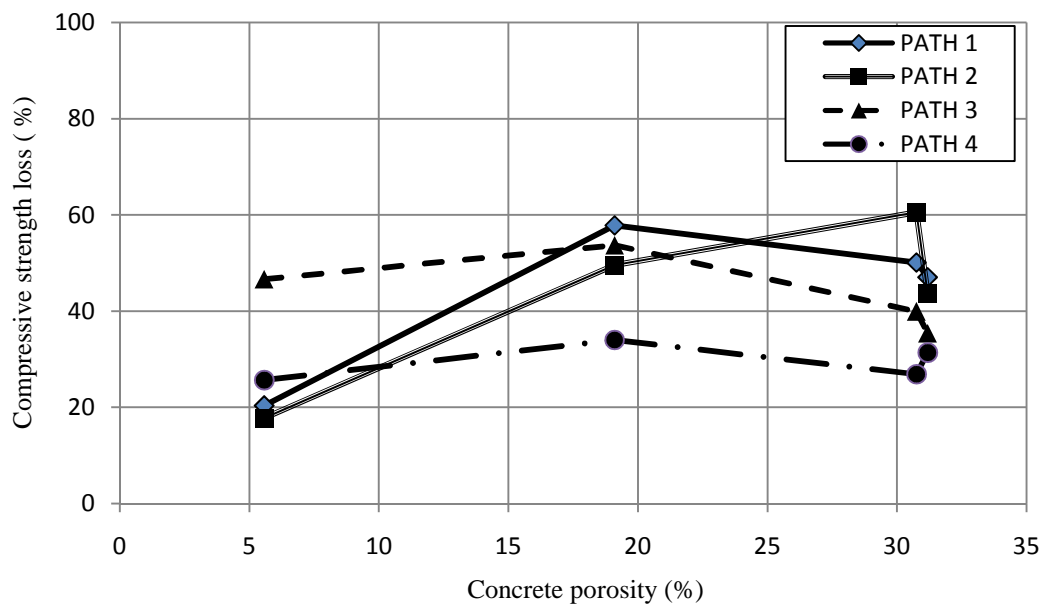


Figure 5.28 Compressive strength loss (%) at 600° C with respect to concrete porosity for 20 MPa concrete at different heating paths.

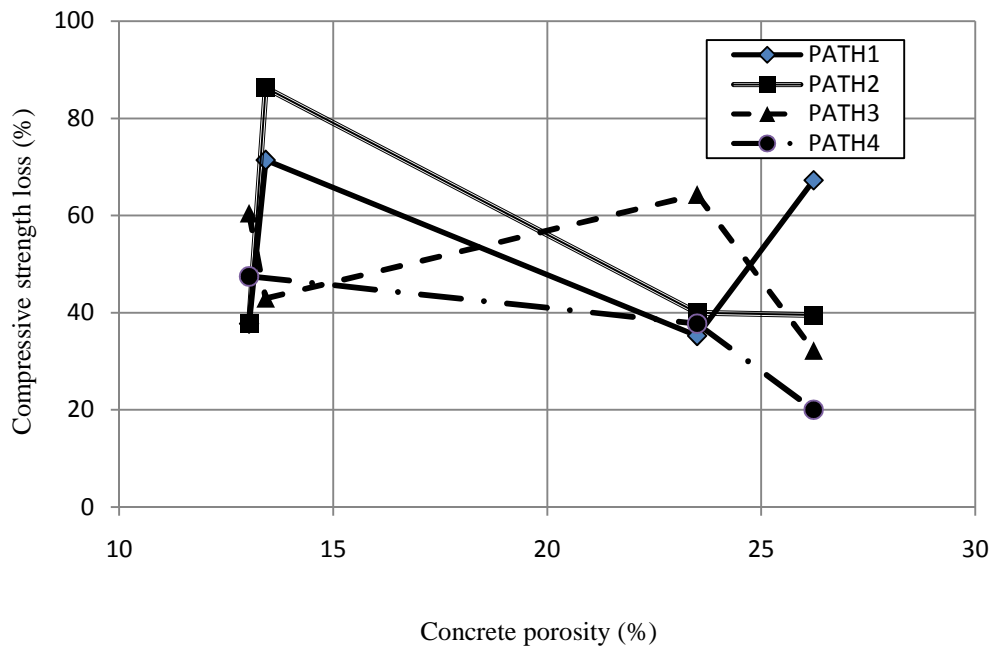


Figure 5.29 Compressive strength loss (%) at 600° C with respect to concrete porosity for 35 MPa concrete at different heating paths.

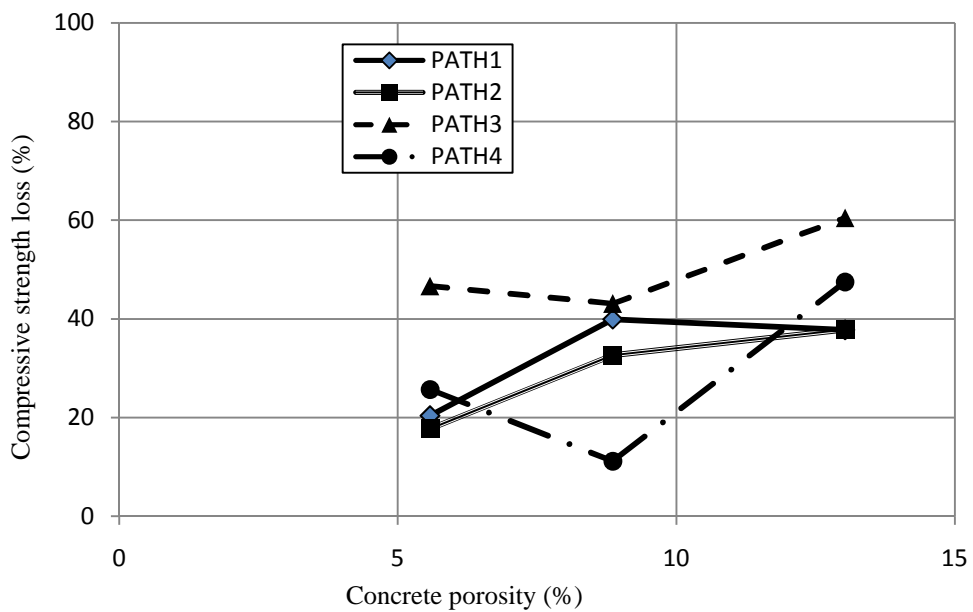


Figure 5.30 Compressive strength loss (%) at 600° C for stone aggregate concrete at different heating paths.

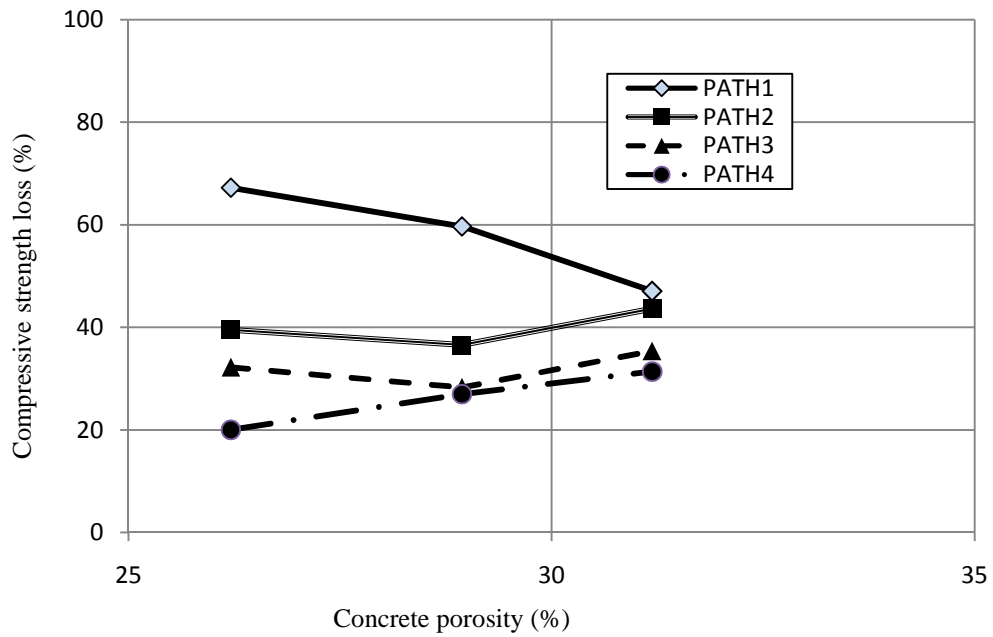


Figure 5.31 Compressive strength loss (%) at 600° C for brick aggregate concrete at different heating paths.

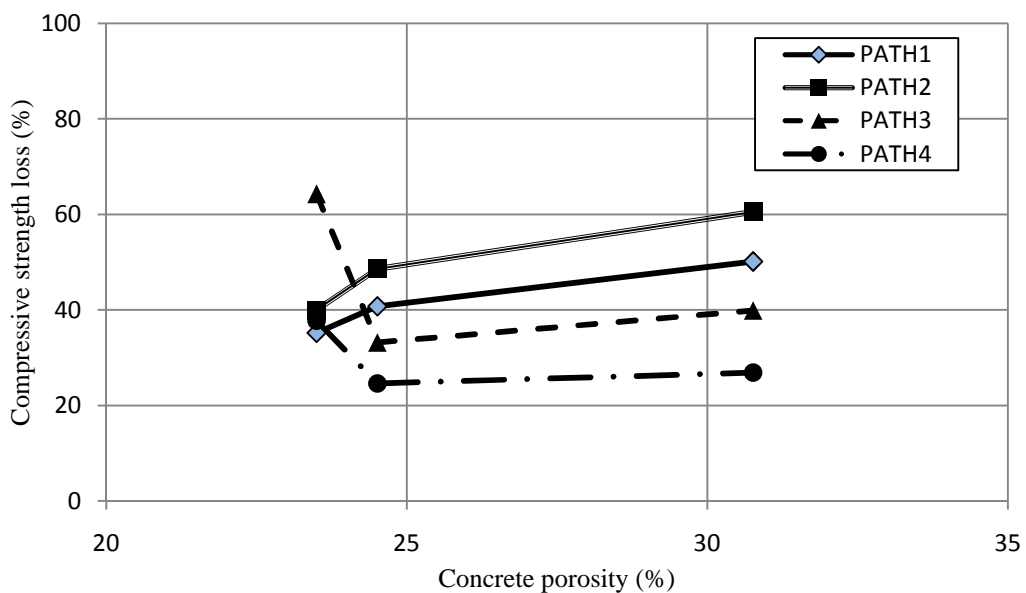


Figure 5.32 Compressive strength loss (%) at 600° C for recycled brick aggregate concrete at different heating paths.

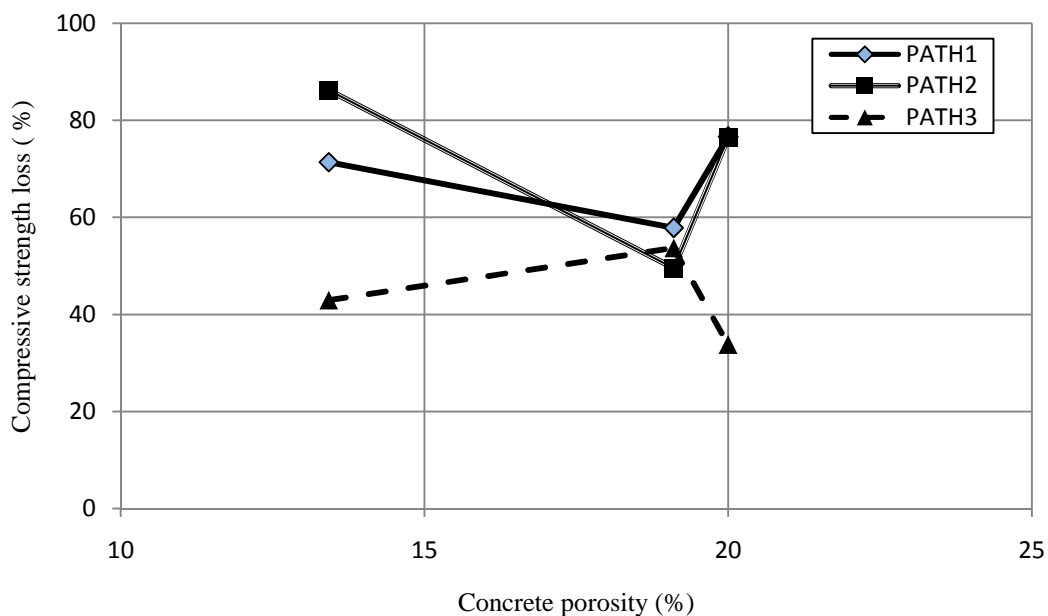


Figure 5.33 Compressive strength loss (%) at 600° C for recycled stone aggregate concrete at different heating paths

5.2.5 Residual compressive strength at different temperatures and heating paths

It has been clearly observed from Figures 5.34 to 5.45 that residual compressive strength after heat treatment is inversely proportional to temperature to which the specimens were subjected to. At a fast heating path (PATH 1, Fig. 1.3, Sec. 1.5) residual compressive strength is low and relatively high at slower heating rate (PATH 2 - 4). These findings are in conformity with past study results (Toumi, et al. 2009, Saad et al. 1996).

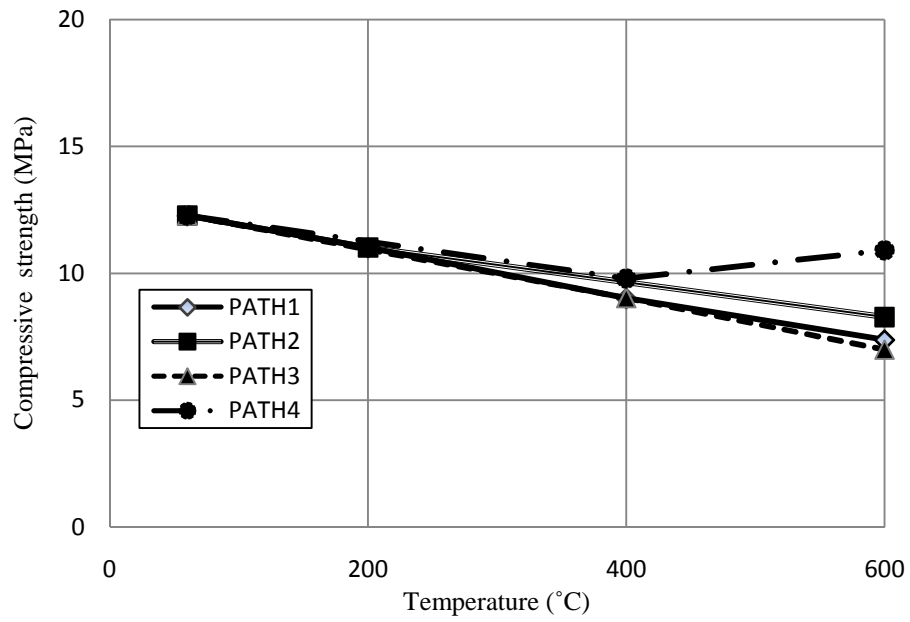


Figure 5.34 Residual compressive strength at different heating paths for S10 concrete.

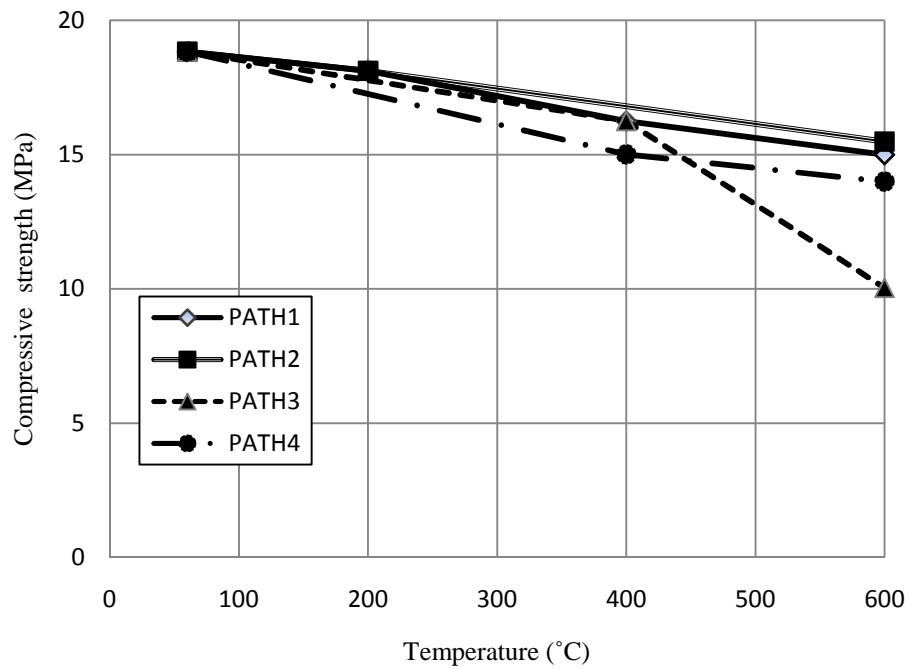


Figure 5.35 Residual compressive strength at different heating paths for S20 concrete.

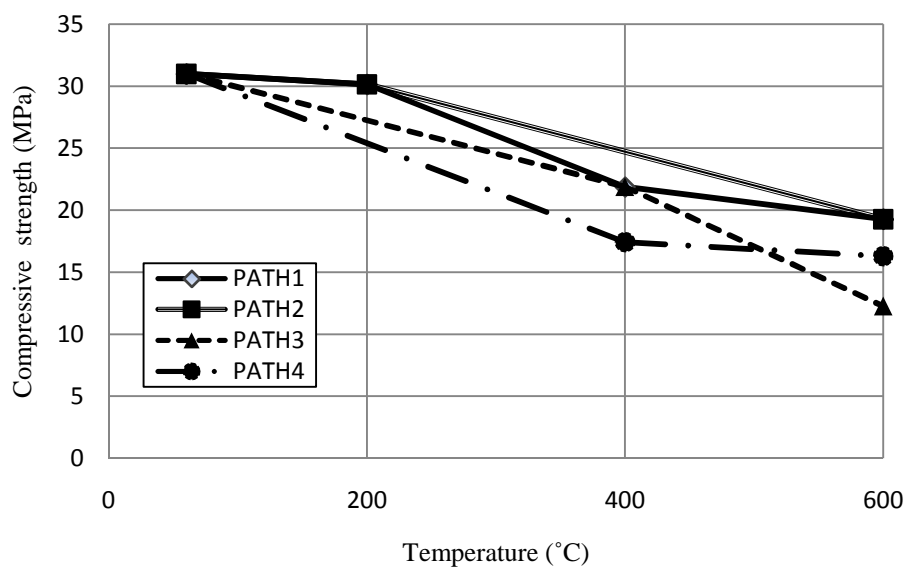


Figure 5.36 Residual compressive strength at different heating paths for S35 concrete.

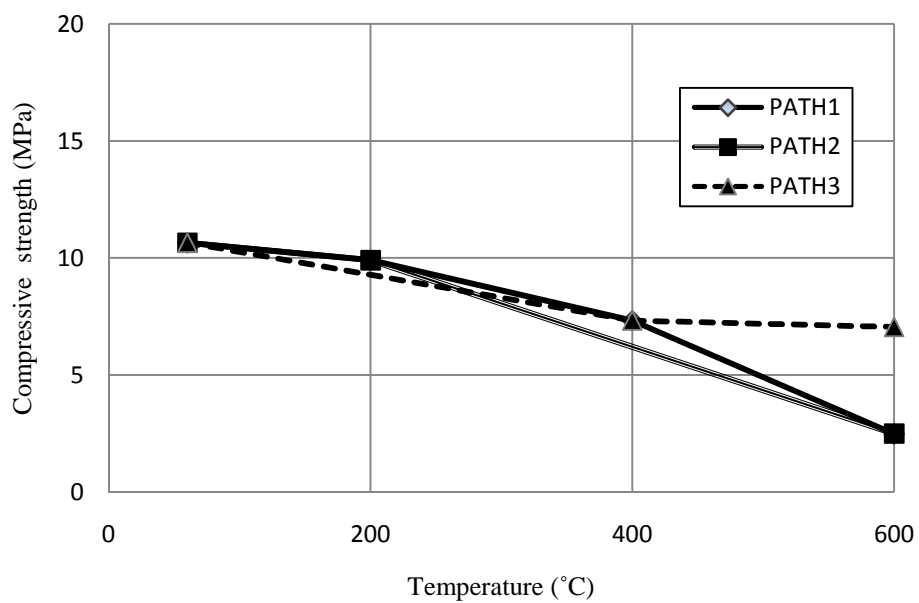


Figure 5.37 Residual compressive strength at different heating paths for RS10 concrete.

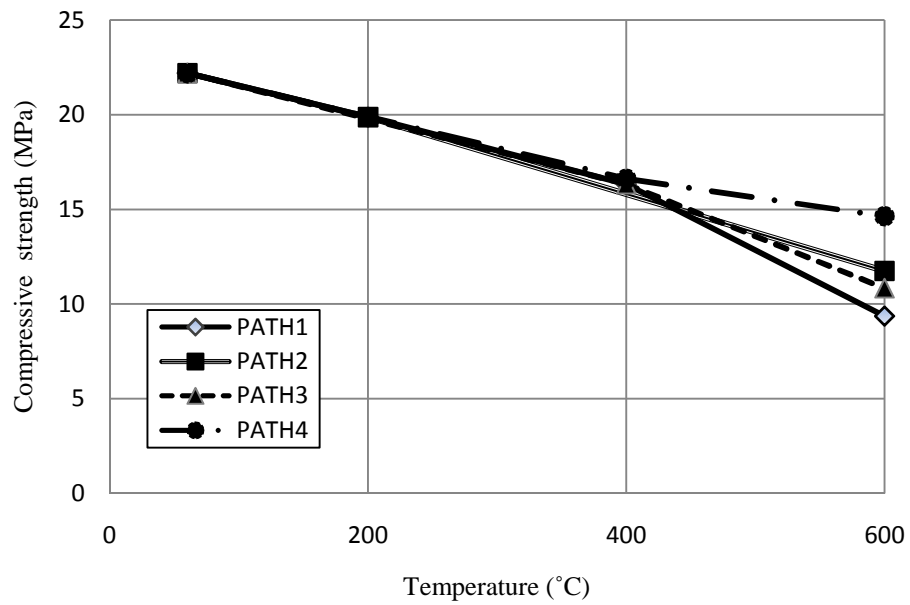


Figure 5.38 Residual compressive strength at different heating paths for RS20 concrete.

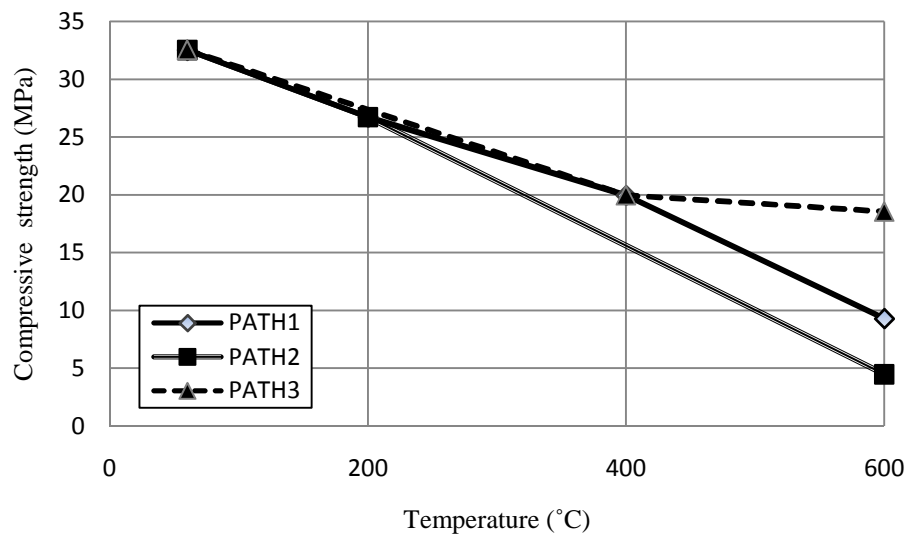


Figure 5.39 Residual compressive strength at different heating paths for RS35 concrete.

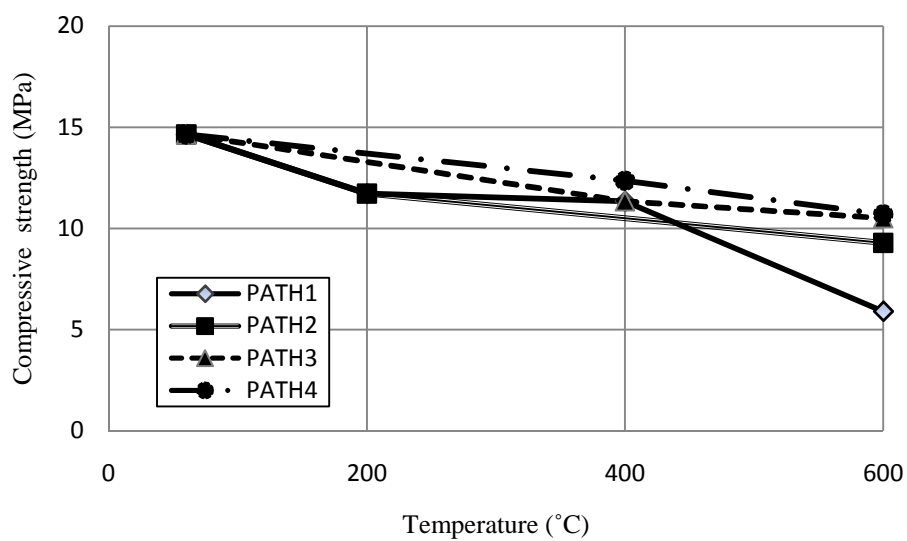


Figure 5.40 Residual compressive strength at different heating paths for B10 concrete.

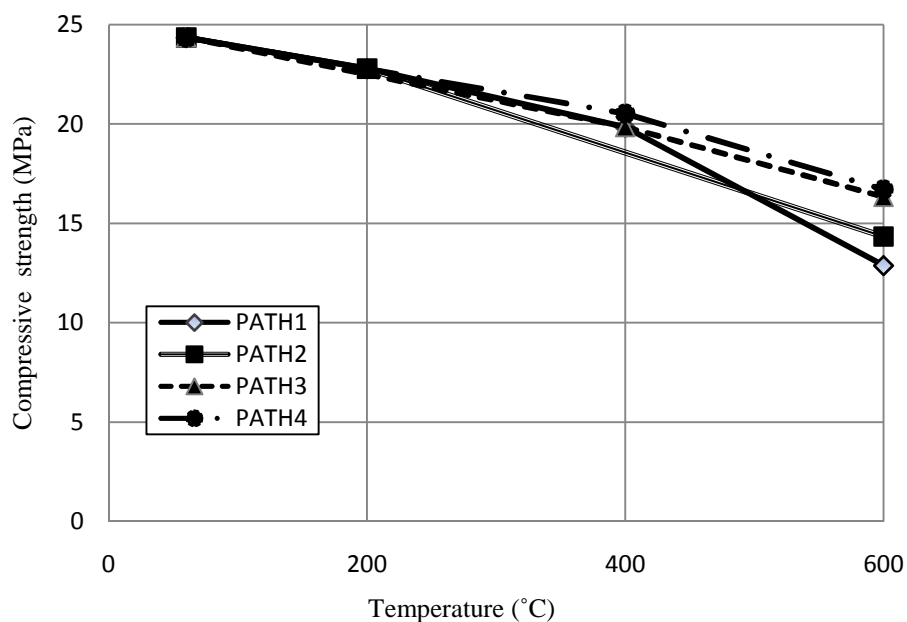


Figure 5.41 Residual compressive strength at different heating paths for B20 concrete.

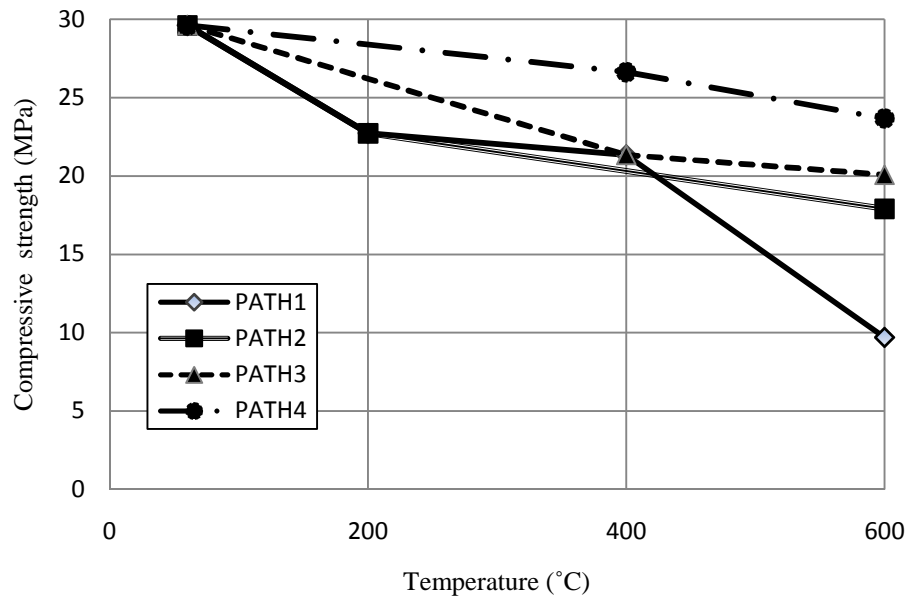


Figure 5.42 Residual compressive strength at different heating paths for B35 concrete.

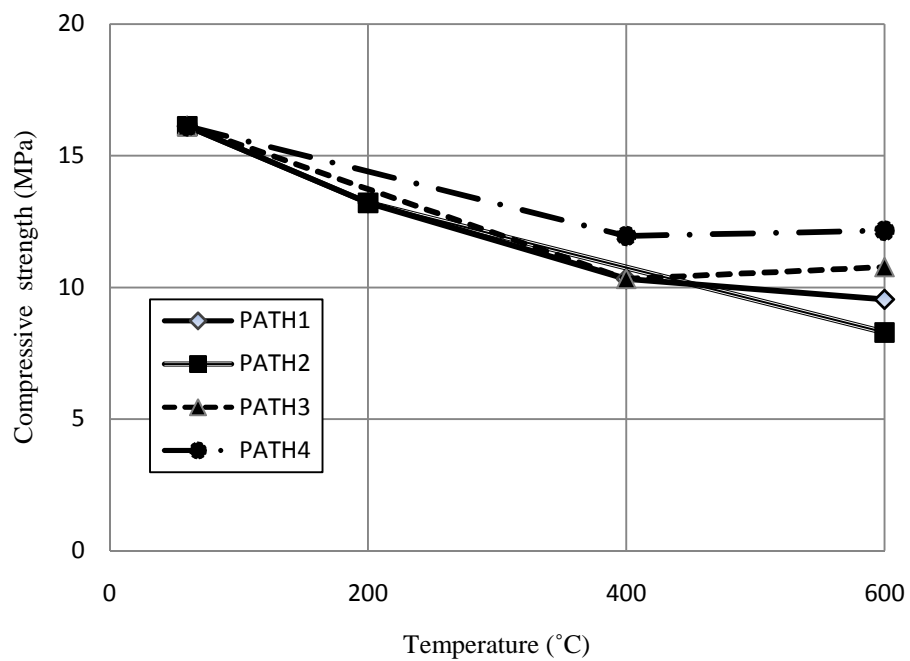


Figure 5.43 Residual compressive strength at different heating paths for RB10 concrete.

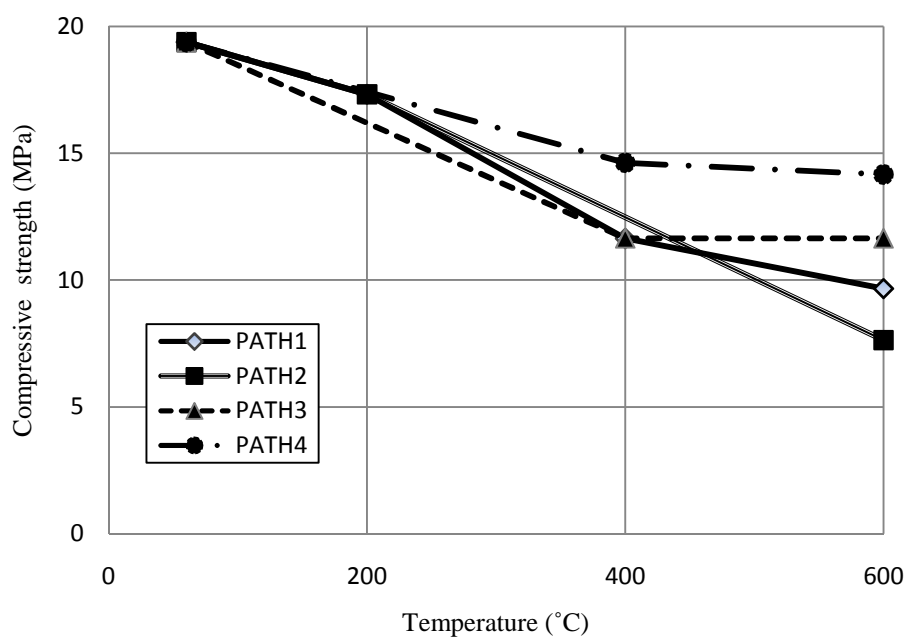


Figure 5.44 Residual compressive strength at different heating paths for RB20 concrete.

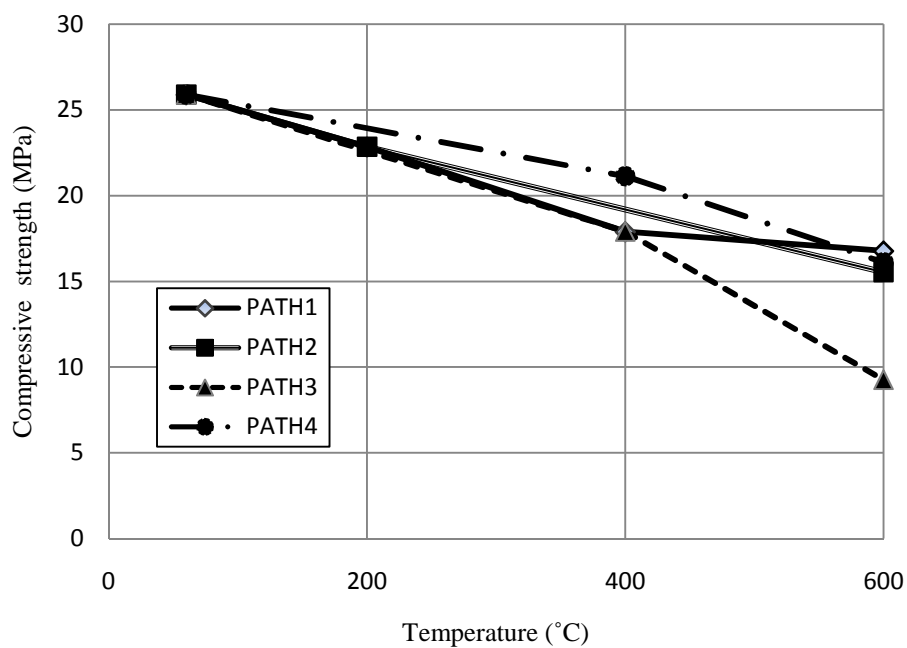


Figure 5.45 Residual compressive strength at different heating paths for RB35 concrete.

5.2.6 Mass loss (%) at 600° C with respect to coarse aggregate porosity and concrete porosity for different types of concrete

In Figures 5.46 and 5.49 averages of mass losses of concrete of all types of aggregate with respect to coarse aggregate porosity and concrete porosity are presented. Statistical significance of averaging is shown by marking high and low points. It has been observed that there is a trend of increasing mass loss with increase of both coarse aggregate porosity and concrete porosity. Figures 5.36 and 5.37 show the loss of mass with respect to coarse aggregate porosity and concrete porosity for different heating paths. It is found that mass loss is proportional to porosity of both coarse aggregate and concrete. Mass loss due to heating phenomenon for all aggregate concrete varies from 5% to 15% for different strength grade concrete. Mass loss is maximum in PATH 3 (Fig. 1.3, Sec. 1.5) but it could be in PATH 4. This may be due to the reason that the samples of heating PATH 4 were tested after a long time from casting.

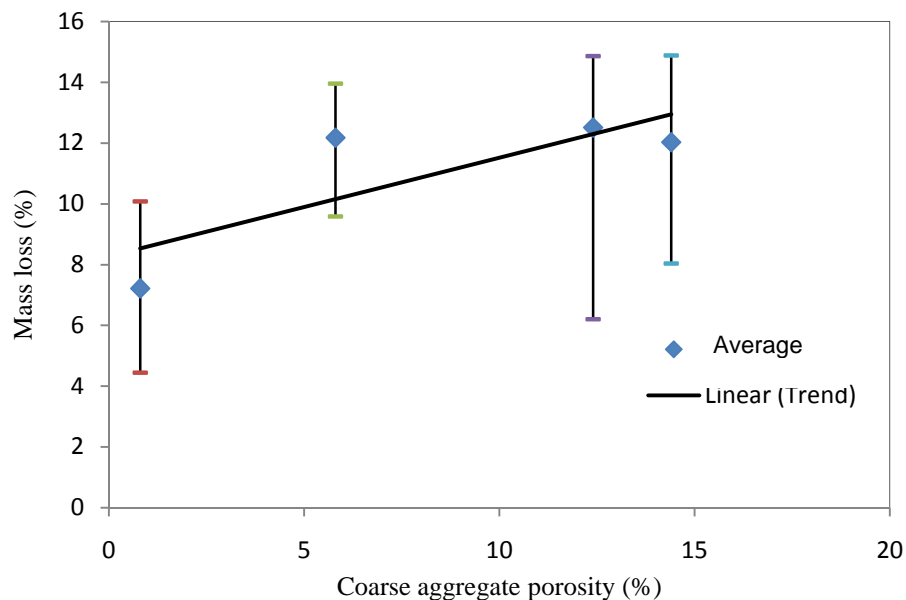


Figure 5.46 Mass loss (%) at 600° C with respect to coarse aggregate porosity for all types of concrete.

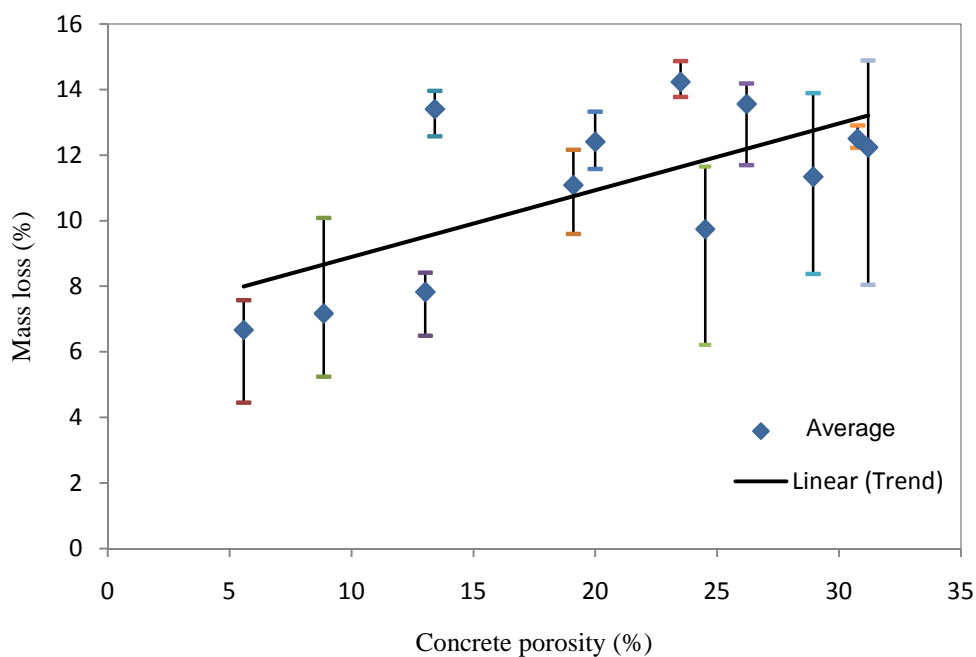


Figure 5.47 Mass loss (%) at 600° C with respect to concrete porosity for all types of concrete.

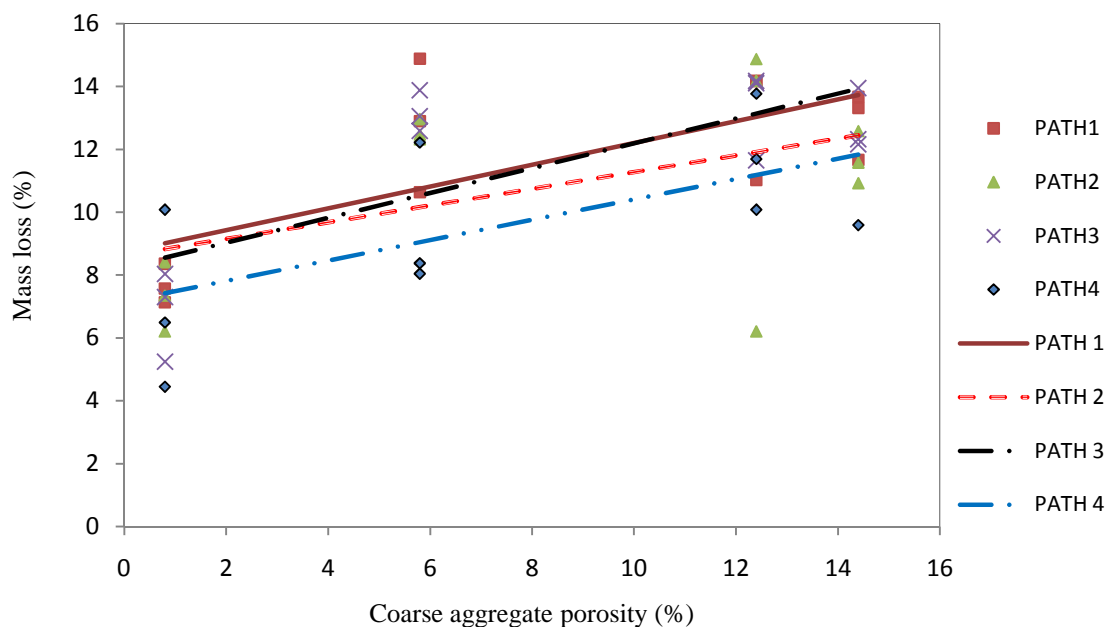


Figure 5.48 Mass loss (%) at 600° C with respect to coarse aggregate porosity at different heating paths for all types of concrete.

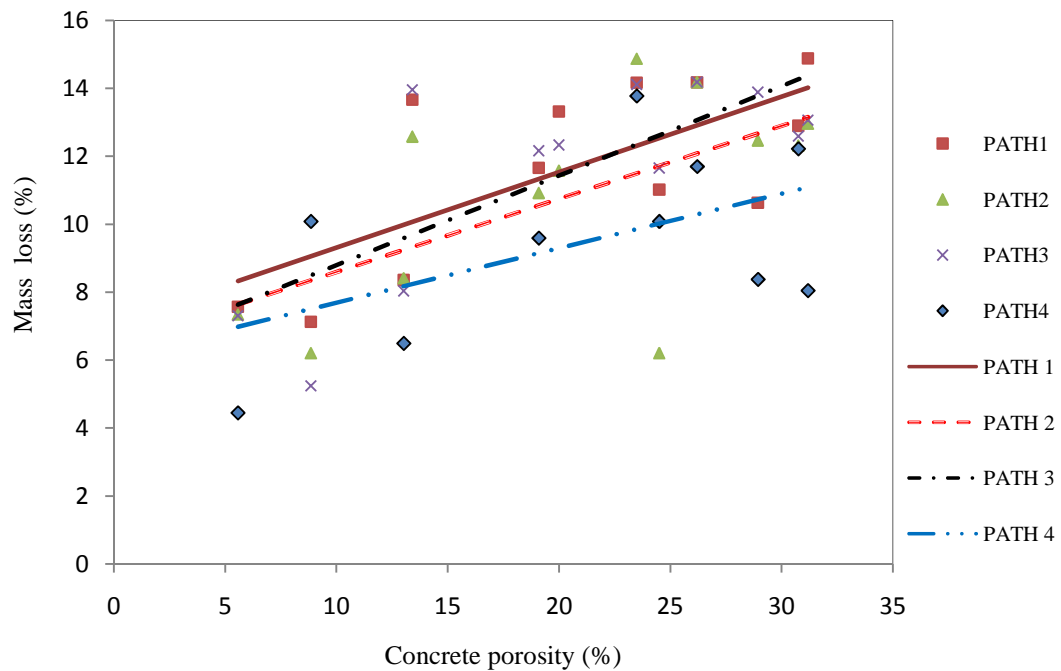


Figure 5.49 Mass loss (%) at 600°C with respect to concrete porosity at different heating paths for all types of concrete.

5.2.7 Mass loss (%) at different temperatures for different types of concrete at different heating paths

It has been observed from Figures 5.50 to 5.61 mass loss due to heating phenomenon for stone aggregate concrete varies from 6% to 8% for different strength grade concrete at heating PATH 1, 2 and 3 but in heating PATH 4 (Fig. 1.3, Sec. 1.5) mass loss is about 5% which is lower than that of other heating paths because samples of heating PATH 4 were tested after a long time from casting and moisture were evaporated. Mass loss of recycled stone aggregate concrete, brick aggregate concrete and recycled brick aggregate concrete due to heat episodes vary from 10% to 15% for different strength grade concrete at heating PATH 1, 2, 3, and 4.

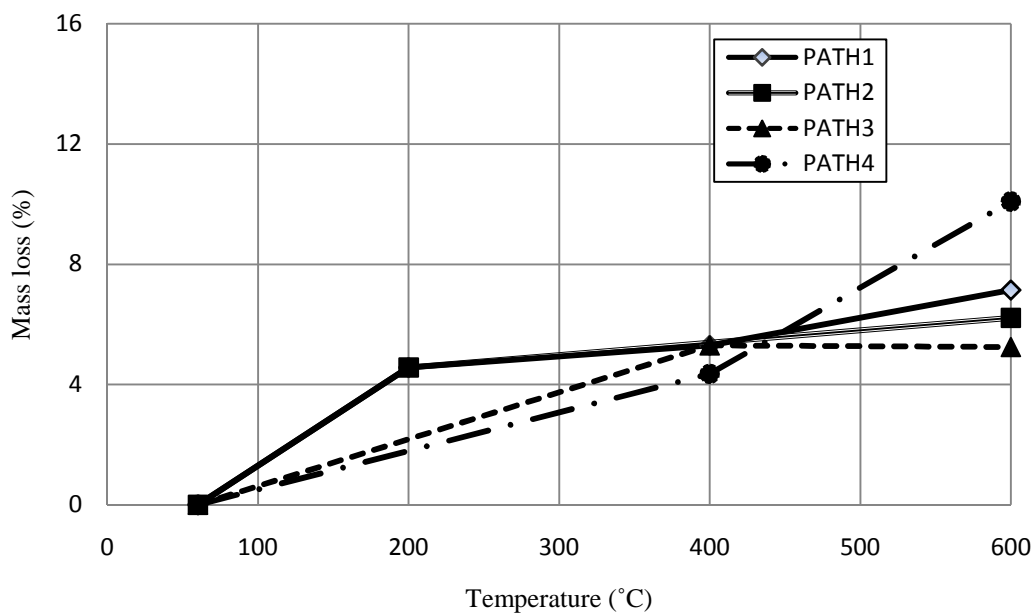


Figure 5.50 Mass loss (%) at different temperatures and different heating paths for S10 concrete.

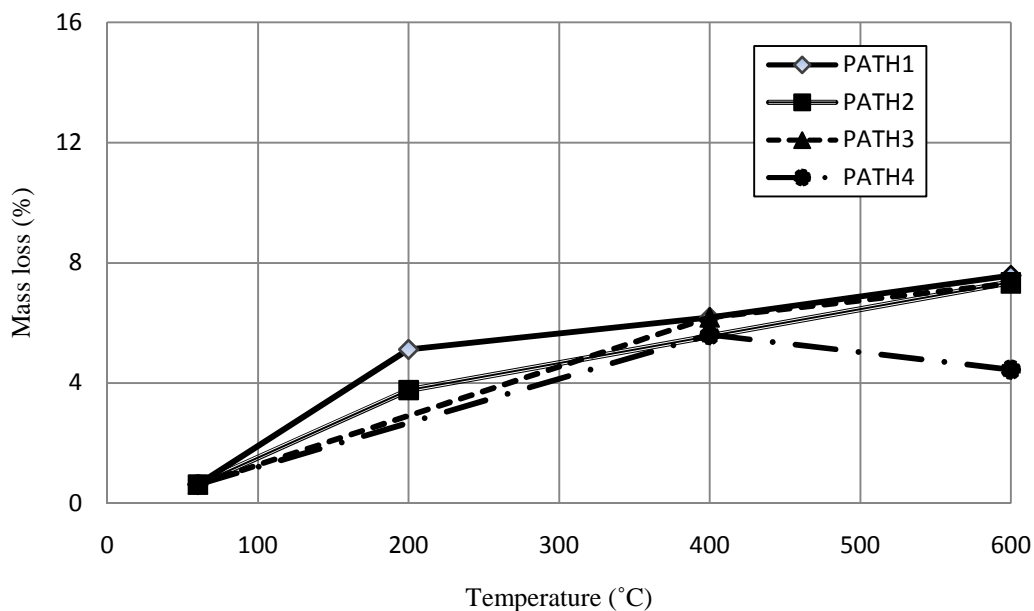


Figure 5.51 Mass loss (%) at different temperatures and different heating paths for S20 concrete.

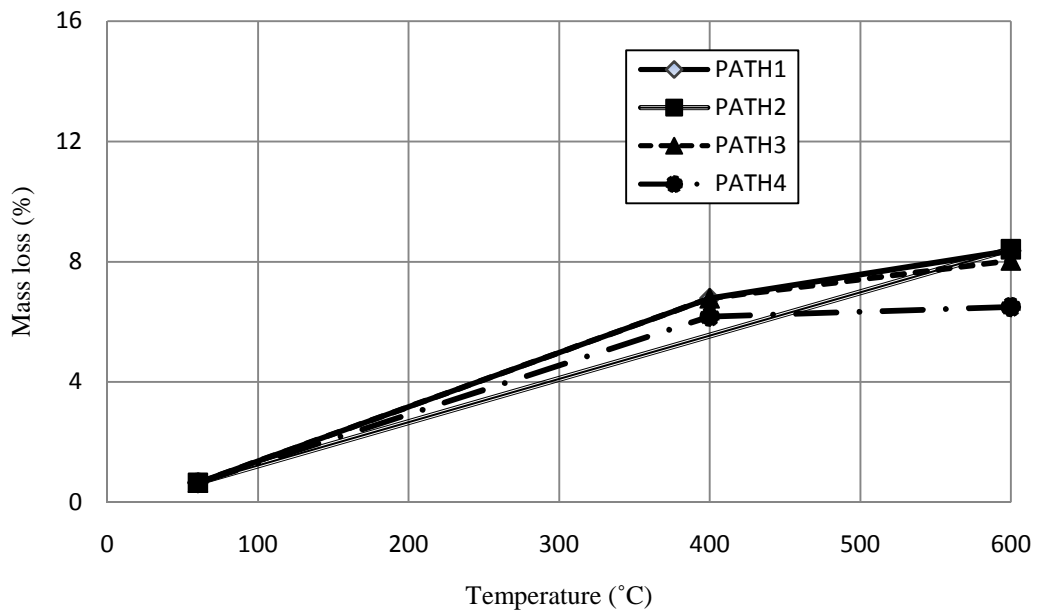


Figure 5.52 Mass loss (%) at different temperatures and different heating paths for S35 concrete.

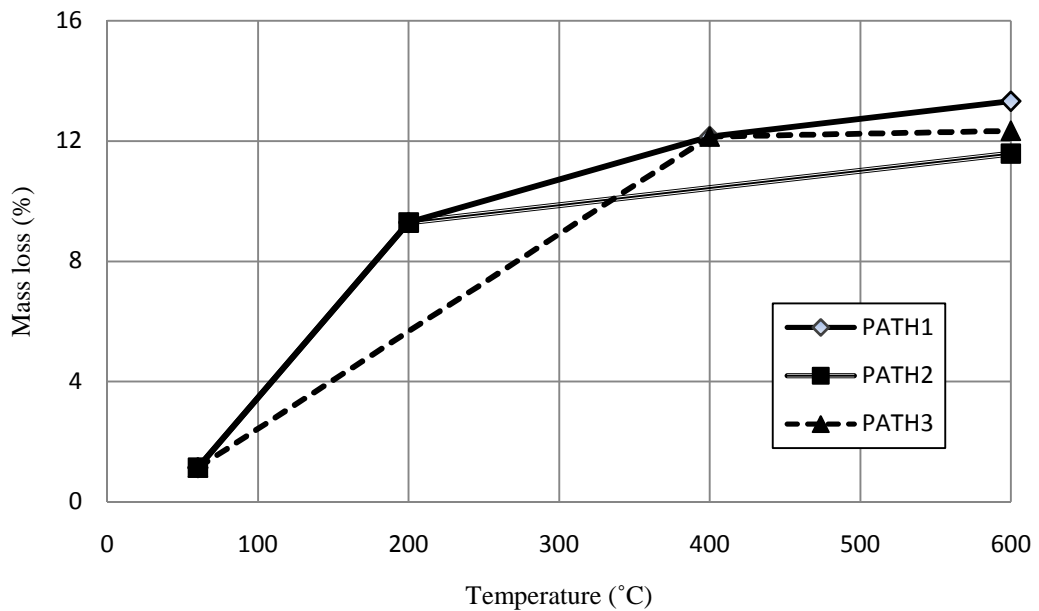


Figure 5.53 Mass loss (%) at different temperatures and different heating paths for RS10 concrete.

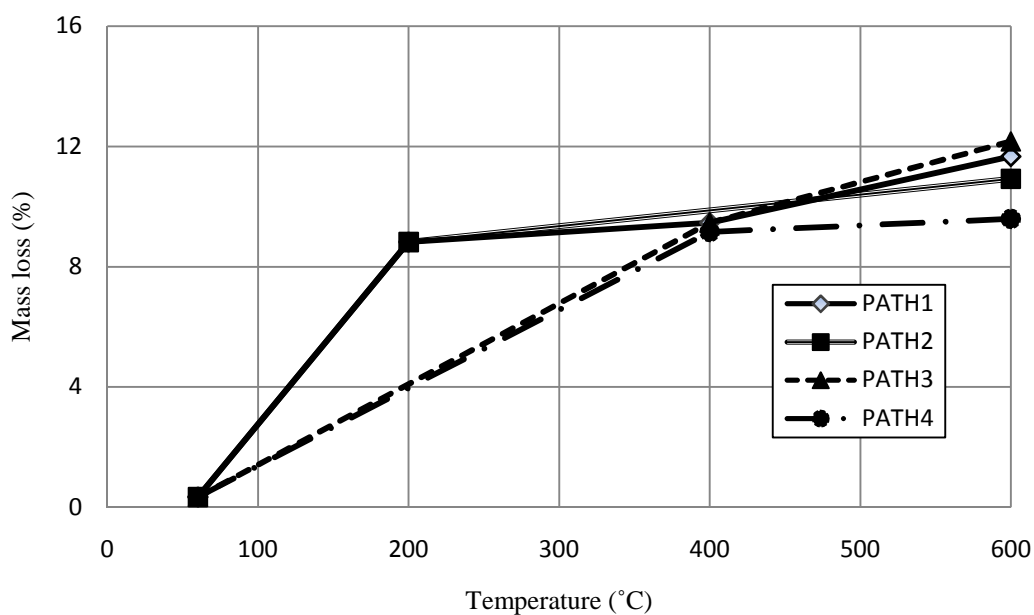


Figure 5.54 Mass loss (%) at different temperatures and different heating paths for RS20 concrete.

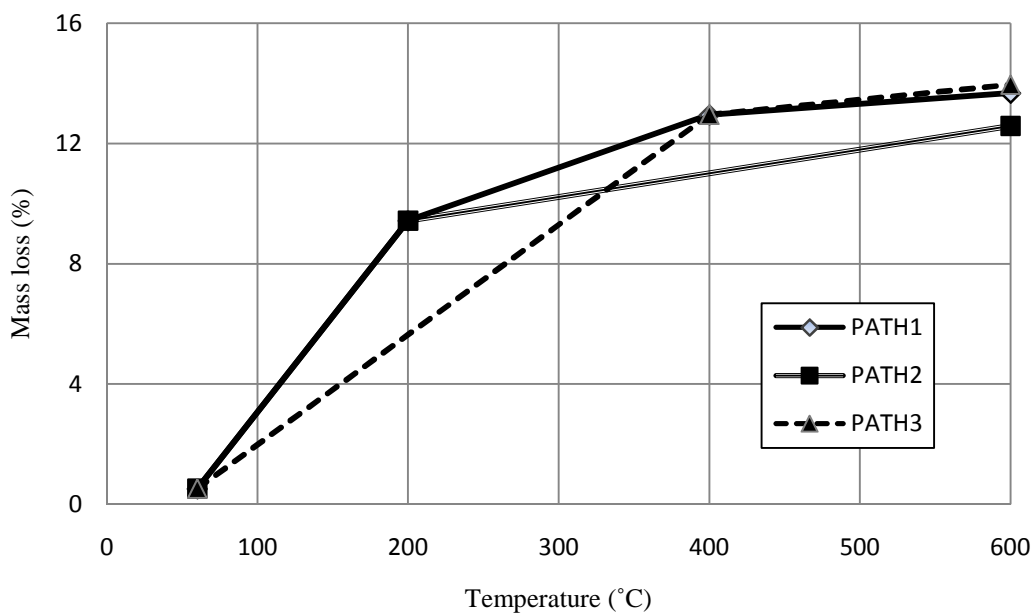


Figure 5.55 Mass loss (%) at different temperatures and different heating paths for RS35 concrete.

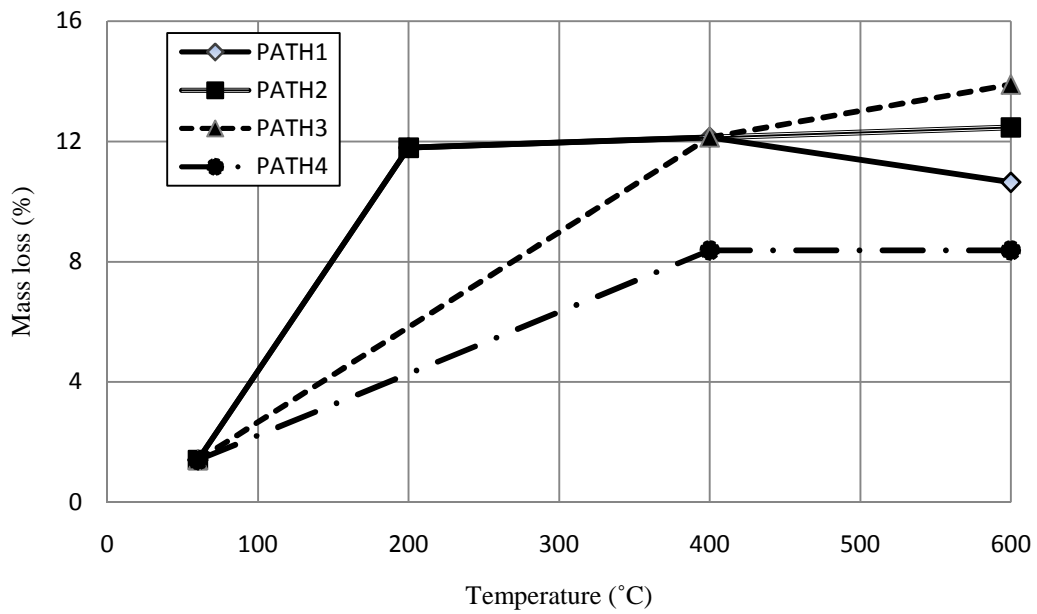


Figure 5.56 Mass loss (%) at different temperatures and different heating paths for B10 concrete.

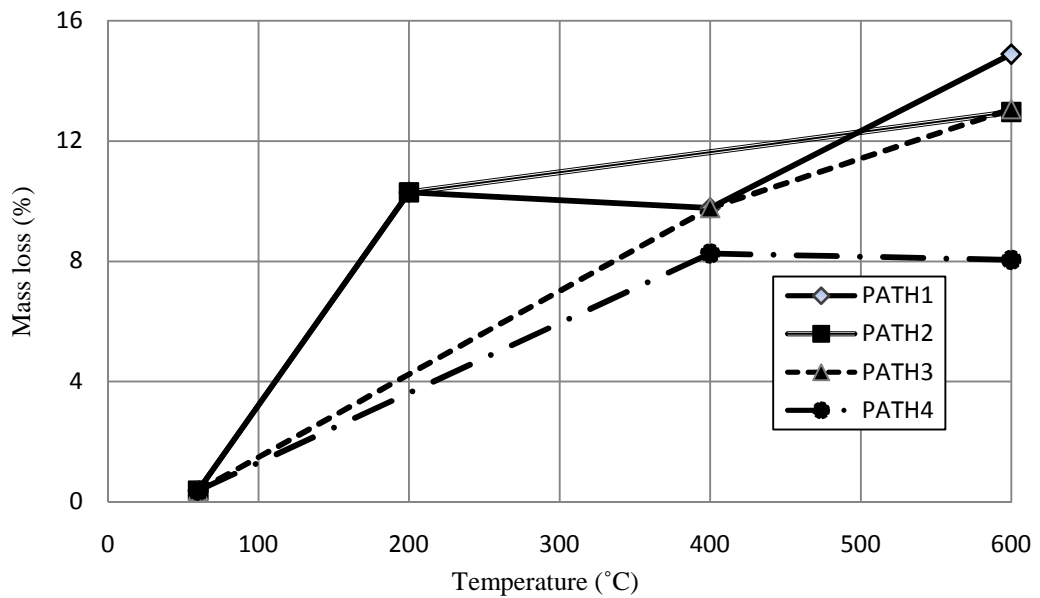


Figure 5.57 Mass loss (%) at different temperatures and different heating paths for B20 concrete.

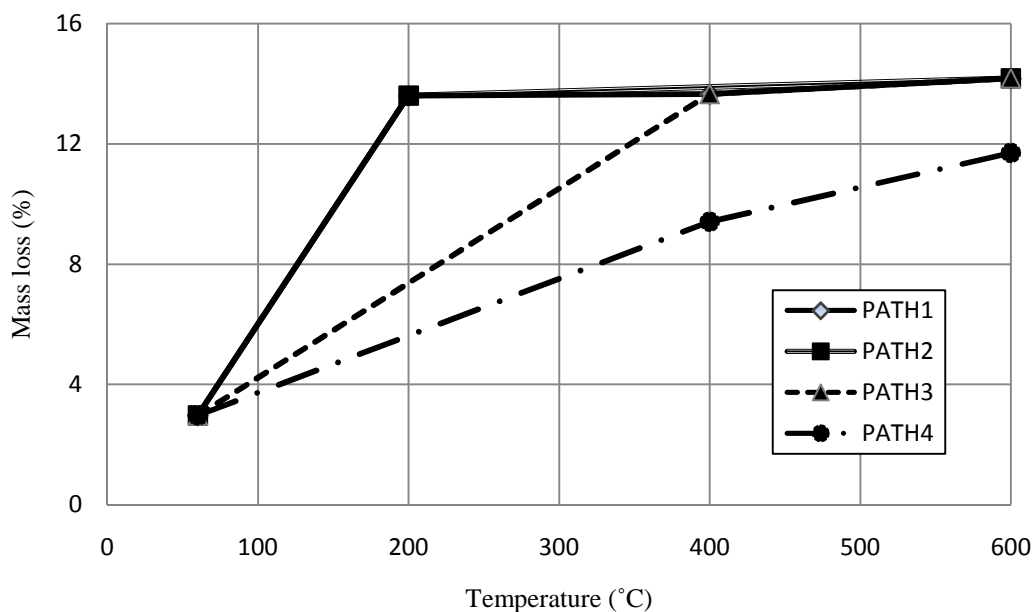


Figure 5.58 Mass loss (%) at different temperatures and different heating paths for B35 concrete.

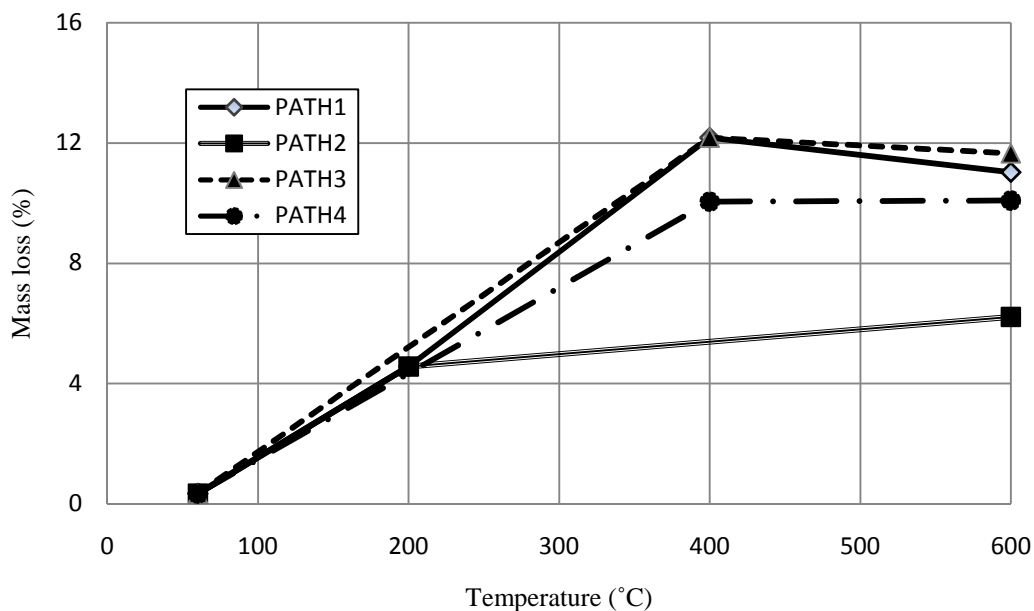


Figure 5.59 Mass loss (%) at different temperatures and different heating paths for RB10 concrete.

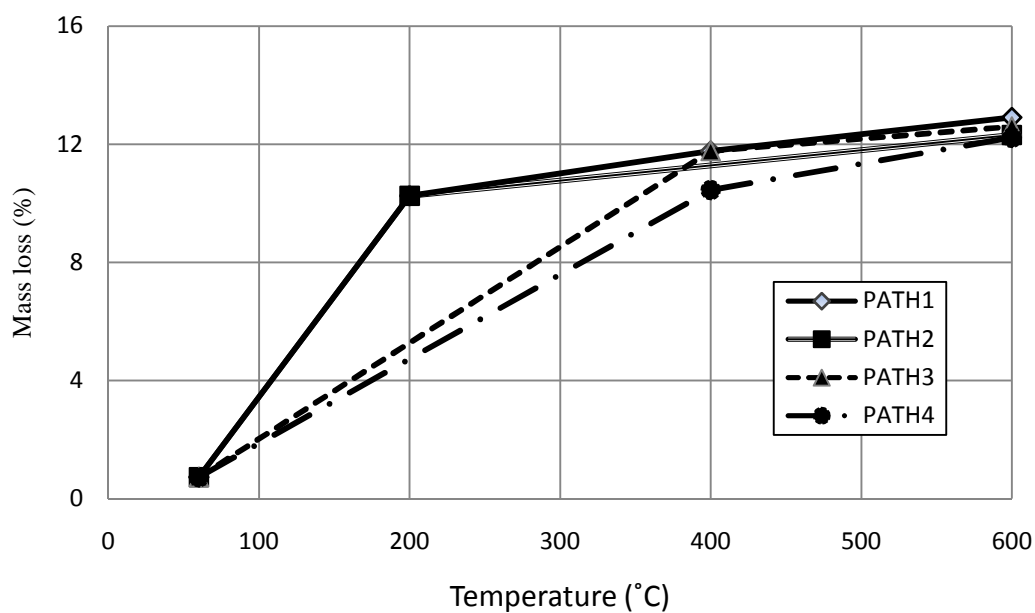


Figure 5.60 Mass loss (%) at different temperatures and different heating paths for RB20

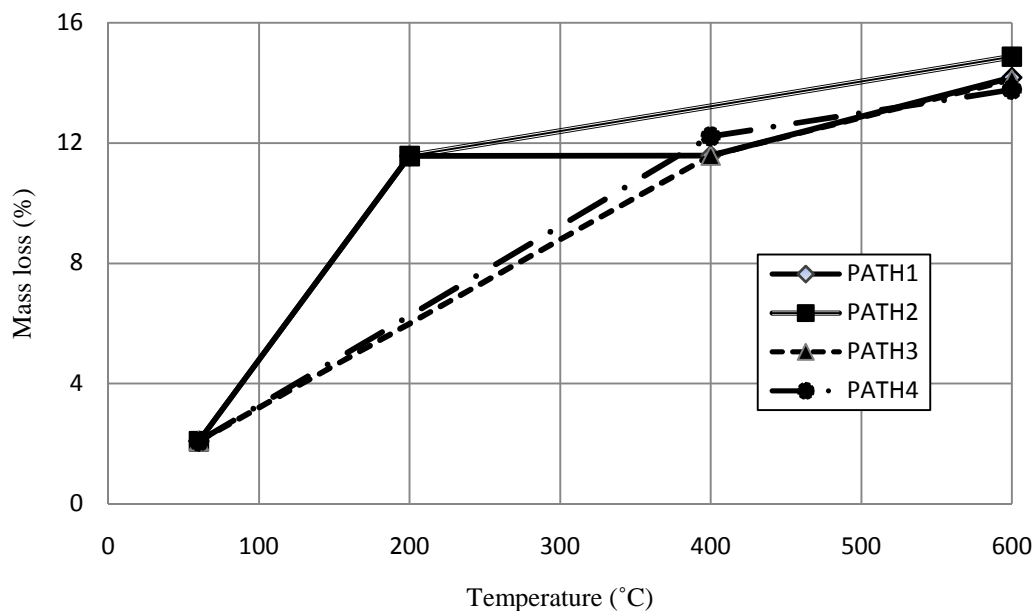


Figure 5.61 Mass loss (%) at different temperatures and different heating paths for RB35

6.1 GENERAL

The compressive behavior of concrete after a heat (possibly induced by fire) episode is not well characterized. Stone aggregate, brick aggregate, recycled stone aggregate recycled brick aggregate have different physical properties in terms of strength, absorption capacity, porosity, modulus of elasticity, Poisson's ratio and unit weight. These aggregates have important effect on the behavior of concrete after high temperature episodes. To characterize those effects, 384 nos. normal strength concrete (10 MPa, 20 MPa, and 35 MPa) cylinder specimens were produced using four types of aggregate and mechanical properties were tested after heat treatment at different temperature. The effect of such temperature episodes on compressive strength and loss of mass relating the porosity of coarse aggregate and concrete were studied.

6.2 EFFECT OF STRENGTH

Experimental results generally indicate that compressive strength loss is proportional to temperature to which the specimens were subjected to. In a particular aggregate type compressive strength loss was found to be higher for concrete with high initial strength. It is clear that compressive strength loss of high strength concretes made of all types of aggregates is more than that of low strength concrete exposed to high temperature episode. Effect of concrete strength on loss of mass after a fire episode is found insignificant.

6.3 EFFECT OF HEATING RATE

Compressive strength loss is seen to be proportional to the rate of heating. Furthermore, to attain a specific ultimate temperature in all heating PATHs when heat input is gradually increased in PATH 1 to PATH 4, the strength loss was found to

decrease at an inverse relation (Sec. 5.2.2). It is also observed that the same trend of decreasing rate of compressive strength loss with increase of heat input irrespective of coarse aggregate and grade (strength) of concrete. In a fast heating path, where less heat input used, compressive strength loss is found to be higher but gradually decreased with increase of heat input in heating PATHs generally having relatively slower heating rate. Furthermore, it is also observed from the study that mass loss increases with increase of both temperature and rate of heating for different strength grade concrete made of different aggregates exposed to high temperature episodes.

6.4 EFFECT OF COARSE AGGREGATE

It is observed from experiments that coarse aggregate has significant effect on behavior of concrete exposed to high temperature. It is observed from the study that there is a range of coarse aggregate porosity (3% to 8%) in between which compressive strength loss is high after high temperature exposure. Beyond this band of coarse aggregate porosity, compressive strength loss is relatively low for concrete of coarse aggregate having both low and high value of porosity. Furthermore, it is also apparent that there is a range of concrete porosity (10% to 20%) in between which compressive strength loss is high and beyond this band of concrete porosity, compressive strength loss is low for concrete having both high and low values of porosity. Compressive strength loss of brick aggregate concrete is higher than stone aggregate concrete. Compressive strength loss is maximum in low strength concrete of recycled stone aggregate and minimum in concrete of stone aggregate. Furthermore, it has been found that mass loss is proportional to porosity of both coarse aggregate and concrete. Mass loss is less for concrete of stone aggregate and little higher for recycled stone aggregate concrete, brick aggregate concrete and recycled brick aggregate concrete after heat treatment for different strength grade concrete.

6.5 SCOPE FOR FUTURE STUDIES

To establish a correlation with compressive strength loss, mass loss of concrete due to high temperature exposure with porosity of coarse aggregate which was aimed in this research. There are further scopes to study in this field to have enough data of residual strength of concrete after fire to support the findings of this study to establish the facts with better confidence. There is a scope for future research on strength loss of reinforced concrete under high temperature. To measure lateral dilation behavior of concrete after heat episodes is also worth exploring. Effects of controlled heating and cooling phases may be studied further.

REFERENCES

Abdel Alim, A. M. K., Abdel Aziz, G. E., El-Mohr, K. A. K, and Salama, G. A., (2009). "Effect of aggregate type on the fire resistance of normal and self compacting concretes" *Engineering Research Journal*, No.122, C47-C62.

Abdel Alim, A. M. K., Abdel Aziz, G. E., El-Mohr, K. A. K, and Salama, G. A., (2009). "Effect of elevated fire temperature and cooling regime on the fire resistance of normal and self-compacting concretes" *Engineering Research Journal*, No.122, C63-C81.

Ahmed, S, and Amin, A. F. M. S, (1998). "Effect of curing conditions on compressive strength of brick aggregate concrete" *Journal of Civil Engineering*, Institution of Engineers, Bangladesh, Vol. CE 26, No. 1.

Akhteruzzaman, A. A., and Hasnat, A. (1983). " Properties of concrete using crushed brick as aggregate" *Concrete International ; Design and Construction*, vol. 5, no. 2, 58-63.

Anand, N., Prince Arulraj, G., (2011). "The Effect of elevated temperature on concrete materials-Aliterature review." *International Journal of Civil and Structural Engineering* vol.1, No. 4.

Alireza, J., Susanto, T., Hooi, T. T. (2008). "High temperature effect on flexural strength of steel-fibre concrete" *The 3rd ACF International Conference ACF/VCA*.

Annerel, E., Taerwe, L, (2009). "Approaches for the assessment of the residual strength of concrete exposed to fire, *Concrete Repair, Rehabilitation and Retrofitting II*, Taylor and Francis Group, London.

ASTM C856 (2005) "Petrographic examination of hardened concrete". American Society for Testing Materials.

ASTM C128-88 (2005) “Test method for density, specific gravity and absorption of fine aggregate”. American Society for Testing Materials.

ASTM C29 (2005) “Test method for unit weight and void in aggregate”. American Society for Testing Materials.

ASTM C39 (2005) “Test method for compressive strength of cylindrical concrete specimens”. American Society for Testing Materials.

ASTM C143 (2005) “Test method for slump of hydraulic cement concrete”. American Society for Testing Materials.

BRE (Building Research Establishment) (1988), “Design of normal concrete mixes”

BS 5328 (1997) “Guide to specifying concrete, method of specifying concrete mixes”. British Standards.

BS 882 (1992) “Specification for aggregates from natural sources for concrete”. British Standards.

BS 12 (1996) “Specification for Portland cement”. British Standards.

BS EN 1992-1-2 (1995) “Eurocode 2, Design of concrete structures: Part 1-2 : Structural fire design” European Committee for Standardization, Brussels.

Bastami, M., Chakabi-Khiabani, A., Baghbadrani, M., Kordi, M., (2011). “Performance of High strength concrete at elevated temperatures.” *Scintia Iranica*.

Benjamin I. A. (1962). “Fire resistance of reinforced concrete” Symposium on fire resistance of concrete, SP-5. Detroit: American Concrete Institute, 25–39.

Buck, A. D., (1977). “Recycled concrete as a source of aggregate” *ACI J.* 74 (5), 212-219.

Bazant, Z. P., Kaplan, M. F. (1996). "Concrete at High Temperatures, Material Properties and Mathematical Models" Longman Group, Essex.

Bingol, A. F., Gul, R., (2003). "Compressive strength of lightweight aggregate concrete exposed to high temperatures" Indian Journal of Engineering and Materials Sciences, Vol. 11, pp. 68-72.

Cachim, P. B., (2009). "Mechanical properties of brick aggregate concrete" Const. Build. Mater. 23, 1292-1297.

Cheng F. P., Kodur V. K. R., Wang, T. C. (2004). "Stress-strain curve for high strength concrete at elevated temperatures, Journal of Materials in Civil Engineering, V.16, No. 1 pp. 84-94.

Davis, H. S. (1967). "Effects of high temperature exposure on concrete" Materials Research and Standards, ASTM International, 452-459.

Debieb, F. and Kenai, S. (2008). "The use of coarse and fine crushed bricks as aggregate in concrete" Build. Mater. 22, 868-893.

Fletcher, I. A., Welch, S., Torero, J. L., Carvel, R. O., and Usmani, A., (2007). "Behavior of concrete structures in fire." Thermal Science, Vol. 11 , No. 2, pp. 37-52.

Frondisto Yannas, S (1977). "Waste concrete as aggregate for new concrete" ACI J. 74 (8), 373-376.

Hachemi, S., Ounis, A., Chabi, S., (2014). "Evaluation of residual mechanical and physical properties of concrete at elevated temperatures" International Journal of Civil, Architectural, Structural, Urban Science and Engineering, Vol: 8 No. 2.

Ikponmwosa, E. E., Salau, M. A. (2010). "Effect of heat on laterised concrete" Maejo Int. J. Sci. Technol. 4(01), 33-42.

Islam, M. M., (2011). “Interaction diagrams for square concrete columns confined with fibre reinforced polymer wraps” M. Sc. Engg. Thesis, Department of Civil Engineering, Bangladesh University of Engineering and Technology (BUET).

Khaliq, W., and Kodur, V. K. R., (2011). “Effect of high temperature on tensile strength of different types of high strength concrete.” ACI Materials Journal Title no. 108-M42.

Kim, G., Y. Kim, Y., S., Lee. T. G., (2009). “Mechanical properties of high strength concrete subjected to high temperature by stressed test.” Transaction of Nonferrous Metals Society of China 19, s128-s133.

Kulkarni, D. B., Patil, S. N, (2011). “Comparative study of effect of sustained high temperature on strength properties of self compacting concrete and ordinary concrete.” International Journal of Engineering and Technology vol.3(2), 106-118.

Kumar, R., Bhattacharjee, B. (2003). “Porosity, pore distribution and in situ strength of concrete” Cement and concrete research 33.

Kodur, V. K. R., Sultan, M. A. (2003). “Effect of temperature on thermal properties of high strength concrete” Journal of Materials in Civil Engineering, V.15, No. 2 pp. 101-107.

Khlah, F. M., Devenny, A. S. (2004). “Recycling of demolished masonry rubble as coarse aggregate in concrete: review, J. Mater. Civ. Eng. 16 (4), 331-340.

Khoury G. A., Majorana C. E., Pesavento, F., Schrefler B. A. (2002). “Modelling of heated concrete” Magazine of Concrete Research , Vol: 8, No: 2.

Lankard D. R., Birkimer D. L., Fondfriest F. F., Snyder M. J. (1971). “Effects of moisture content on structural properties of Portland cement concrete exposed to temperatures up to 500° F” Temperature and Concrete, Sp-25. Detroit: American Concrete Institute, PP.59-102.

Lo, T. Y., Cui, H. Z. (2003). "Effect of porous light weight aggregate on strength on concrete" Department of Building and Construction, City University of Hong Kong, Materials Letters 58, 916-919.

Lee, K. K. (2008). "Evaluation of concrete behavior under high temperature" Umi Microform 3315418.

Malhotra, H. L., (1956). "The effect of temperature on compressive strength of concrete" Magazine of Concrete Research, V. 8(22), 85-94.

Morita, T., Saito, H., Kumagai, H. (1992). "Residual mechanical properties of high strength members at exposed to high temperature-Part-1: Test on material properties" Architectural Institute of Japan, Niigata.

Mansur, M. A., Wee, T. H., and Cheran L.S. (1999). "Crushed bricks as coarse aggregate for concrete" ACI Mater. J. 96(4), 478-484.

Neville A. M., (1995). "Properties of concrete" Fourth edition, Longman Group UK Limited, Harlow, Essex England, United Kingdom.

Pimienta P., Anton O., Mindeguia J., Avenel R., Cuypers H., Cesmat E., (2010). "Fire protection of concrete structures exposed to fast fires" 4th International Symposium on Tunnel Safety and Security, Frankfurt am Main, Germany.

Phan, L. T., Carino N. J. (2001). "Mechanical properties of high strength concrete at elevated temperatures" NISTIR 6726.

Phan, L. T. (1996). "Fire performance of high strength concrete" A report of the state of the art, National Institute of Standards and Technology, pp. 105 Gaithersburg, MD.

Poon, C. S. (1997). "Management and recycling of demolition waste in Hong Kong" Waste Manage. Res. 15, 561-572.

Phan, L. T., Carino N. J. (2003). “Code provisions for high strength concrete strength-temperature relationship at elevated temperatures” *Materials and Structures*, 36(156), pp. 91-98.

Phan, L, T., Carino, N. J. (2000). “Fire performance of high strength concrete: research needs” *Building and Fire Research Laboratory, National Institute of Standards and Technology, USA*.

Saad, M., Abo-El-Enein, Hanna, G. B., and Kotkata, (1996). “Effect of temperature on physical and mechanical properties of concrete containing silica fume.” *Cement and Concrete Research*, Vol. 26, No. 5, pp. 669-675.

Schneider U. (1976). “Behavior of concrete under thermal steady state and non-steady fire and materials, pp.103–115.

Toumi, B., Resheidat, M., Guemmadi, Z., and Chabil, H. (2009). “Coupled effect of high temperature on residual strength of normal and high strength concrete.” *Jordan Journal of Civil Engineering* vol.3, No. 4.

T. Zdražil, F. Vodák, O. Kapičková (2004). “Effect of temperature and age of concrete on strength – porosity relation” Vol. 44 No. 1, pp.52-56.

William, K., Xi, Y., Lee, K., Kim, B. (2009). “Thermal response of reinforced concrete structures in nuclear power plants” *University of Colorado, SESM No.02*.

Zhang, B., Bicanic, N., Pearce, C. J., Balabanic, G. (2000). “Residual fracture properties of normal and high strength concrete subject to elevated temperatures” *Magazine of Concrete Research*, No. 2, 123-136.

APPENDIX A

Table A.1 Sample of collected compressive strength data

| Type of coarse aggregate | Specimen ID | Temperature episode | Specimen number | Compressive strength after temperature episodes (Mpa) | | | |
|--------------------------|-------------|---------------------|-----------------|---|-------|-------|-------|
| | | | | 60° | 200° | 400° | 600° |
| Stone chips | S10 | Heating PATH 1 | 1.00 | 15.42 | 12.71 | 9.70 | 8.38 |
| | | | 2.00 | 11.04 | 11.19 | 10.19 | 9.09 |
| | | | 3.00 | 12.23 | 11.79 | 9.78 | 7.30 |
| | | | 4.00 | 14.32 | 11.43 | 8.90 | 7.09 |
| | | | Average | 13.25 | 11.78 | 9.64 | 7.96 |
| | | | % Loss | | 11.09 | 27.24 | 39.91 |
| Stone chips | S10 | Heating PATH 2 | 1.00 | | | | 7.78 |
| | | | 2.00 | | | | 7.33 |
| | | | 3.00 | | | | 10.51 |
| | | | 4.00 | | | | 10.75 |
| | | | Average | | | | 9.09 |
| | | | % Loss | | | | 31.39 |
| Stone chips | S10 | Heating PATH 3 | 1.00 | | | | 8.36 |
| | | | 2.00 | | | | 8.13 |
| | | | 3.00 | | | | 7.28 |
| | | | 4.00 | | | | 6.97 |
| | | | Average | | | | 7.68 |
| | | | % Loss | | | | 42.02 |
| Stone chips | S10 | Heating PATH 4 | 1.00 | | 11.83 | | 11.24 |
| | | | 2.00 | | 12.04 | | 12.84 |
| | | | 3.00 | | 12.13 | | 14.19 |
| | | | 4.00 | | 14.11 | | 11.44 |
| | | | Average | | 12.53 | | 12.43 |
| | | | % Loss | | 20.46 | | 21.22 |

Table A.2 Sample of collected mass loss data

| Type of coarse aggregate | Specimen ID | Temperature episode | Specimen number | Specimen weight loss (%) after temperature episodes | | | |
|--------------------------|-------------|---------------------|-----------------|---|------|------|-------|
| | | | | 60° | 200° | 400° | 600° |
| Stone chips | S10 | Heating PATH 1 | 1.00 | 0 | 3.89 | 3.94 | 7.69 |
| | | | 2.00 | 0 | 3.89 | 5.33 | 6.57 |
| | | | 3.00 | 0 | 5.19 | 5.33 | 6.57 |
| | | | 4.00 | 0 | 5.26 | 6.57 | 7.69 |
| | | | Average % Loss | 0 | 4.56 | 5.29 | 7.13 |
| Stone chips | S10 | Heating PATH 2 | 1.00 | | | | 6.57 |
| | | | 2.00 | | | | 5.19 |
| | | | 3.00 | | | | 6.57 |
| | | | 4.00 | | | | 6.49 |
| | | | Average % Loss | | | | 6.21 |
| Stone chips | S10 | Heating PATH 3 | 1.00 | | | | 5.26 |
| | | | 2.00 | | | | 5.19 |
| | | | 3.00 | | | | 5.26 |
| | | | 4.00 | | | | 5.26 |
| | | | Average % Loss | | | | 5.24 |
| Stone chips | S10 | Heating PATH 4 | 1.00 | | 4.42 | | 10.22 |
| | | | 2.00 | | 4.22 | | 9.96 |
| | | | 3.00 | | 3.96 | | 9.83 |
| | | | 4.00 | | 4.78 | | 10.30 |
| | | | Average % Loss | | 4.35 | | 10.08 |

Table A.3 Concrete porosity and coarse aggregate porosity

| Types of concrete | Design strength (MPa) | Specimen ID | Concrete porosity (%) (Through absorption) | Coarse aggregate porosity (%) (Through absorption) |
|--------------------------|-----------------------|-------------|--|--|
| Stone aggregate | 10 | S10 | 8.86 | 0.8 |
| Stone aggregate | 20 | S20 | 5.58 | 0.8 |
| Stone aggregate | 35 | S35 | 13.03 | 0.8 |
| Recycled stone aggregate | 10 | RS10 | 20.00 | 5.8 |
| Recycled stone aggregate | 20 | RS20 | 19.10 | 5.8 |
| Recycled stone aggregate | 35 | RS35 | 13.42 | 5.8 |
| Recycled brick aggregate | 10 | RB10 | 24.51 | 12.4 |
| Recycled brick aggregate | 20 | RB20 | 30.76 | 12.4 |
| Recycled brick aggregate | 35 | RB35 | 23.50 | 12.4 |
| Brick aggregate | 10 | B10 | 28.94 | 14.4 |
| Brick aggregate | 20 | B20 | 31.19 | 14.4 |
| Brick aggregate | 35 | B35 | 26.21 | 14.4 |

Table A.4 Mass loss data

| Specimen mass loss (%) after temperature episodes | | | | | | |
|--|--------------|-------------|------|------|------|-------|
| | | Temperature | 60° | 200° | 400° | 600° |
| S10 | Heating PATH | 1 | 0 | 4.56 | 5.29 | 7.13 |
| | | 2 | 0 | 4.56 | 0 | 6.21 |
| | | 3 | 0 | 0 | 5.29 | 5.24 |
| | | 4 | 0 | 0 | 4.35 | 10.08 |
| Specimen mass loss (%) after temperature episodes at | | | | | | |
| | | Temperature | 60° | 200° | 400° | 600° |
| S20 | Heating PATH | 1 | 0.62 | 5.11 | 6.17 | 7.57 |
| | | 2 | 0.62 | 3.76 | 0 | 7.35 |
| | | 3 | 0.62 | 0 | 6.17 | 7.30 |
| | | 4 | 0.62 | 0 | 5.60 | 4.45 |

| Specimen mass loss (%) after temperature episodes | | | | | | |
|---|-----------------|---|------|-------|-------|-------|
| | Temperature | | 60° | 200° | 400° | 600° |
| S35 | Heating PATH | 1 | 0.65 | 12.5 | 6.77 | 8.36 |
| | | 2 | 0.65 | 12.5 | 0 | 8.41 |
| | | 3 | 0.65 | 0 | 6.77 | 8.04 |
| | | 4 | 0.65 | 0 | 6.17 | 6.49 |
| Specimen mass loss (%) after temperature episodes | | | | | | |
| | Temperature | | 60° | 200° | 400° | 600° |
| RS10 | Heating PATH | 1 | 1.13 | 9.28 | 12.15 | 13.32 |
| | | 2 | 1.13 | 9.28 | 0 | 11.58 |
| | | 3 | 1.13 | 0 | 12.15 | 12.33 |
| | | 4 | 0 | 0 | 0 | 0 |
| Specimen mass loss (%) after temperature episodes | | | | | | |
| | Temperature | | 60° | 200° | 400° | 600° |
| RS20 | Heating PATH | 1 | 0.34 | 8.82 | 9.46 | 11.66 |
| | | 2 | 0.34 | 8.82 | 0 | 10.92 |
| | | 3 | 0.34 | 0 | 9.46 | 12.16 |
| | | 4 | 0.34 | 0 | 9.16 | 9.59 |
| Specimen mass loss (%) after temperature episodes | | | | | | |
| | Temperature | | 60° | 200° | 400° | 600° |
| RS35 | Heating PATH | 1 | 0.52 | 9.43 | 12.95 | 13.67 |
| | | 2 | 0.52 | 9.43 | 0 | 12.58 |
| | | 3 | 0.52 | 0 | 12.95 | 13.95 |
| | | 4 | 0 | 0 | 0 | 0 |
| Specimen weight loss (%) after temperature episodes | | | | | | |
| | Temperature | | 60° | 200° | 400° | 600° |
| B10 | Heating PATH | 1 | 1.40 | 11.79 | 12.13 | 10.64 |
| | | 2 | 1.40 | 11.79 | 0 | 12.47 |
| | | 3 | 1.40 | 0 | 12.13 | 13.89 |
| | | 4 | 1.40 | 0 | 8.38 | 8.38 |
| Specimen weight loss (%) after temperature episodes | | | | | | |
| | Temperature | | 60° | 200° | 400° | 600° |
| B20 | Heating PATH | 1 | 0.37 | 10.29 | 9.77 | 14.88 |
| | | 2 | 0.37 | 10.29 | 0 | 12.96 |
| | | 3 | 0.37 | 0 | 9.77 | 13.06 |
| | | 4 | 0.37 | 0 | 8.26 | 8.05 |
| Specimen weight loss (%) after temperature episodes | | | | | | |
| | Temperature | | 60° | 200° | 400° | 600° |
| B35 | Heating PATH | 1 | 2.97 | 13.60 | 13.65 | 14.18 |
| | | 2 | 2.97 | 13.60 | 0 | 14.18 |
| | | 3 | 2.97 | 0 | 13.65 | 14.18 |
| | | 4 | 2.97 | 0 | 9.41 | 11.70 |

| Specimen weight loss (%) after temperature episodes | | | | | | |
|---|-----------------|-------------|------|------|-------|-------|
| | | Temperature | 60° | 200° | 400° | 600° |
| RB10 | Heating PATH | 1 | 0.34 | 4.56 | 12.18 | 11.02 |
| | | 2 | 0.34 | 4.56 | 0 | 6.21 |
| | | 3 | 0.34 | 0 | 12.18 | 11.65 |
| | | 4 | 0.34 | 0 | 10.05 | 10.08 |

| Specimen weight loss (%) after temperature episodes | | | | | | |
|---|-----------------|-------------|------|-------|-------|-------|
| | | Temperature | 60° | 200° | 400° | 600° |
| RB20 | Heating PATH | 1 | 0.73 | 10.26 | 11.76 | 12.90 |
| | | 2 | 0.73 | 10.26 | 0 | 12.31 |
| | | 3 | 0.73 | 0 | 11.76 | 12.59 |
| | | 4 | 0.73 | 0 | 10.45 | 12.22 |

| Specimen weight loss (%) after temperature episodes | | | | | | |
|---|-----------------|-------------|------|-------|-------|-------|
| | | Temperature | 60° | 200° | 400° | 600° |
| RB35 | Heating PATH | 1 | 2.08 | 11.56 | 11.58 | 14.17 |
| | | 2 | 2.08 | 11.56 | 0 | 14.87 |
| | | 3 | 2.08 | 0 | 11.58 | 14.11 |
| | | 4 | 2.08 | 0 | 12.22 | 13.77 |

Table A.5 Residual compressive strength data

| Compressive strength after temperature episodes (MPa) | | | | | | |
|---|-----------------|-------------|------|------|------|------|
| | | Temperature | 60° | 200° | 400° | 600° |
| S10 | Heating PATH | 1 | 12.3 | 11.0 | 9.0 | 7.4 |
| | | 2 | 12.3 | 11.0 | 0 | 8.3 |
| | | 3 | 12.3 | 0 | 9.0 | 7.0 |
| | | 4 | 12.3 | 11.0 | 9.8 | 10.9 |
| Compressive strength after temperature episodes (MPa) | | | | | | |
| | | Temperature | 60° | 200° | 400° | 600° |
| S20 | Heating PATH | 1 | 18.8 | 18.1 | 16.2 | 15.0 |
| | | 2 | 18.8 | 18.1 | 0 | 15.5 |
| | | 3 | 18.8 | 0 | 16.2 | 10.0 |
| | | 4 | 18.8 | 18.1 | 15.0 | 14 |
| Compressive strength after temperature episodes (MPa) | | | | | | |
| | | Temperature | 60° | 200° | 400° | 600° |
| S35 | Heating PATH | 1 | 31.0 | 30.2 | 21.9 | 19.3 |
| | | 2 | 31.0 | 30.2 | 0 | 19.3 |
| | | 3 | 31.0 | 0 | 21.9 | 12.2 |
| | | 4 | 31.0 | 30.2 | 17.4 | 16.3 |
| Compressive strength after temperature episodes (MPa) | | | | | | |
| | | Temperature | 60° | 200° | 400° | 600° |
| RS10 | Heating PATH | 1 | 10.7 | 9.9 | 7.3 | 2.49 |
| | | 2 | 10.7 | 9.9 | 0 | 2.50 |
| | | 3 | 10.7 | 0 | 7.3 | 7.06 |
| | | 4 | 0 | 9.9 | 0 | 0 |
| Compressive strength after temperature episodes (MPa) | | | | | | |
| | | Temperature | 60° | 200° | 400° | 600° |
| RS20 | Heating PATH | 1 | 22.2 | 19.9 | 16.3 | 9.4 |
| | | 2 | 22.2 | 19.9 | 0 | 11.8 |
| | | 3 | 22.2 | 0 | 16.3 | 10.8 |
| | | 4 | 22.2 | 19.9 | 16.6 | 14.7 |
| Compressive strength after temperature episodes (MPa) | | | | | | |
| | | Temperature | 60° | 200° | 400° | 600° |
| RS35 | Heating PATH | 1 | 32.5 | 26.7 | 19.9 | 9.3 |
| | | 2 | 32.5 | 26.7 | 0 | 4.5 |
| | | 3 | 32.5 | 0 | 19.9 | 18.6 |
| | | 4 | 0 | 0 | 0 | 0 |

| Compressive strength after temperature episodes (MPa) | | | | | | |
|---|-----------------|-------------|------|------|------|------|
| | | Temperature | 60° | 200° | 400° | 600° |
| B10 | Heating PATH | 1 | 14.7 | 11.7 | 11.3 | 5.9 |
| | | 2 | 14.7 | 11.7 | 0 | 9.3 |
| | | 3 | 14.7 | 0 | 11.3 | 10.5 |
| | | 4 | 14.7 | 11.7 | 12.4 | 10.7 |
| Compressive strength after temperature episodes (MPa) | | | | | | |
| | | Temperature | 60° | 200° | 400° | 600° |
| B20 | Heating PATH | 1 | 24.4 | 22.8 | 19.9 | 12.9 |
| | | 2 | 24.4 | 22.8 | 0 | 14.3 |
| | | 3 | 24.4 | 0 | 19.9 | 16.3 |
| | | 4 | 24.4 | 22.8 | 20.5 | 16.7 |
| Compressive strength after temperature episodes (MPa) | | | | | | |
| | | Temperature | 60° | 200° | 400° | 600° |
| B35 | Heating PATH | 1 | 29.6 | 22.7 | 21.3 | 9.7 |
| | | 2 | 29.6 | 22.7 | 0 | 17.9 |
| | | 3 | 29.6 | 0 | 21.3 | 20.1 |
| | | 4 | 29.6 | 22.7 | 26.6 | 23.7 |
| Compressive strength after temperature episodes (MPa) | | | | | | |
| | | Temperature | 60° | 200° | 400° | 600° |
| RB10 | Heating PATH | 1 | 16.1 | 13.2 | 10.3 | 9.5 |
| | | 2 | 16.1 | 13.2 | 0 | 8.3 |
| | | 3 | 16.1 | 0 | 10.3 | 10.8 |
| | | 4 | 16.1 | 13.2 | 12.0 | 12.2 |
| Compressive strength after temperature episodes (MPa) | | | | | | |
| | | Temperature | 60° | 200° | 400° | 600° |
| RB20 | Heating PATH | 1 | 19.4 | 17.3 | 11.6 | 9.7 |
| | | 2 | 19.4 | 17.3 | 0 | 7.6 |
| | | 3 | 19.4 | 0 | 11.6 | 11.6 |
| | | 4 | 19.4 | 17.3 | 14.6 | 14.2 |
| Compressive strength after temperature episodes (MPa) | | | | | | |
| | | Temperature | 60° | 200° | 400° | 600° |
| RB35 | Heating PATH | 1 | 25.9 | 22.9 | 17.9 | 16.8 |
| | | 2 | 25.9 | 22.9 | 0 | 15.5 |
| | | 3 | 25.9 | 0 | 17.9 | 9.3 |
| | | 4 | 25.9 | 22.9 | 21.1 | 16.1 |

Table A.6 Compressive strength loss data

| Compressive strength loss (%) after temperature episodes | | | | | | |
|--|-----------------|---|-----|-------|-------|-------|
| | Temperature | | 60° | 200° | 400° | 600° |
| S10 | Heating PATH | 1 | 0 | 12.71 | 28.56 | 39.91 |
| | | 2 | 0 | 12.71 | 0 | 32.63 |
| | | 3 | 0 | 0 | 28.56 | 43.07 |
| | | 4 | 0 | 12.71 | 10.43 | 11.15 |
| Compressive strength loss (%) after temperature episodes | | | | | | |
| | Temperature | | 60° | 200° | 400° | 600° |
| S20 | Heating PATH | 1 | 0 | 3.76 | 13.74 | 20.35 |
| | | 2 | 0 | 3.76 | 0 | 17.75 |
| | | 3 | 0 | 0 | 13.74 | 46.66 |
| | | 4 | 0 | 3.76 | 20.28 | 25.67 |
| Compressive strength loss (%) after temperature episodes | | | | | | |
| | Temperature | | 60° | 200° | 400° | 600° |
| S35 | Heating PATH | 1 | 0 | 2.69 | 29.37 | 37.75 |
| | | 2 | 0 | 2.69 | 0 | 37.81 |
| | | 3 | 0 | 0 | 29.37 | 60.49 |
| | | 4 | 0 | 2.69 | 43.76 | 47.46 |
| Compressive strength loss (%) after temperature episodes | | | | | | |
| | Temperature | | 60° | 200° | 400° | 600° |
| RS10 | Heating PATH | 1 | 0 | 6.96 | 31.16 | 76.64 |
| | | 2 | 0 | 6.96 | 0 | 76.49 |
| | | 3 | 0 | 0 | 31.16 | 33.74 |
| | | 4 | 0 | 6.96 | 0 | 0 |
| Compressive strength loss (%) after temperature episodes | | | | | | |
| | Temperature | | 60° | 200° | 400° | 600° |
| RS20 | Heating PATH | 1 | 0 | 10.46 | 26.45 | 57.83 |
| | | 2 | 0 | 10.46 | 0 | 49.56 |
| | | 3 | 0 | 0 | 26.45 | 53.71 |
| | | 4 | 0 | 10.46 | 25.14 | 34.02 |
| Compressive strength loss (%) after temperature episodes | | | | | | |
| | Temperature | | 60° | 200° | 400° | 600° |
| RS35 | Heating PATH | 1 | 0 | 17.82 | 38.63 | 71.37 |
| | | 2 | 0 | 17.82 | 0 | 86.24 |
| | | 3 | 0 | 0 | 38.63 | 42.93 |
| | | 4 | 0 | 0 | 0 | 0 |

| Compressive strength loss (%) after temperature episodes | | | | | | |
|--|-----------------|---|-----|-------|-------|-------|
| | Temperature | | 60° | 200° | 400° | 600° |
| B10 | Heating PATH | 1 | 0 | 19.95 | 22.62 | 59.69 |
| | | 2 | 0 | 19.95 | 0 | 36.58 |
| | | 3 | 0 | 0 | 22.62 | 28.27 |
| | | 4 | 0 | 19.95 | 15.64 | 26.97 |
| Compressive strength loss (%) after temperature episodes | | | | | | |
| | Temperature | | 60° | 200° | 400° | 600° |
| B20 | Heating PATH | 1 | 0 | 6.42 | 18.48 | 47.07 |
| | | 2 | 0 | 6.42 | 0 | 43.63 |
| | | 3 | 0 | 0 | 18.48 | 35.41 |
| | | 4 | 0 | 6.42 | 15.71 | 31.39 |
| Compressive strength loss (%) after temperature episodes | | | | | | |
| | Temperature | | 60° | 200° | 400° | 600° |
| B35 | Heating PATH | 1 | 0 | 23.25 | 27.90 | 67.24 |
| | | 2 | 0 | 23.25 | 0 | 39.54 |
| | | 3 | 0 | 0 | 27.90 | 32.20 |
| | | 4 | 0 | 23.25 | 10.07 | 20.03 |
| Compressive strength loss (%) after temperature episodes | | | | | | |
| | Temperature | | 60° | 200° | 400° | 600° |
| RB10 | Heating PATH | 1 | 0 | 18.06 | 35.95 | 40.80 |
| | | 2 | 0 | 18.06 | 0 | 48.60 |
| | | 3 | 0 | 0 | 35.95 | 33.20 |
| | | 4 | 0 | 18.06 | 25.85 | 24.63 |
| Compressive strength loss (%) after temperature episodes | | | | | | |
| | Temperature | | 60° | 200° | 400° | 600° |
| RB20 | Heating PATH | 1 | 0 | 10.60 | 39.91 | 50.13 |
| | | 2 | 0 | 10.60 | 0 | 60.56 |
| | | 3 | 0 | 0 | 39.91 | 39.91 |
| | | 4 | 0 | 10.60 | 24.51 | 26.90 |
| Compressive strength loss (%) after temperature episodes | | | | | | |
| | Temperature | | 60° | 200° | 400° | 600° |
| RB35 | Heating PATH | 1 | 0 | 11.78 | 30.87 | 35.22 |
| | | 2 | 0 | 11.78 | 0 | 40.01 |
| | | 3 | 0 | 0 | 30.87 | 64.26 |
| | | 4 | 0 | 11.78 | 18.40 | 37.77 |

Table A.7 Summary of mix design for 32 (dia-100mm & height-200mm) cylinders of each type

| Type of concrete | free water content (kg) | cement content (kg) | Total aggregate content (kg) | Fine Aggregate content (kg) | Coarse Aggregate content (kg) |
|------------------|-------------------------|---------------------|------------------------------|-----------------------------|-------------------------------|
| S10 | 14.41 | 17.84 | 127.67 | 51.07 | 76.60 |
| S20 | 14.41 | 22.65 | 123.55 | 49.42 | 74.13 |
| S35 | 15.44 | 30.28 | 114.89 | 42.51 | 72.38 |
| B10 | 14.41 | 17.84 | 127.67 | 51.07 | 76.60 |
| B20 | 14.41 | 22.65 | 123.55 | 49.42 | 74.13 |
| B35 | 15.44 | 30.28 | 103.22 | 38.19 | 65.03 |
| RS10 | 14.41 | 17.84 | 127.67 | 51.07 | 76.60 |
| RS20 | 14.41 | 22.65 | 123.55 | 49.42 | 74.13 |
| RS35 | 15.44 | 30.28 | 110.43 | 40.86 | 69.57 |
| RB10 | 14.41 | 17.84 | 127.67 | 51.07 | 76.60 |
| RB20 | 14.41 | 22.65 | 123.55 | 49.42 | 74.13 |
| RB35 | 15.44 | 30.28 | 105.97 | 39.21 | 66.76 |

A.8 Sample calculation of porosity for S10:

Equation used for porosity (through absorption) calculation;

Apparent porosity of concrete, η

$$= \frac{\text{Wt. of sample in SSD condition} - \text{Dry wt. of sample at } 600^{\circ} \text{ C}}{\text{Dry weight of sample at } 600^{\circ} \text{ C}} \times 100\%$$

$$\text{Apparent porosity, } \eta = \frac{3.84 - 3.53}{3.53} \times 100\%$$

$$= 8.86\%$$

Table A.9 Summary of age of concrete

| Age of concrete from casting to testing (days) | | | | | | | |
|--|---------------------|------|------|------|-----|-----|-----|
| Heating PATH | Temperature control | RS10 | RS20 | RS35 | B10 | B20 | B35 |
| 1 | 200 | 34 | 51 | 32 | 62 | 54 | 61 |
| | 400 | 33 | 52 | 31 | 61 | 55 | 60 |
| | 600 | 37 | 36 | 35 | 57 | 39 | 56 |
| 2 | 200+600 | 34 | 51 | 32 | 62 | 54 | 61 |
| 3 | 400+600 | 33 | 52 | 31 | 61 | 55 | 60 |
| 4 | 200+400+600 | | 120 | | 120 | 120 | 120 |

| Heating PATH | Temperature control | S10 | S20 | S35 | RB10 | RB20 | RB35 |
|--------------|---------------------|-----|-----|-----|------|------|------|
| 1 | 200 | 67 | 67 | 73 | 69 | 67 | 71 |
| | 400 | 68 | 68 | 74 | 70 | 68 | 72 |
| | 600 | 64 | 64 | 72 | 67 | 65 | 70 |
| 2 | 200+600 | 67 | 67 | 73 | 69 | 67 | 71 |
| 3 | 400+600 | 68 | 68 | 74 | 70 | 68 | 72 |
| 4 | 200+400+600 | 120 | 120 | 120 | 120 | 120 | 120 |

A.10 Sample calculation of heat input:

Equation used for heat input calculation;

Heat = Electrical power x Time

Heat input in PATH1 (60⁰ – 200⁰) for S10

$$= \frac{\text{Power in watt} \times \text{Time of power supply in second}}{\text{Nos. of sample} \times \text{weight of each sample}} \text{ (J/kg)}$$

$$= \frac{27720 \times 105 \times 60}{16 \times 3.81} \text{ (J/kg)}$$

$$= 2.864\text{E}6 \text{ J/kg}$$

Table A.11 Summary of estimation of heat input

| Concrete type | Temperature episode (°C) | Heat input (J/kg) | Concrete type | Temperature episode (°C) | Heat input (J/kg) |
|---------------|--------------------------|-------------------|---------------|--------------------------|-------------------|
| S10 | 60-200 | 2.864E+06 | B10 | 60-200 | 3.203E+06 |
| | 60-400 | 3.137E+06 | | 60-400 | 3.509E+06 |
| | 60-600 | 3.819E+06 | | 60-600 | 4.271E+06 |
| | 60-200-600 | 6.329E+06 | | 60-200-600 | 7.078E+06 |
| | 60-400-600 | 9.575E+06 | | 60-400-600 | 1.071E+07 |
| | 60-200-400 | 9.138E+06 | | 60-200-400 | 1.022E+07 |
| | 60-200-400-600 | 1.271E+07 | | 60-200-400-600 | 1.422E+07 |
| S20 | 60-200 | 2.742E+06 | B20 | 60-200 | 3.261E+06 |
| | 60-400 | 3.003E+06 | | 60-400 | 3.572E+06 |
| | 60-600 | 3.655E+06 | | 60-600 | 4.349E+06 |
| | 60-200-600 | 6.057E+06 | | 60-200-600 | 7.206E+06 |
| | 60-400-600 | 9.156E+06 | | 60-400-600 | 1.090E+07 |
| | 60-200-400 | 8.747E+06 | | 60-200-400 | 1.041E+07 |
| | 60-200-400-600 | 1.217E+07 | | 60-200-400-600 | 1.447E+07 |
| S35 | 60-200 | 2.818E+06 | B35 | 60-200 | 3.269E+06 |
| | 60-400 | 3.086E+06 | | 60-400 | 3.580E+06 |
| | 60-600 | 3.757E+06 | | 60-600 | 4.358E+06 |
| | 60-200-600 | 6.226E+06 | | 60-200-600 | 7.223E+06 |
| | 60-400-600 | 9.420E+06 | | 60-400-600 | 1.093E+07 |
| | 60-200-400 | 8.990E+06 | | 60-200-400 | 1.043E+07 |
| | 60-200-400-600 | 1.251E+07 | | 60-200-400-600 | 1.451E+07 |
| RS10 | 60-200 | 2.902E+06 | RB10 | 60-200 | 3.142E+06 |
| | 60-400 | 3.178E+06 | | 60-400 | 3.441E+06 |
| | 60-600 | 3.869E+06 | | 60-600 | 4.189E+06 |
| | 60-200-600 | 6.411E+06 | | 60-200-600 | 6.941E+06 |
| | 60-400-600 | 9.700E+06 | | 60-400-600 | 1.050E+07 |
| | 60-200-400 | 9.257E+06 | | 60-200-400 | 1.002E+07 |
| | 60-200-400-600 | 1.288E+07 | | 60-200-400-600 | 1.394E+07 |
| RS20 | 60-200 | 2.976E+06 | RB20 | 60-200 | 3.329E+06 |
| | 60-400 | 3.259E+06 | | 60-400 | 3.646E+06 |
| | 60-600 | 3.967E+06 | | 60-600 | 4.439E+06 |
| | 60-200-600 | 6.575E+06 | | 60-200-600 | 7.355E+06 |
| | 60-400-600 | 9.947E+06 | | 60-400-600 | 1.113E+07 |
| | 60-200-400 | 9.493E+06 | | 60-200-400 | 1.062E+07 |
| | 60-200-400-600 | 1.321E+07 | | 60-200-400-600 | 1.477E+07 |
| RS35 | 60-200 | 2.871E+06 | RB35 | 60-200 | 3.098E+06 |
| | 60-400 | 3.144E+06 | | 60-400 | 3.393E+06 |
| | 60-600 | 3.828E+06 | | 60-600 | 4.130E+06 |
| | 60-200-600 | 6.343E+06 | | 60-200-600 | 6.844E+06 |
| | 60-400-600 | 9.596E+06 | | 60-400-600 | 1.036E+07 |
| | 60-200-400 | 9.159E+06 | | 60-200-400 | 9.883E+06 |
| | 60-200-400-600 | 1.274E+07 | | 60-200-400-600 | 1.375E+07 |

B.1 FIRE INCIDENT AND LOSSES IN BANGLADESH

B.1.1 Standard Garments Ltd., Konabari, Gazipur.

A devastating fire broke out at Standard Garments Ltd. Konabari, Gazipur at around 12:30am November 24, 2012. Hearing rumor of death of two garment workers, agitating workers set the fire on two 10-storied buildings of Standard Group. No people were killed. Agitating workers refused fire fighting unit to stop the fire. This is a biggest fire incident in near past in terms of loss of property. Bangladesh Garment Manufacturers and Exporters Association (BGMEA) has termed the fire incident at Standard Group as “sabotage.”



Figure B.1 Fire incident in Standard Garments Ltd., November 24, 2012.

(Sources: Internet)

B.1.2 Tazreen Fashion Factory in Ashulia

A devastating fire broke out in the Tazreen Fashion factory in Ashulia. At least 124 people were killed in the fire and at least 200 were injured. The fire caused by an electrical short circuit, started on the ground floor of the nine-story building. Because of the large amount of fabrics and yarn in the factory, the fire quickly spread to the other floors, which complicates the firefighting operations.



Figure B.2 Fire incident in Tazreen Fashion factory, Ashulia, November 24, 2012.

(Sources: Internet)

Witnesses reported that many workers had been unable to escape through the narrow exits. 12 of the victims died leaping from windows to escape the flame. Maj. Mohammad Mahbub, fire operation director, told press, “had there been at least one emergency exit outside the factory, the casualties would have been much lower”. It is worst ever fire incident in Bangladesh’s history.

B.1.3 Fire in Chemical Factory, Dhaka

A large fire broke out at in a chemical factory in Dhaka June 4, 2010 .At least 104 people were killed and over 100 were injured in this devastating fire according to local media. Mohibul Huq, deputy commissioner of Dhaka district, told the local

media that the fire broke out when an electric transformer exploded igniting a chemical warehouse.

The fire broke out in the old Dhaka city about 9:20 p.m. and it soon spread to some houses in the congested residential area. The firefighters rushed to the spot soon and brought the fire under control after three hours.



Figure B.3 Fire incident in a chemical factory, Old Dhaka, June 4, 2010.

(Sources: Internet)

B.1.4 Ha-Meem Group in Ashulia

At least 23 people were killed and over a hundred injured as Ha-Meem Group's high-rise garment factory in Ashulia, Dhaka due to a devastating fire on December 14, 2010. The fire starts around 10. The cause of the fire is not clear. Firefighters ran out of water. Later Dhaka WASA sent water-carrying vehicle to assist the operations. Many workers, trapped in plumes of smoke and unable to breathe, jumped to their deaths to escape from one of the worst fire accidents in recent memory. A total of six units of firefighters from Savar, Dhamrai, DEPZ, Gazipur and Mirpur drove in and struggled to put out the blaze. Besides, army was called out for rescue operation.



Figure B.4 Fire incident in Ha-Meem group, Ashulia, Dhaka, December 14, 2010.

(Sources: Internet)

B.1.5 Fire in Shoe Factory, Dhaka

A fire broke out at a shoe factory in kayettuli area of Old Dhaka on 24th august .the fire originated at about 6:50 PM from an electric short circuit at the factory and soon reached the other parts of the unit. According to the fire service control room it spreads over the densely populated area, creating panic between people.

Eight units of firefighters from various city stations rushed to the spot and tried to control the fire with the help of local people.

B.2 FIRE INCIDENTS AROUND THE WORLD

B.2.1 Hotel Roosevelt Fire, USA

The Hotel Roosevelt fire was the worst fire that had been seen since 1901 in Florida. This incident occurred on December 29, 1963. At that time the Hotel Roosevelt was one of the two luxury hotels in the city's downtown, with many restaurants and

businesses on its ground floor, including a ballroom and a barber shop. Fire started in the ballroom's ceiling. The old ceiling was deemed a fire hazard, was not removed when the new ceiling was installed, providing kindling for the fire which started from faulty wires.

After a day of recovering the dead, firefighter found 21 residents dead in their beds from smoke inhalation.



Figure B.5 (a) Hotel Roosevelt fire incident, Florida, December 29, 1963.
(Sources: Internet)



Figure B.5 (b) Hotel Roosevelt fire incident, Florida, December 29, 1963.
(Sources: Internet)

B.2.2 Fire at the Ozone Disco Club in Quezon City, Philippine

A fire at the Ozone Disco Club in Quezon City, Philippines broke out shortly after midnight, March 18, 1996 leaving at least 162 people dead. It is officially acknowledged as the worst fire in Philippine history.

At the time of the fire, it was estimated that there were around 350 patrons and 40 club employees inside the disco. Most of the club guests were high school and college students attending graduation or end of the school year celebrations. The final death count was reported as between 160 and 162 people and at least 95 people were injured.



Figure B.6 Fire incident in the Ozone Disco Club in Quezon City, Philippines, March 18, 1996.

B.2.3 Kader Toy Factory Fire, Thailand

A fire broke out on May 10, 1993 at a toy factory in Thailand. It is considered as the worst industrial factory fire in history. 188 people were killed and over 500 were seriously injured. Most of the victims were young female worker from rural families.

At about 4 PM on May 10, 1993, a small fire was discovered on the first floor of the E-shaped building. Workers, located in the upper floors, were instructed to keep

working because they were told the fire was said to be minor. This part of the building was dedicated to the storage of finished products and the fire spread quickly. Other parts of the factory were full of raw materials which also burned very fast. Workers in the first building who tried to escape found the ground floor exit doors locked and the stairwells soon collapsed.

Many workers jumped from the building in order to escape. Firefighters arrived at the factory 4:40 PM but it was already late. The fire spread extremely quickly because of the presence of the combustible plastics and fabrics.

B.2.4 2010 Shanghai Fire , China

The 2010 Shanghai Fire was devastating fire that destroyed a 28 story high rise apartment building in the city of Shanghai, China. More than 58 people were killed and at least 70 others were injured. On November 15, 2010 the fire began at 2:15 PM local time around the 10th floor. It took over 80 fire engines and several hours to contain the fire. Firefighters were able to save over 100 people.

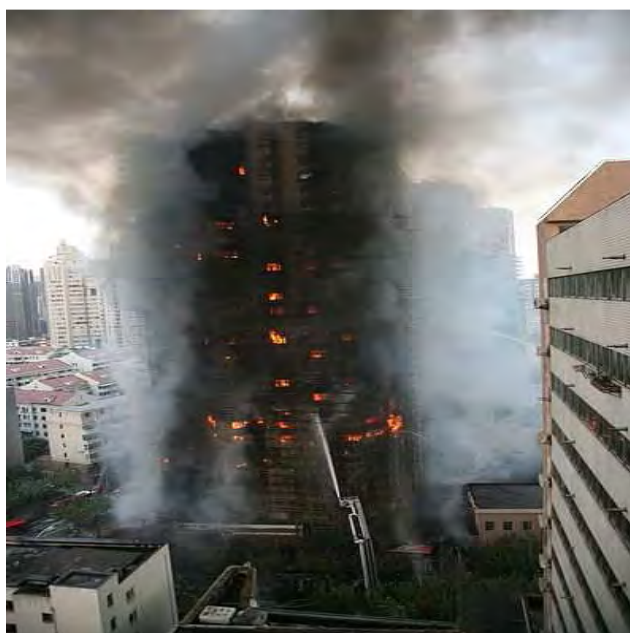


Figure B.7 (a) Shanghai fire, China, November 15, 2010.

(Sources: Internet)



Figure B.7 (b) Shanghai fire, China, November 15, 2010.

(Sources: Internet)

B.2.5 Santiago Prison Fire, Chile

A devastating fire broke out in the San Miguel prison in Santiago, Chile on December 8, 2010. More than 81 people were killed, making it country's deadliest prison incident.

The fire broke out at 5:30 AM on the 3rd floor during a fight between rival gangs who set mattresses alight. Local firefighters took around three hours to bring the fire under control.

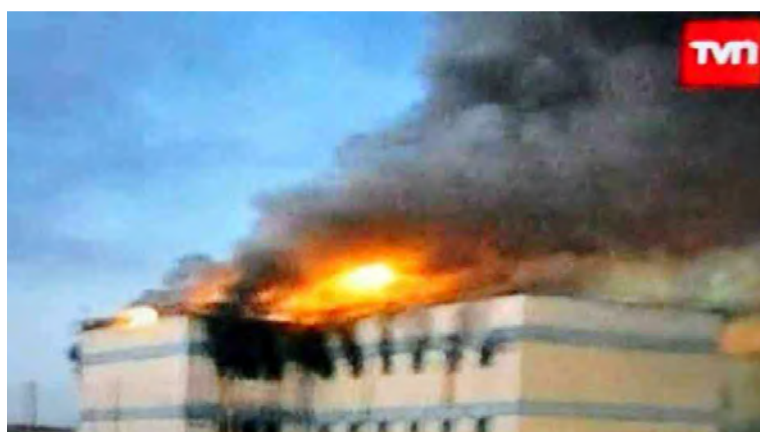


Figure B.8 Santiago prison fire, Chile, December 8, 2010.

(Sources: Internet)

Photographs of materials and activities.

C.1 Material used



Figure C.1 Stone aggregate



Figure C.2 Brick aggregate



Figure C.3 Recycled brick aggregate



Figure C.4 Recycled stone aggregate



Figure C.5 Sylhet sand



Figure C.6 Cement



Figure C.7 Water

C.2 Casting of materials.



Figure C.8 Fresh concrete



Figure C.9 Compaction of concrete sample



Figure C.10 Hammering

C.3 Curing and marking of sample



Figure C.11 Marking of sample



Figure C.12 Sample of concrete cylinder



Figure C.13 Curing of sample

C.4 Burning and testing

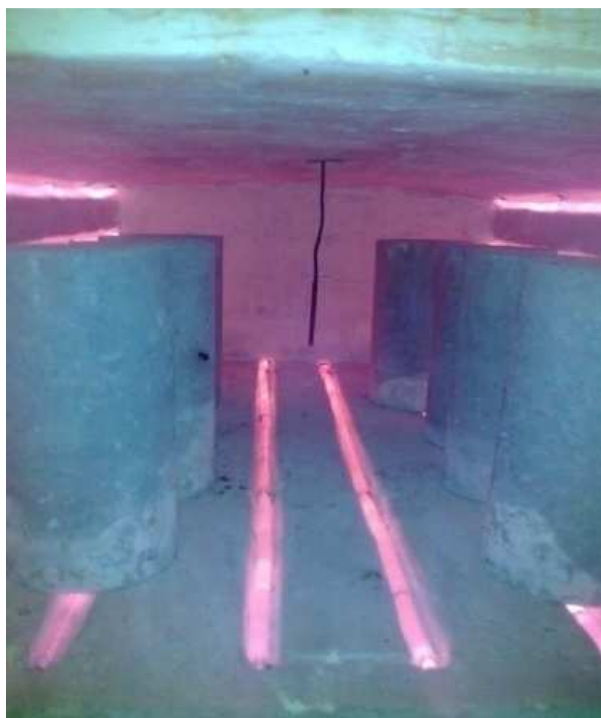


Figure C.14 Burning of sample



Figure C.15 Crushing strength test



Figure C.16 Failure pattern after testing